HRPT
High Resolution Powder Diffractometer for Thermal Neutrons

http://sinq.web.psi.ch/hrpt

Vladimir Pomjakushin
Laboratory for Neutron Scattering, ETHZ and PSI

AIC Information Day on "Large Facilities for Crystallography Studies: Synchrotron and Neutron sources"
October 19th, 2009 , Paul Scherrer Institut, Villigen, Switzerland

Instead of introduction (1): HRPT history

- Design, construction (CERCA) started ~1991
- Commissioned in 1999. HRPT father is Peter Fisher

Instead of introduction (2): Applications of HRPT diffractometer

1) Precise structure refinement complementary to x-rays
2) Magnetic ordering phenomena
3) Direct structure solution. Phase analysis of (new) materials

Instead of introduction (2): Applications of HRPT diffractometer

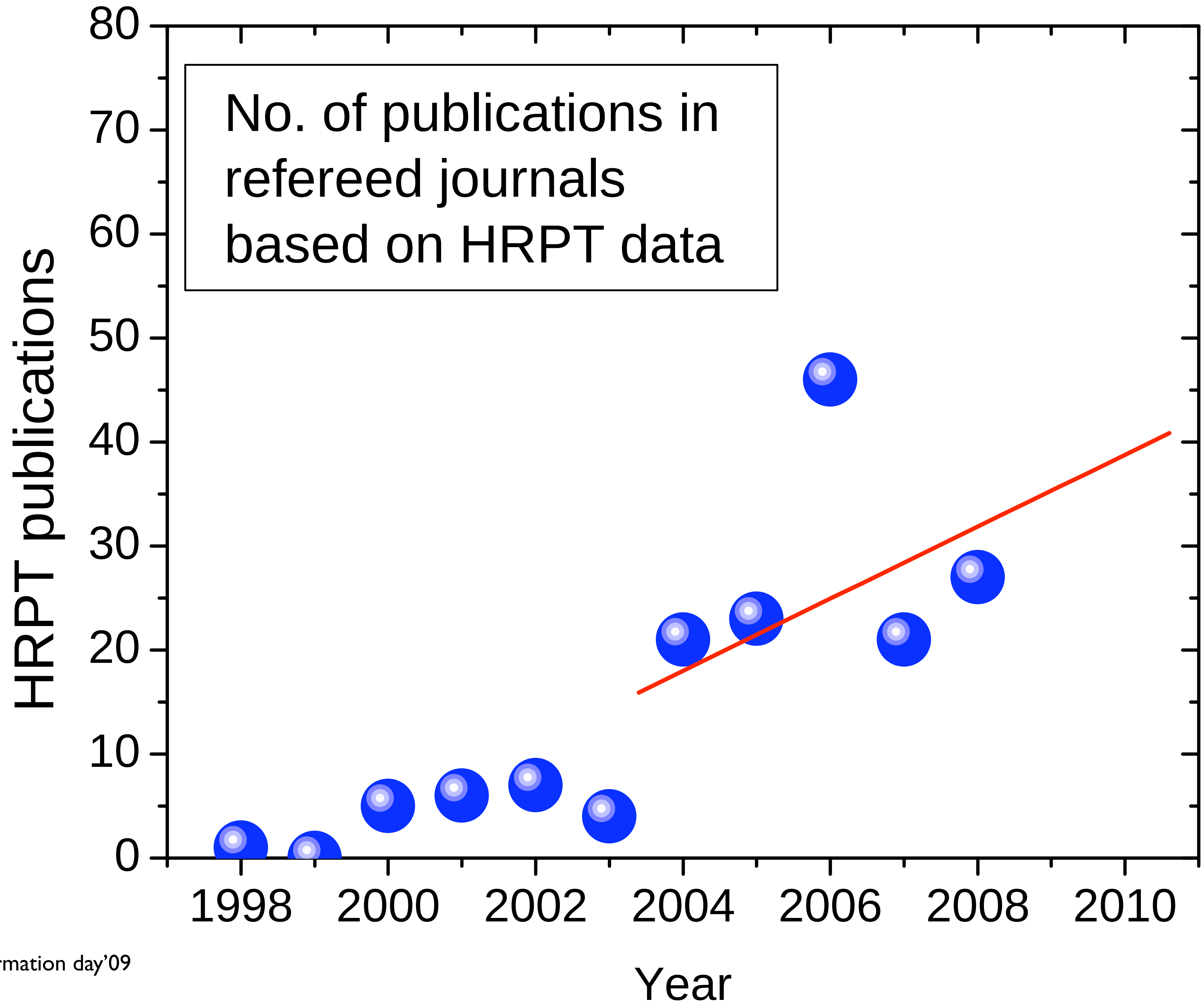

More information about HRPT

Google
Switzerland

More information about HRPT

Google Switzerland

HRPT neutron

More information about HRPT

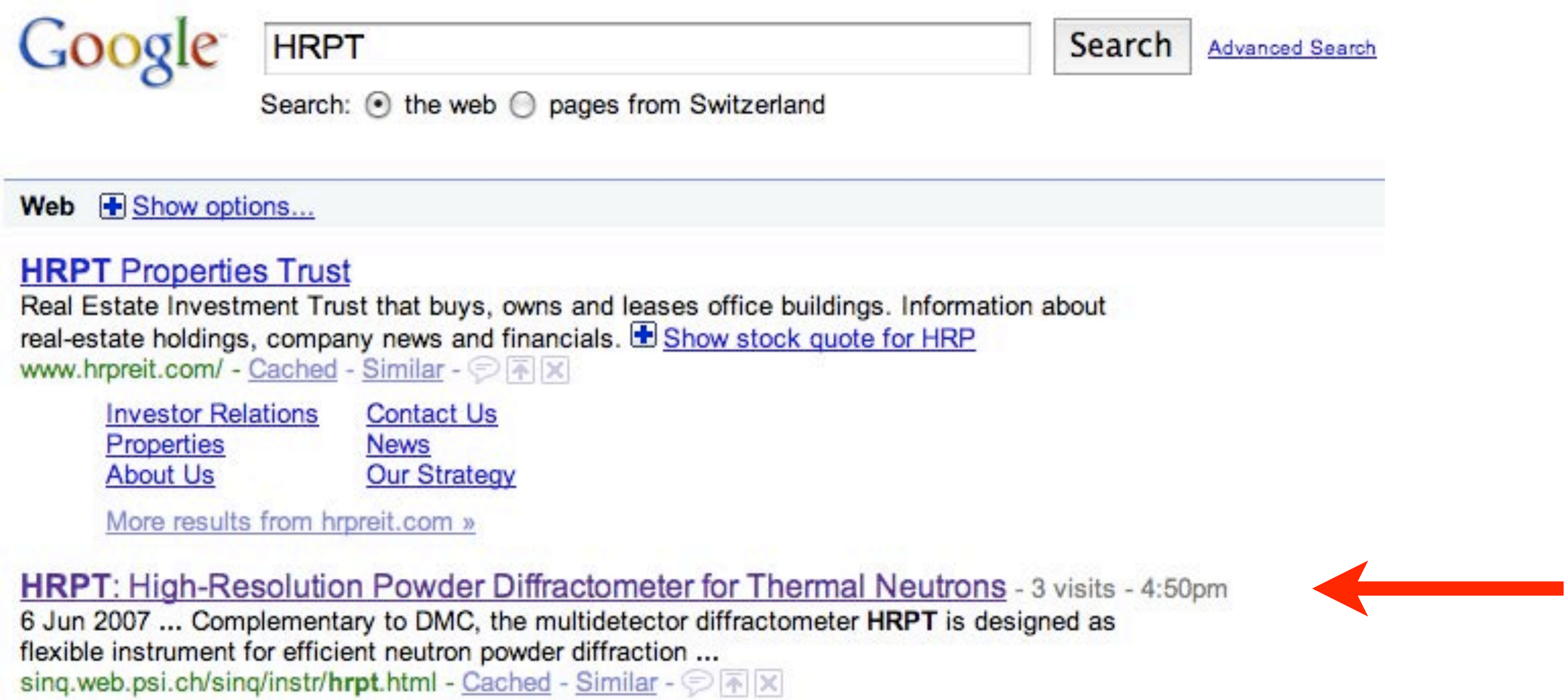

Powder neutron diffractometers

European Portal for Neutron Scattering

http://pathfinder.neutron-eu.net

Powder neutron diffractometers

European Portal for Neutron Scattering

http://pathfinder.neutron-eu.net

SINQ/PSI, CH	DMC, HRPT, POLDI
LLB, FR	G41, G42
ISIS, UK	GEM, HRPD, PEARL
FRM-II, DE	SPODI
FLNP/Dubna, RU	HRFD, DN2, DN12
ILL, FR	D20, D2B

Powder ND at SINQ/PSI

HRPT - High Resolution Powder Diffractometer for Thermal Neutrons at SINQ

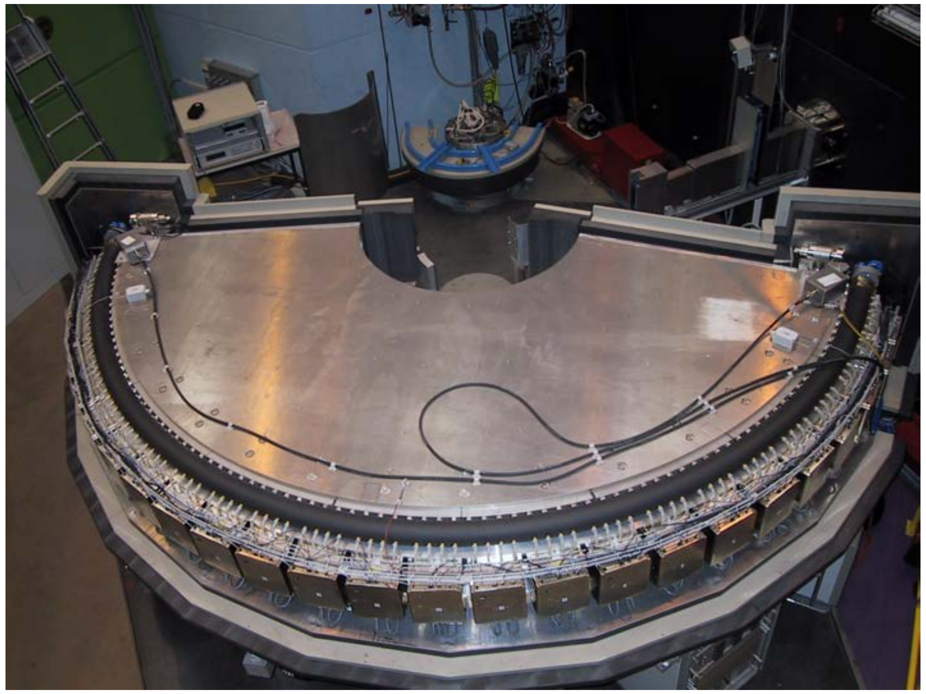

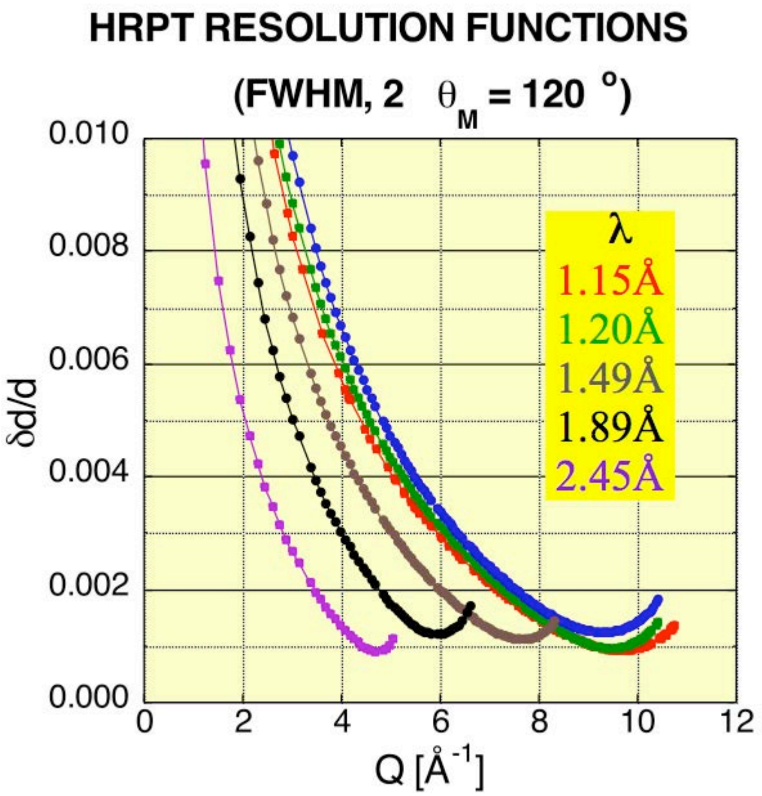

DMC - cold neutron powder diffractometer

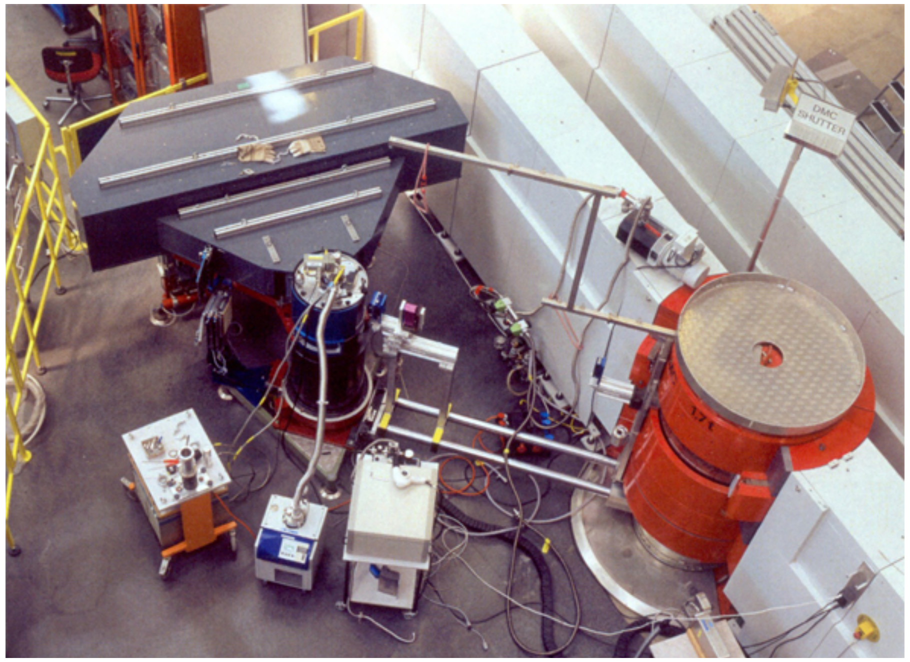

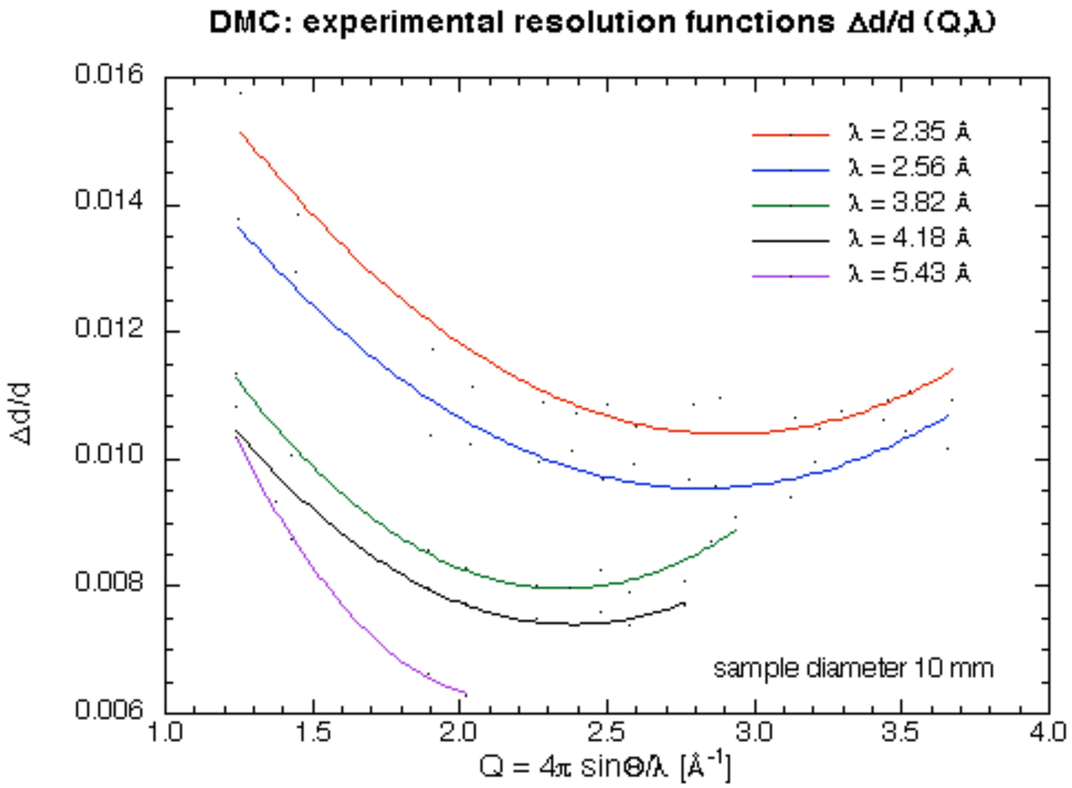

Powder ND at SINQ/PSI

HRPT - High Resolution Powder Diffractometer for Thermal Neutrons at SINQ

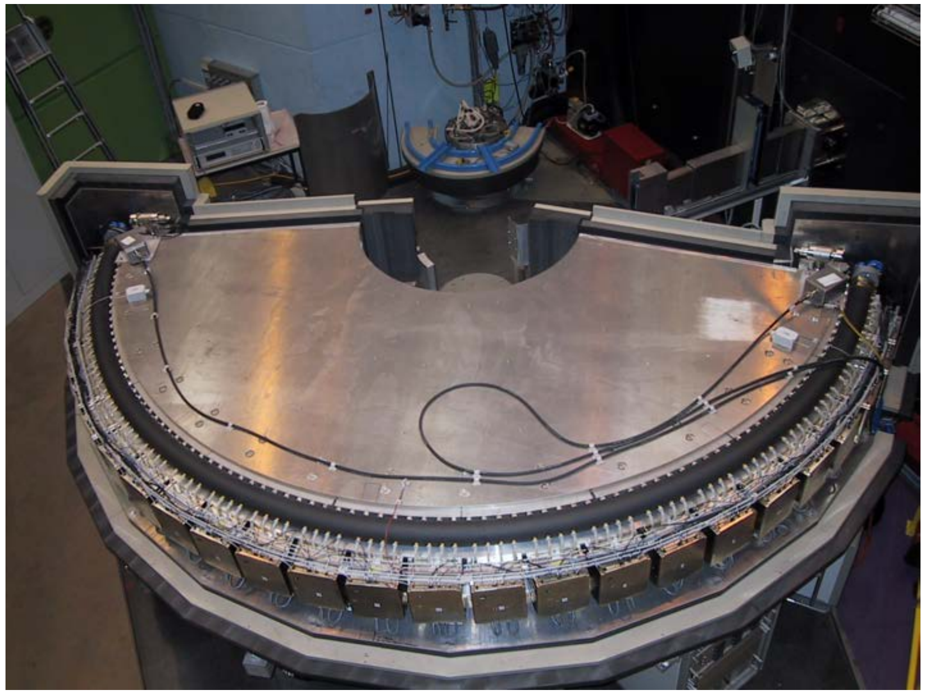

DMC - cold neutron powder diffractometer

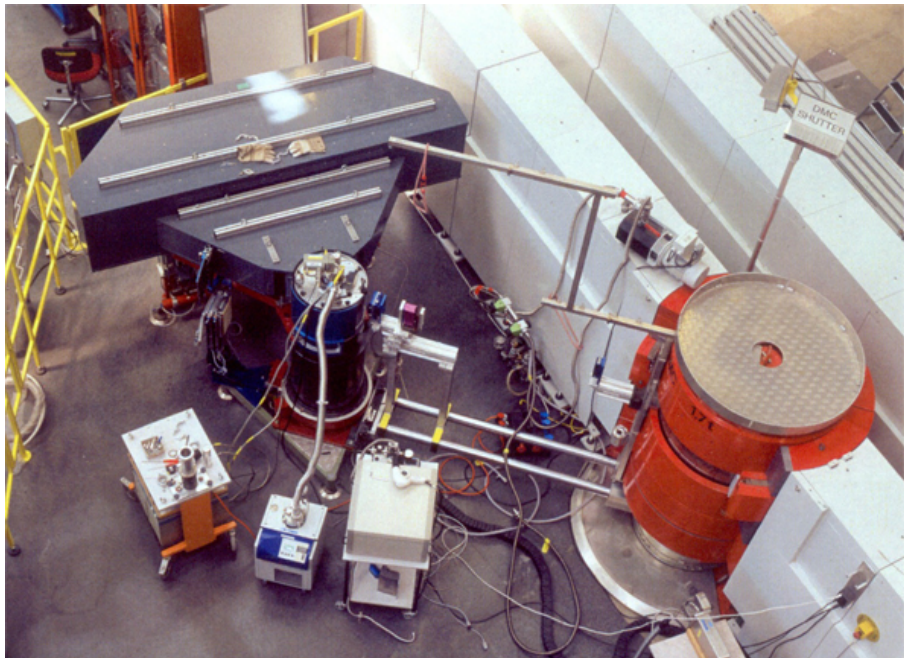

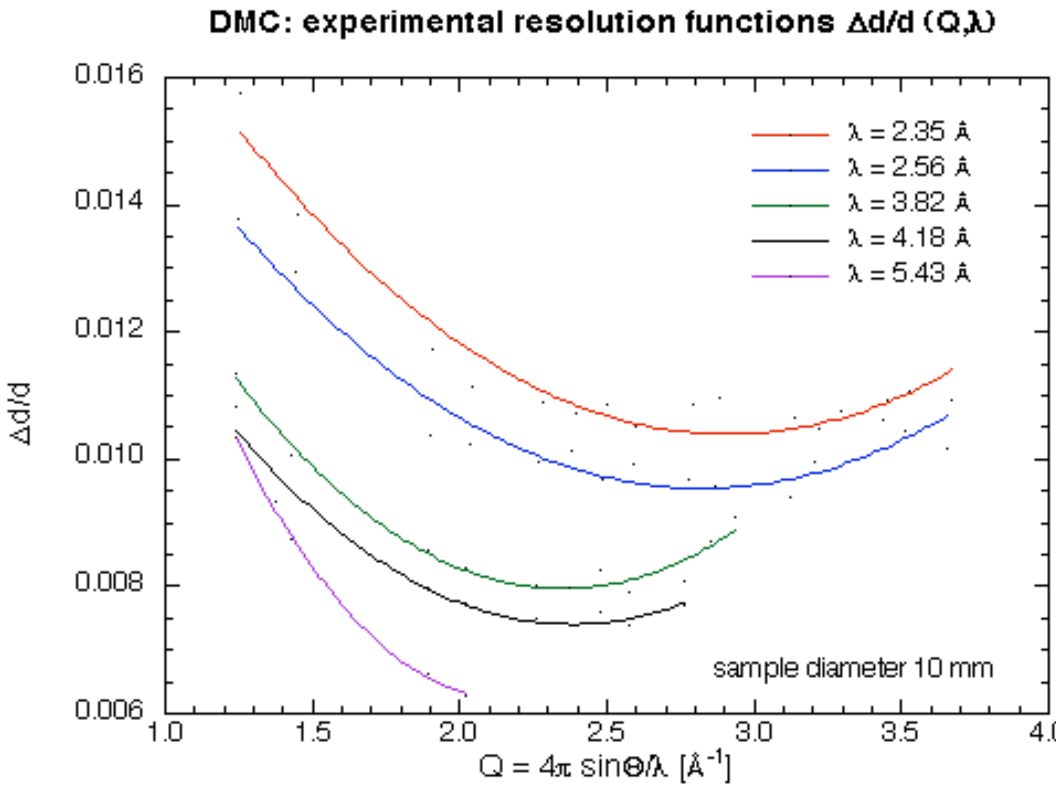

Powder ND at SINQ/PSI

HRPT - High ... **Diffractometer for** ... **powder diffractometer**

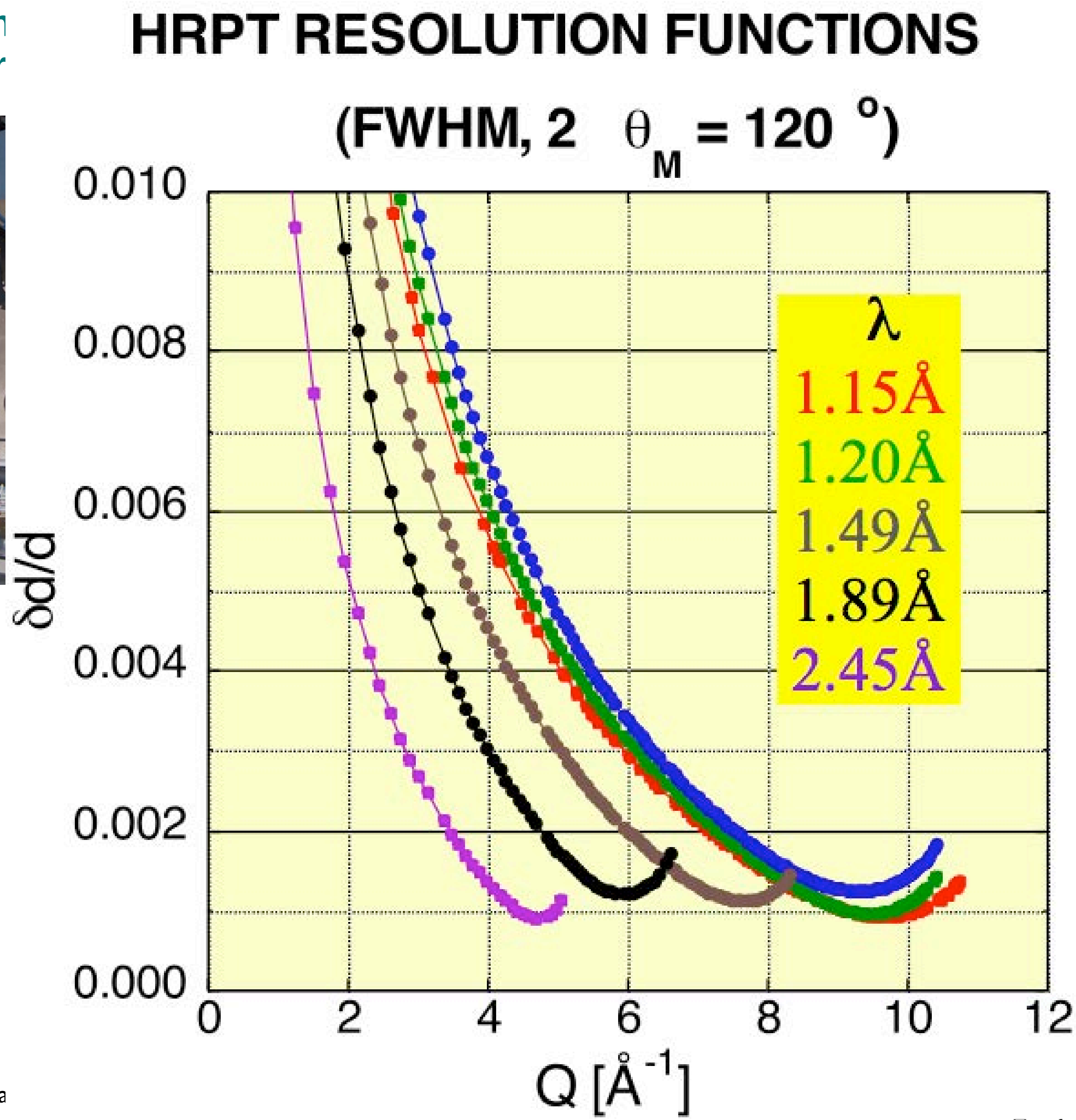

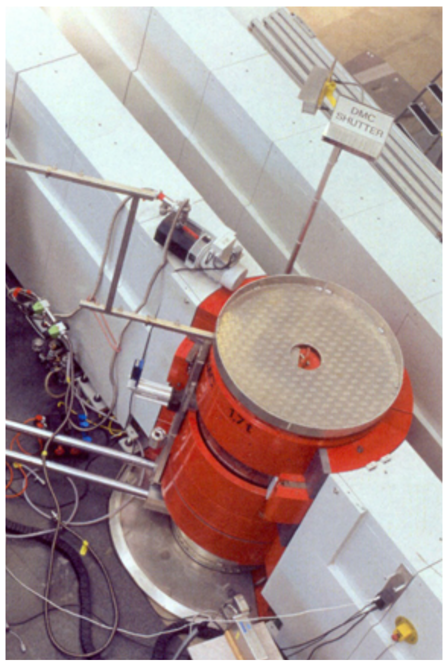

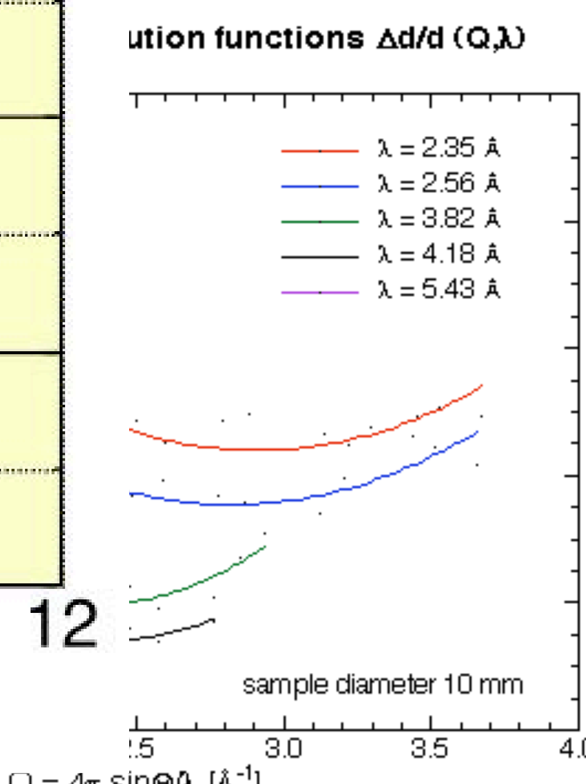

PSI information da

Example of HRPT diffraction pattern

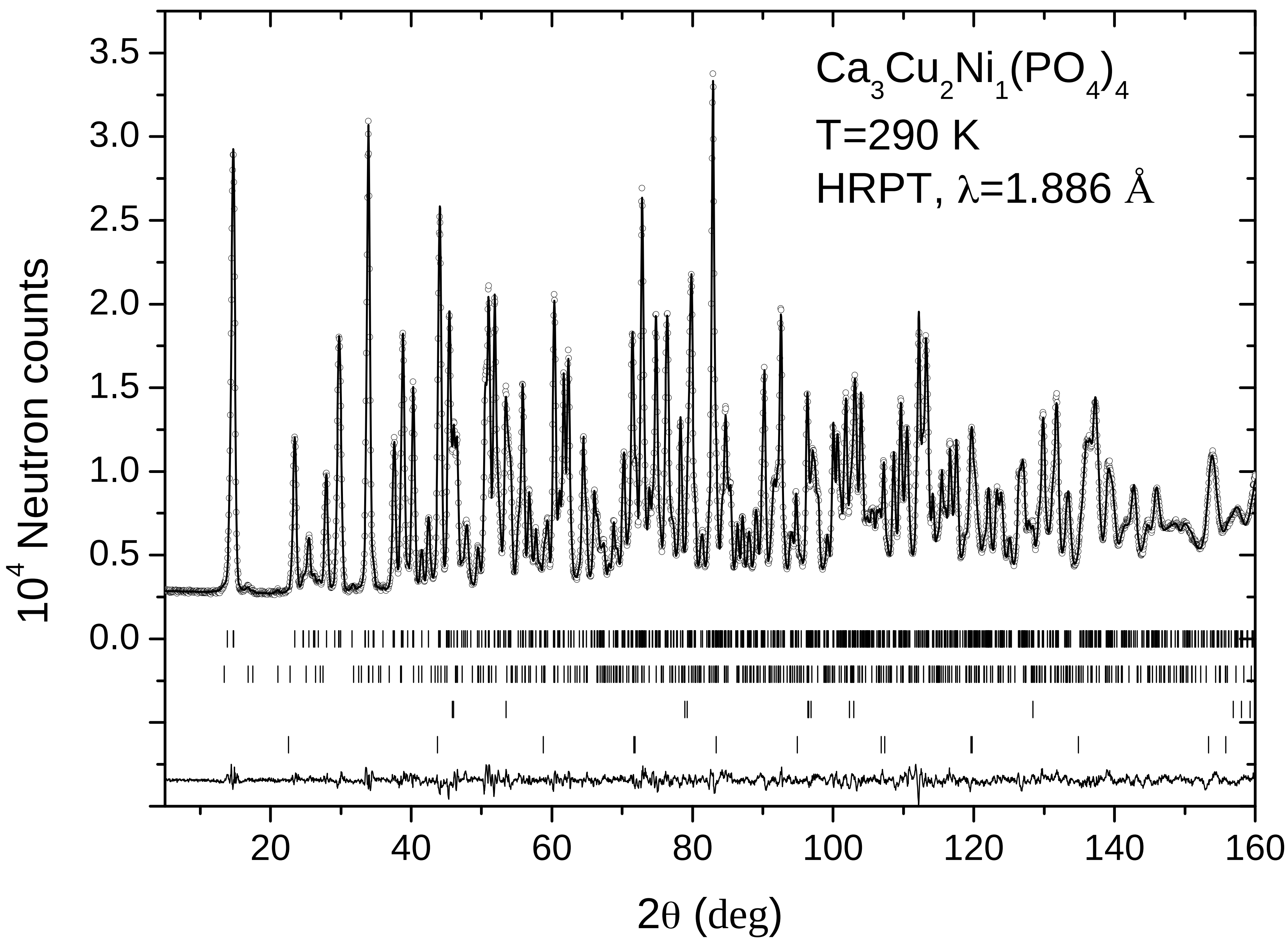

Powder ND at SINQ/PSI

HRPT - High Resolution Powder Diffractometer for Thermal Neutrons at SINQ

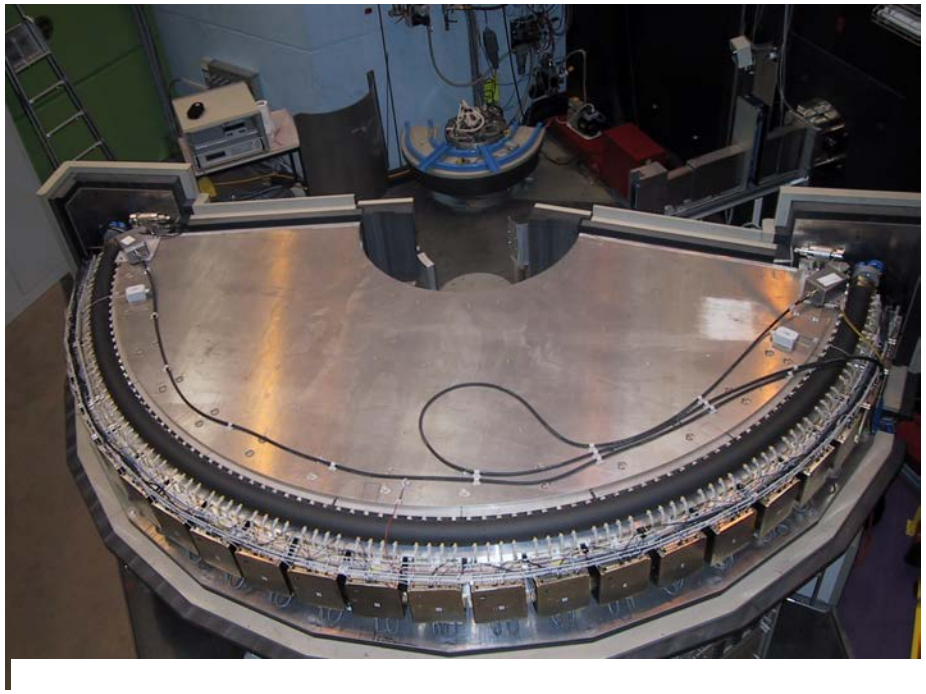

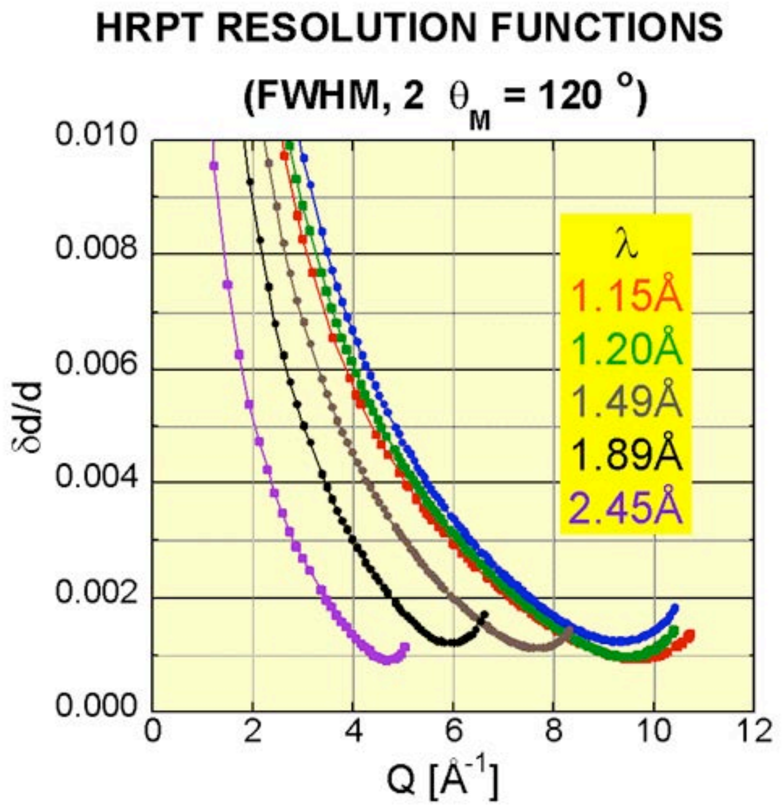

DMC - cold neutron powder diffractometer

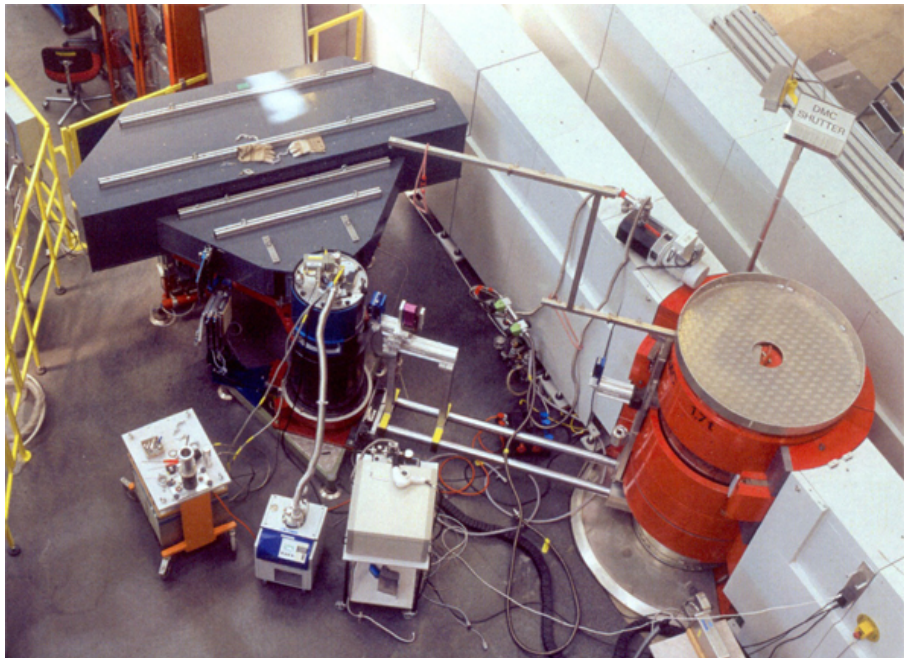

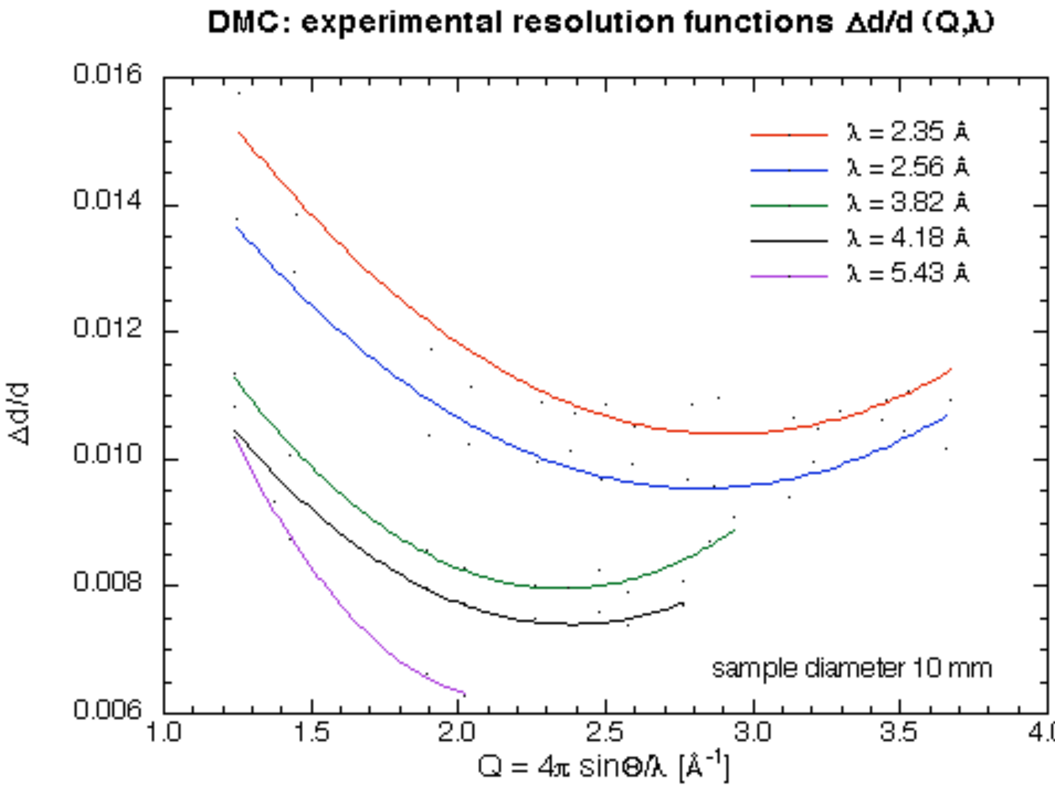

Powder ND at SINQ/PSI

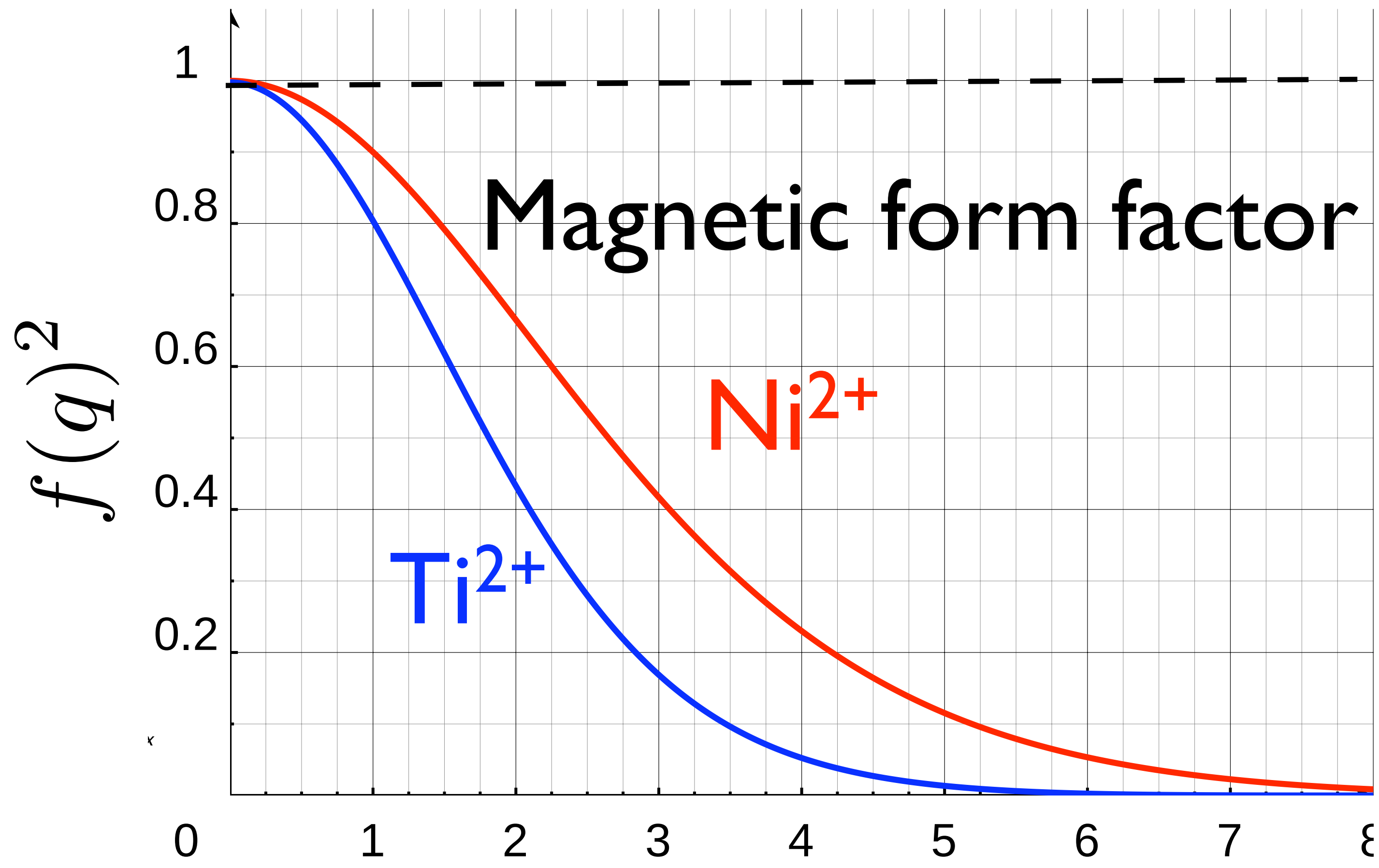

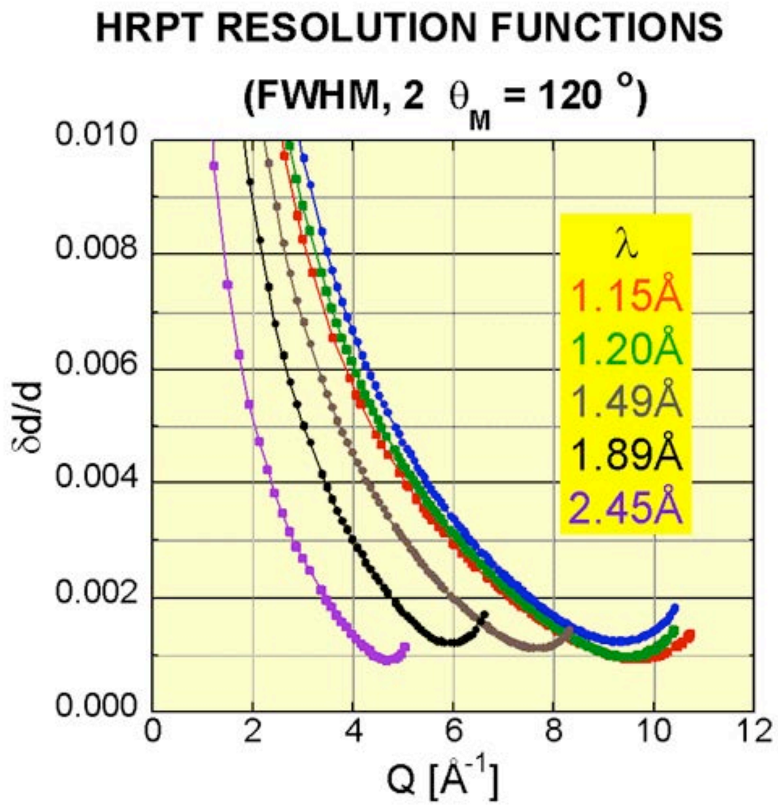

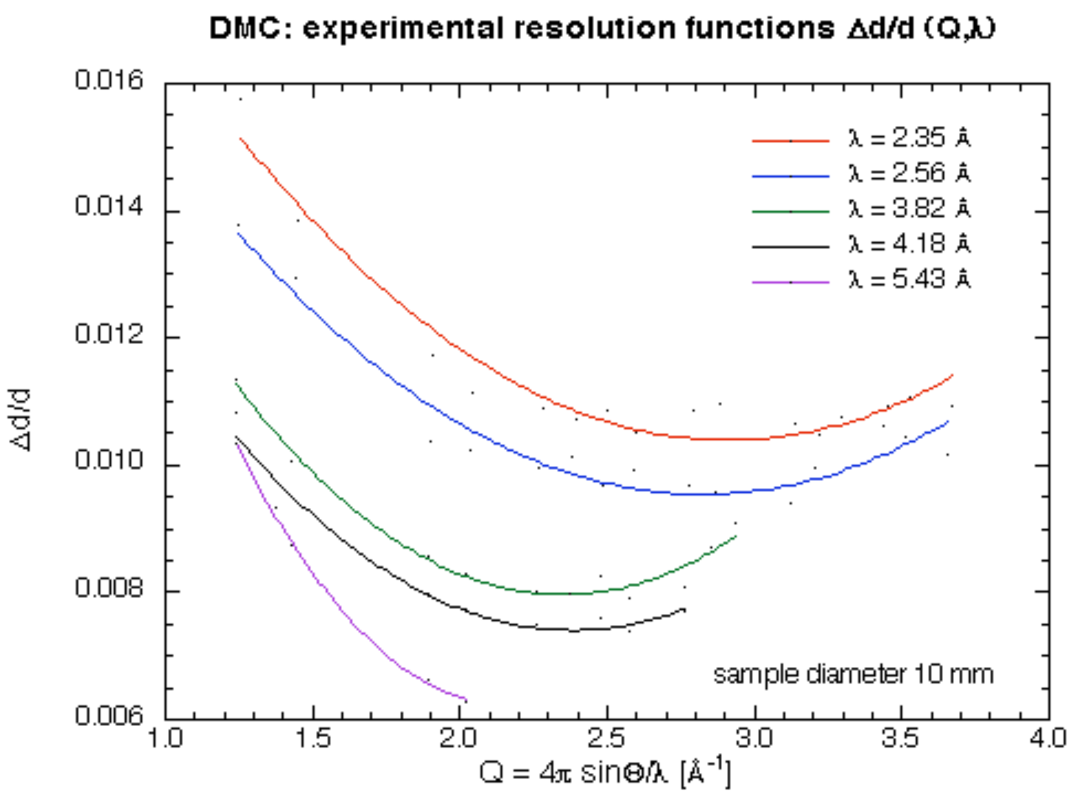

cf. resolution/q-range

HRPT 1.9Å

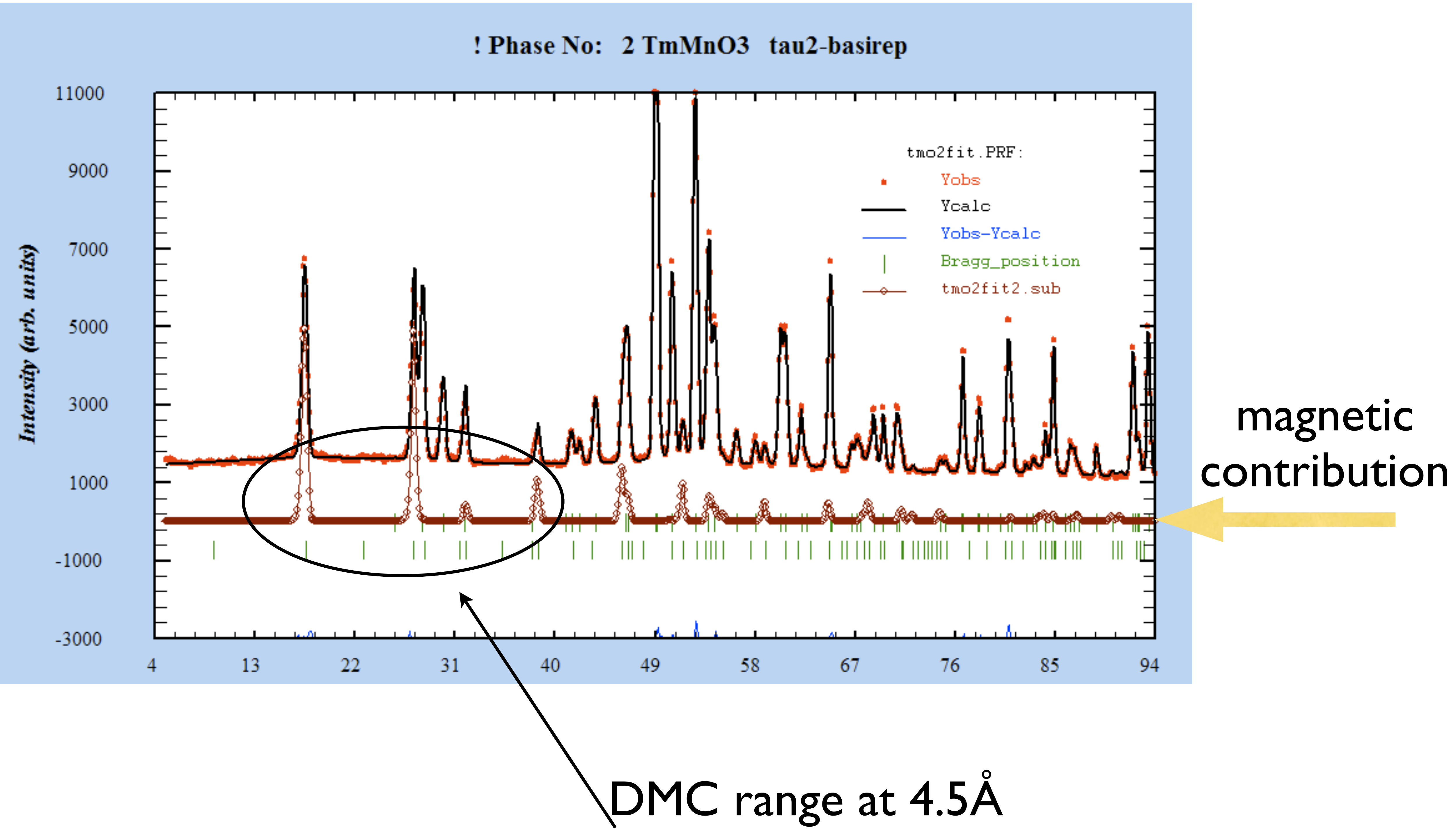

Cf. resolution/q-range

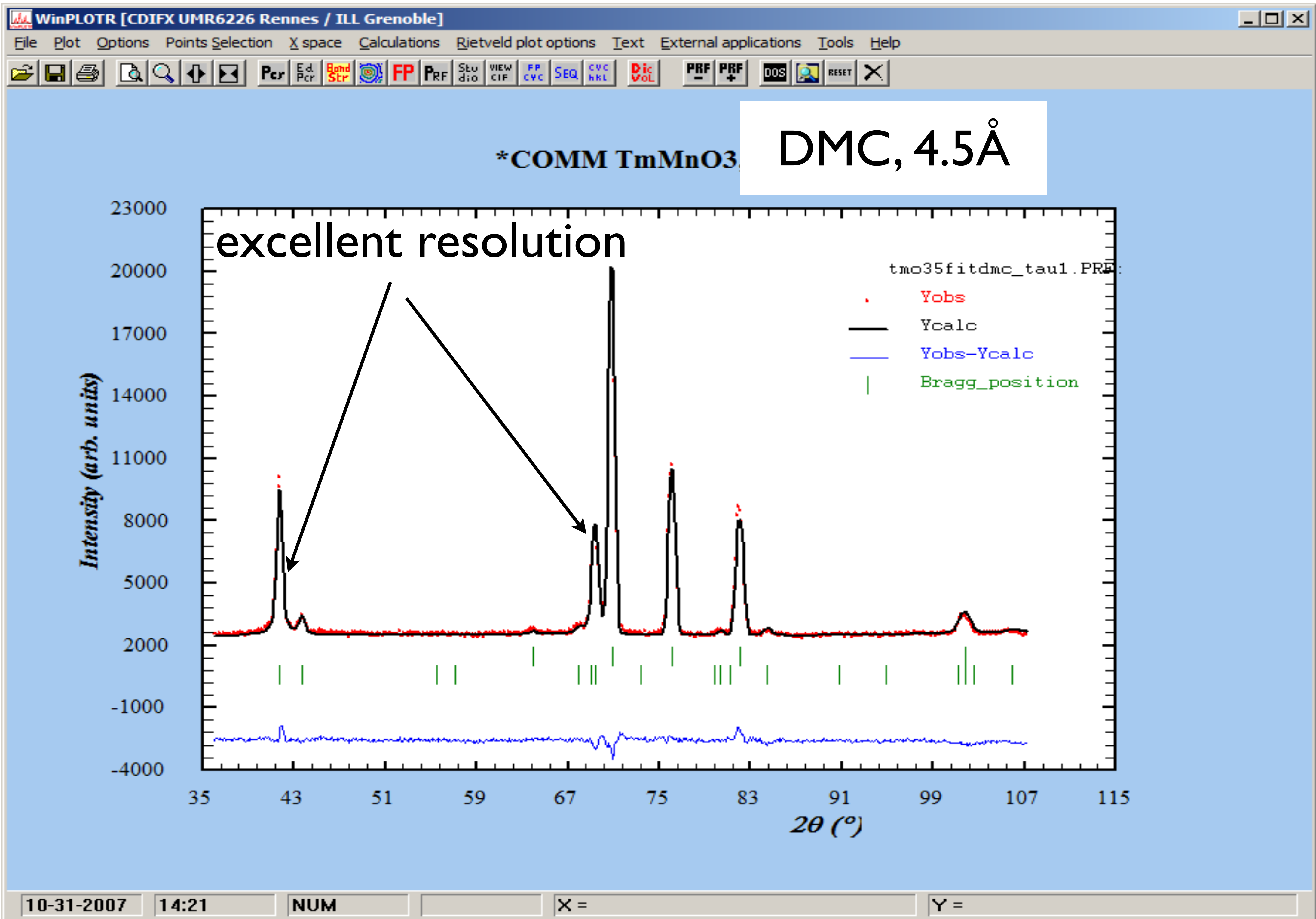

SINQ hall

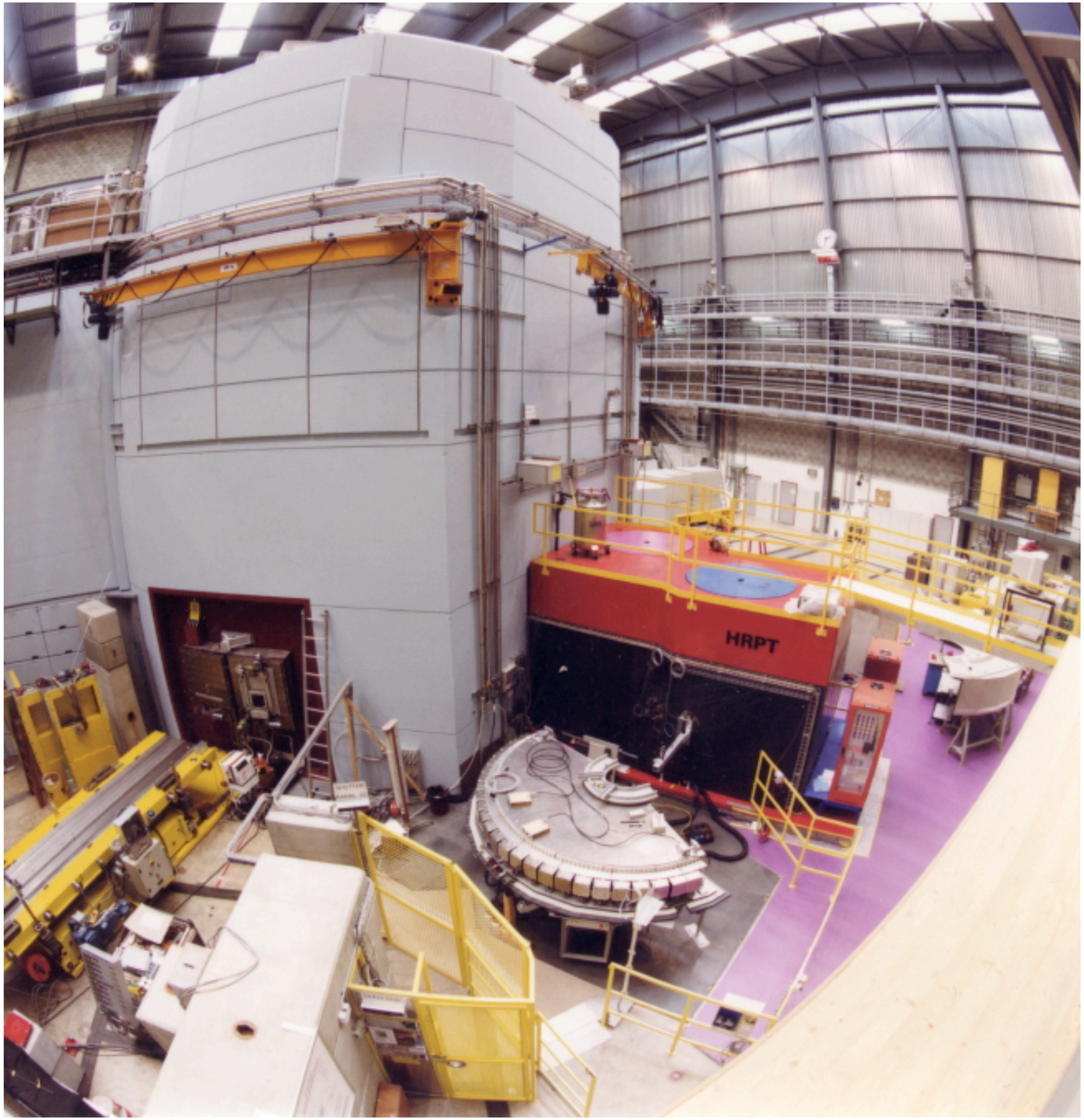

Instrument view at SINQ taget station

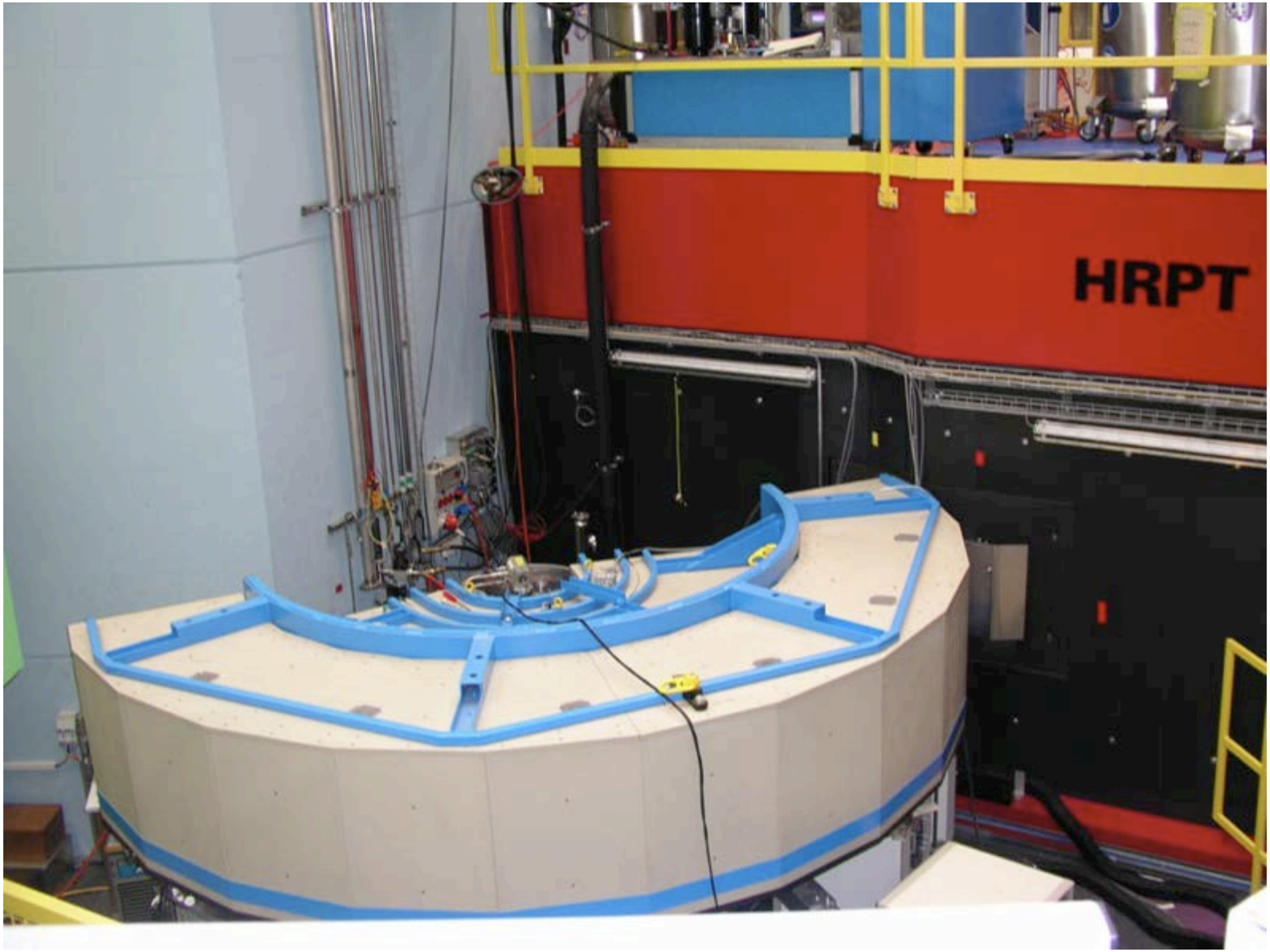

Instrument view at SINQ taget station

Instrument view at SINQ taget station

Instrument view at SINQ taget station

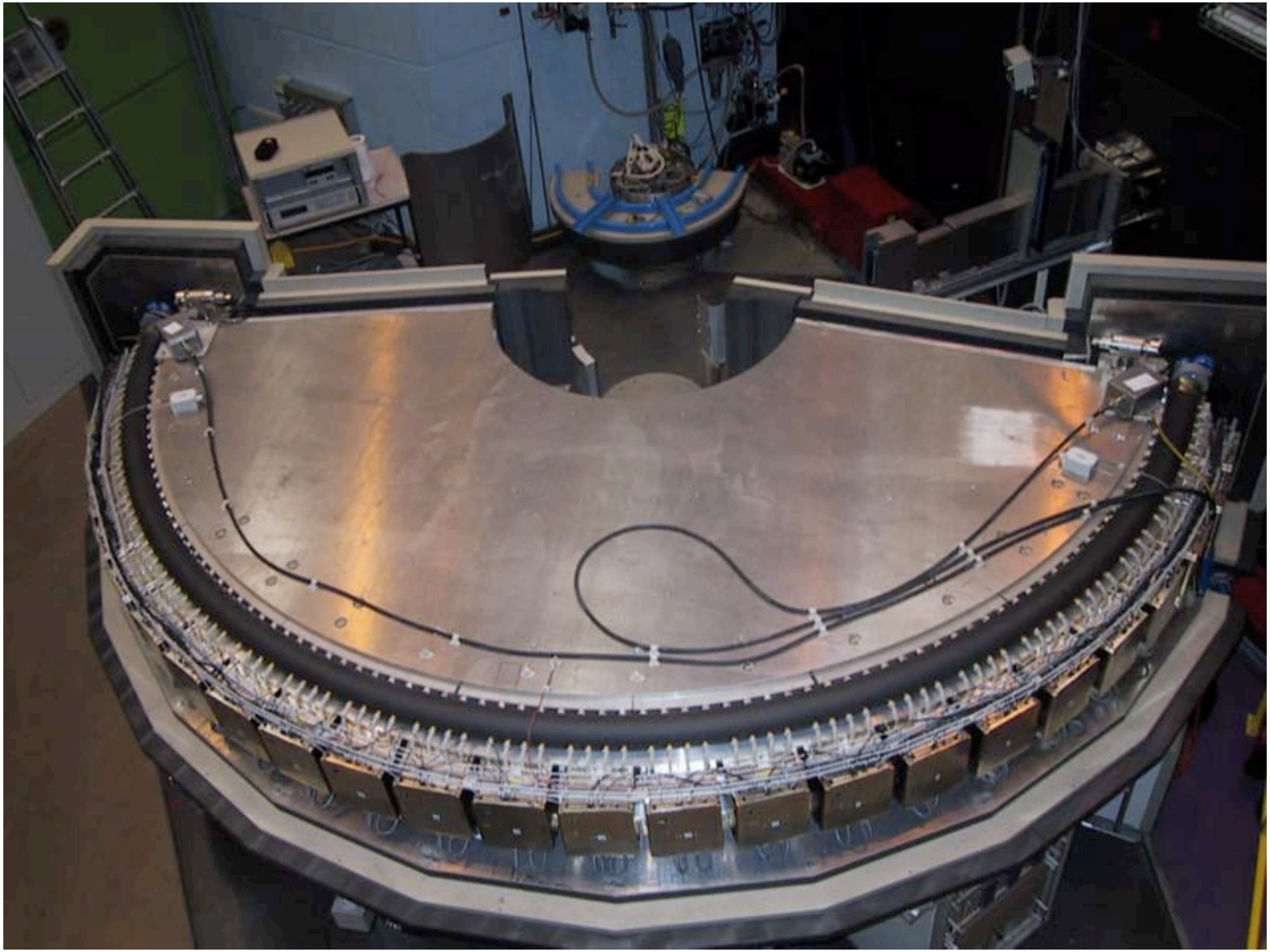

SINQ hall

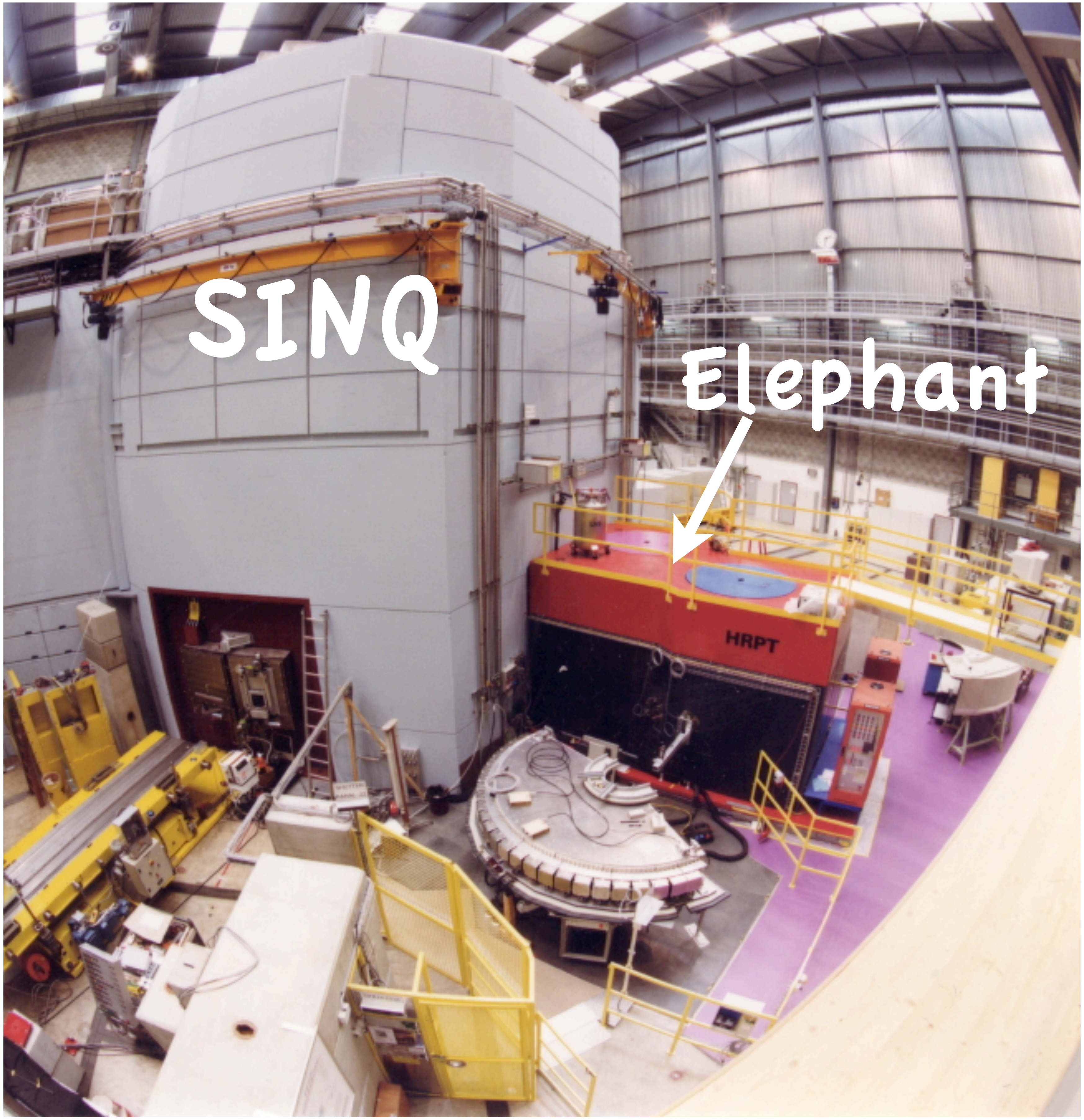

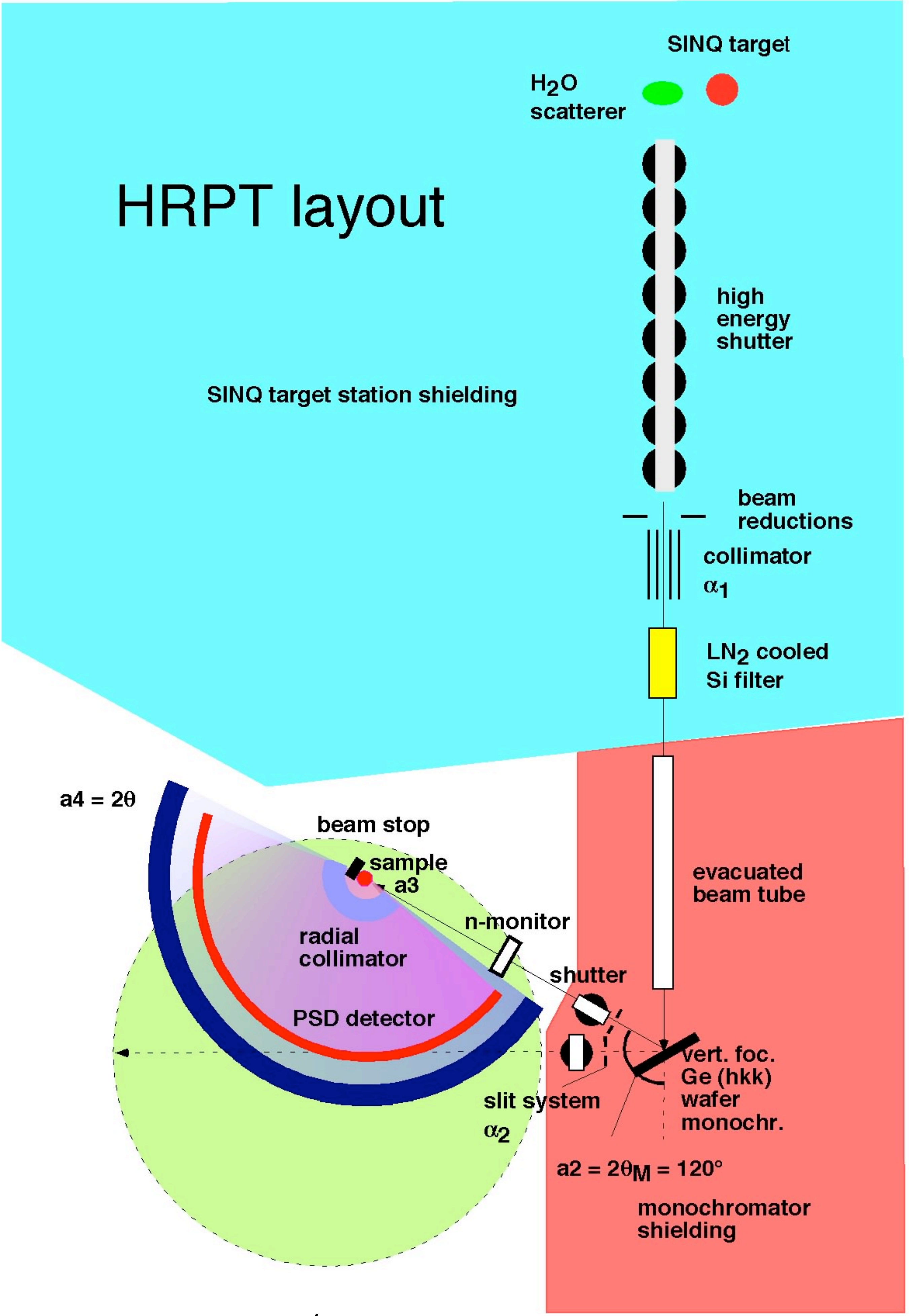

HRPT layout
SINQ target
H_2O scatterer
high energy shutter
SINQ target station shielding
beam reductions
collimator α_1
LN_2 cooled Si filter
evacuated beam tube
a4 = 2θ
beam stop
sample
a3
n-monitor
radial collimator
shutter
PSD detector
vert. foc. Ge (hkk) wafer monochr.
slit system α_2
a2 = $2\theta_M$ = 120°
monochromator shielding

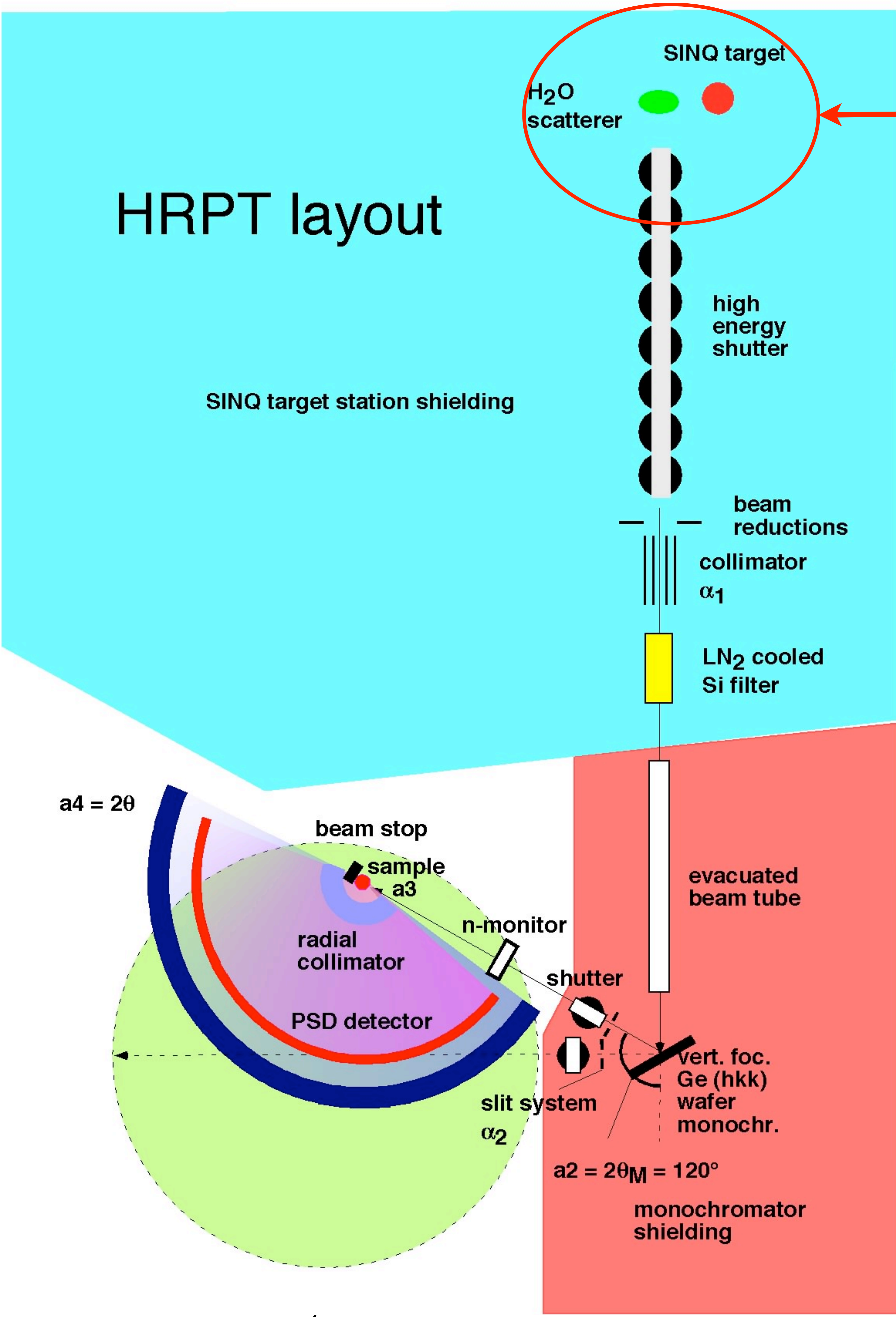

neutron flux from the moderator

Neutron flux from the D_2O moderator at NEUTRA (white beam)

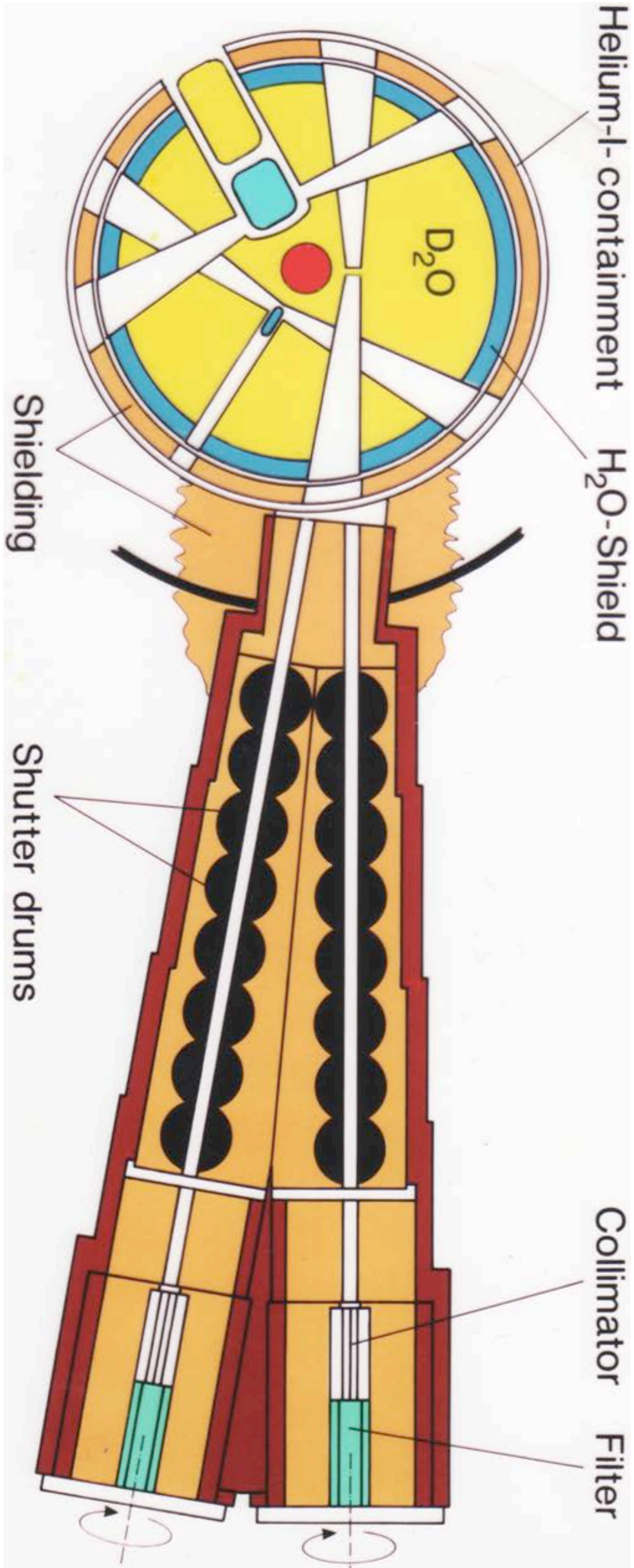

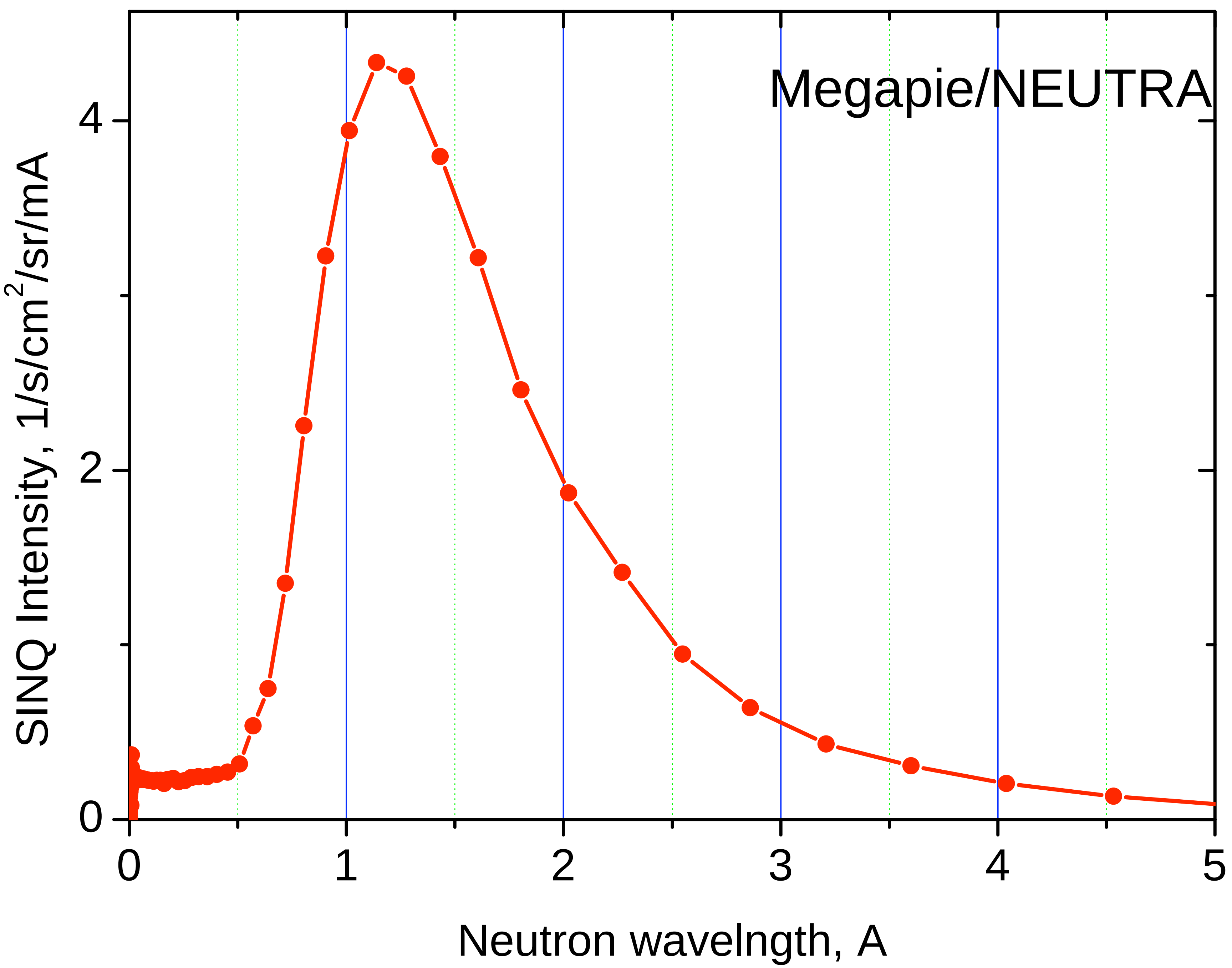

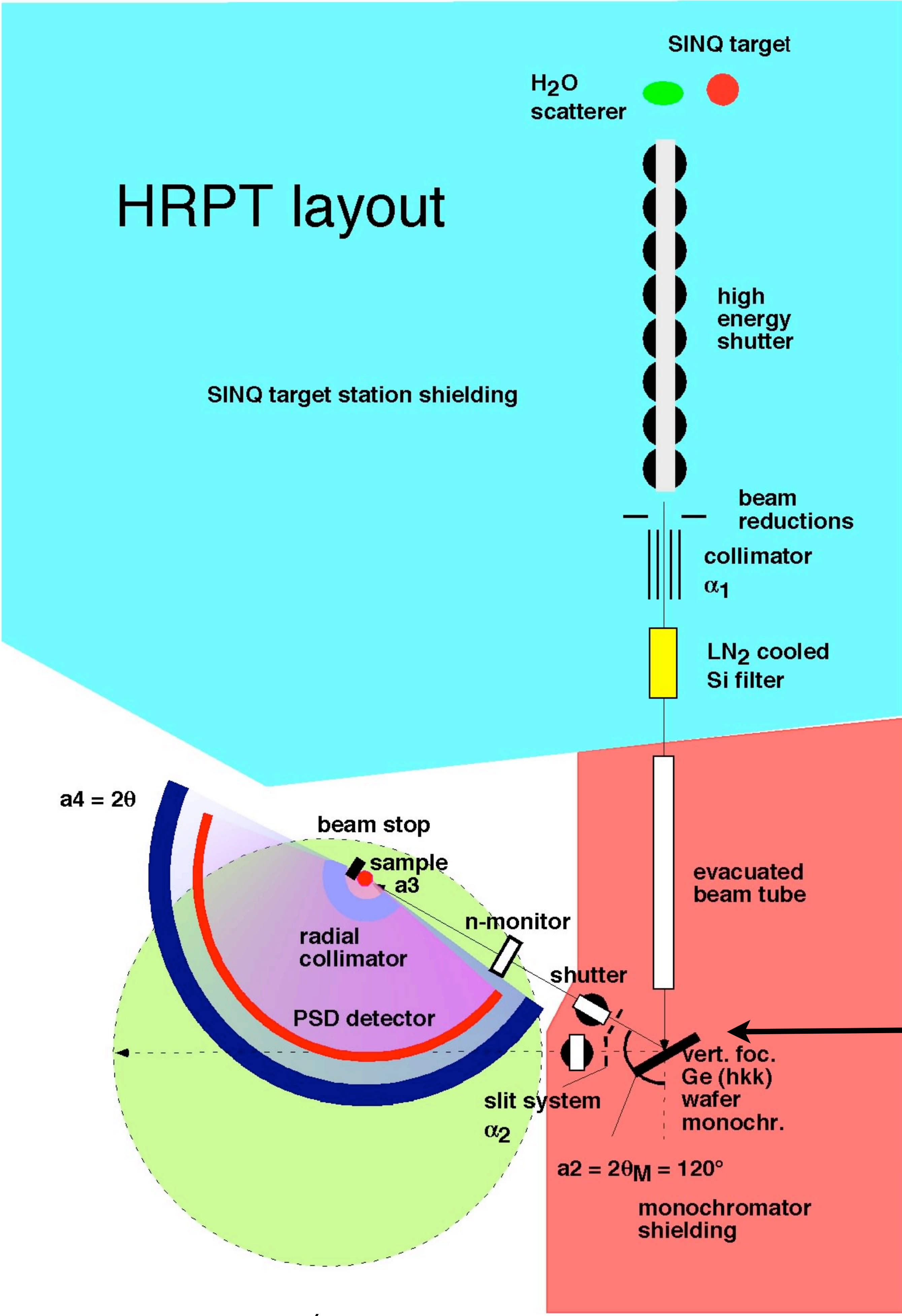

neutron monochromator
fixed 120 take off angle

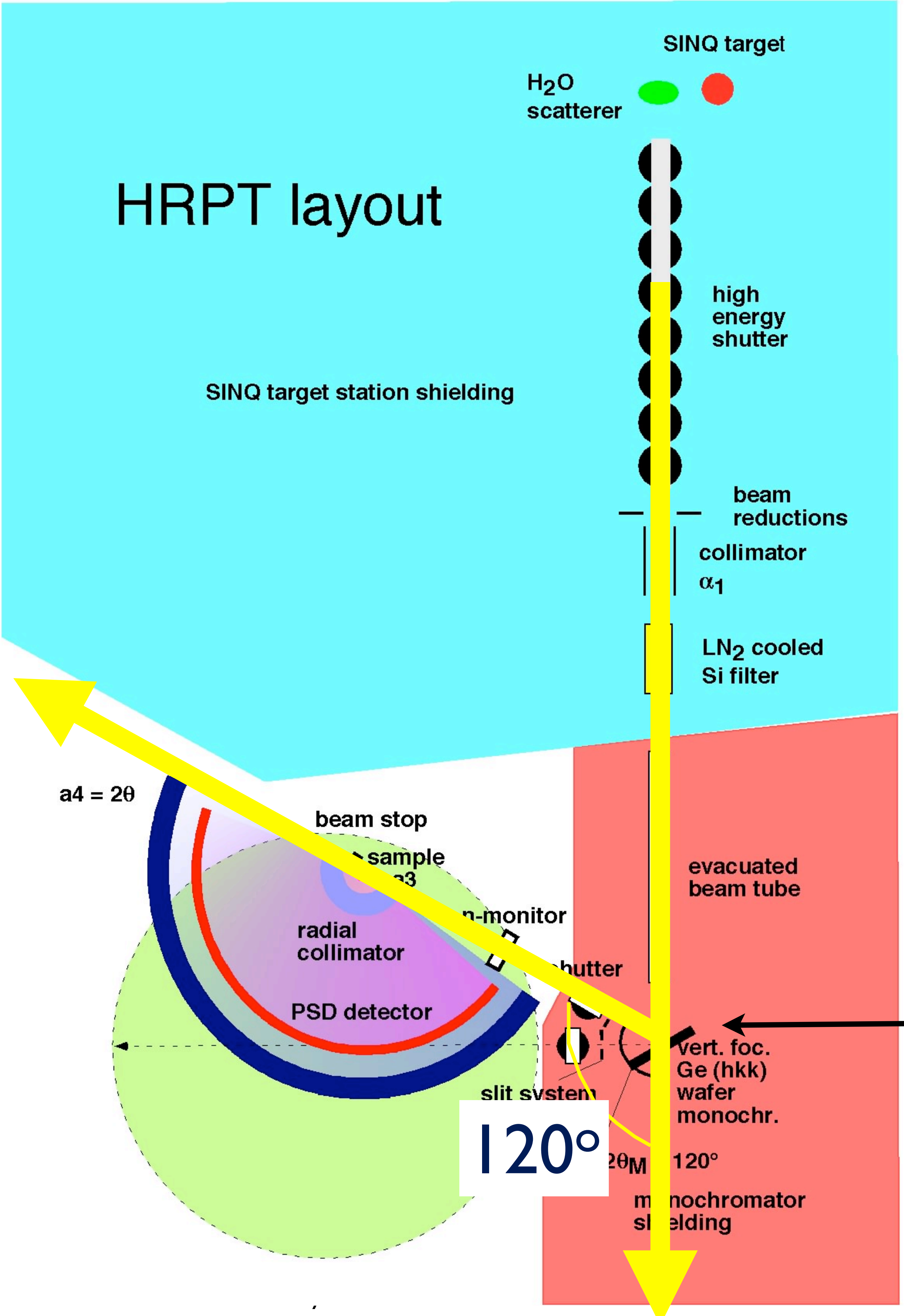

neutron monochromator
fixed 120 take off angle

Ge hkk focusing monochromator

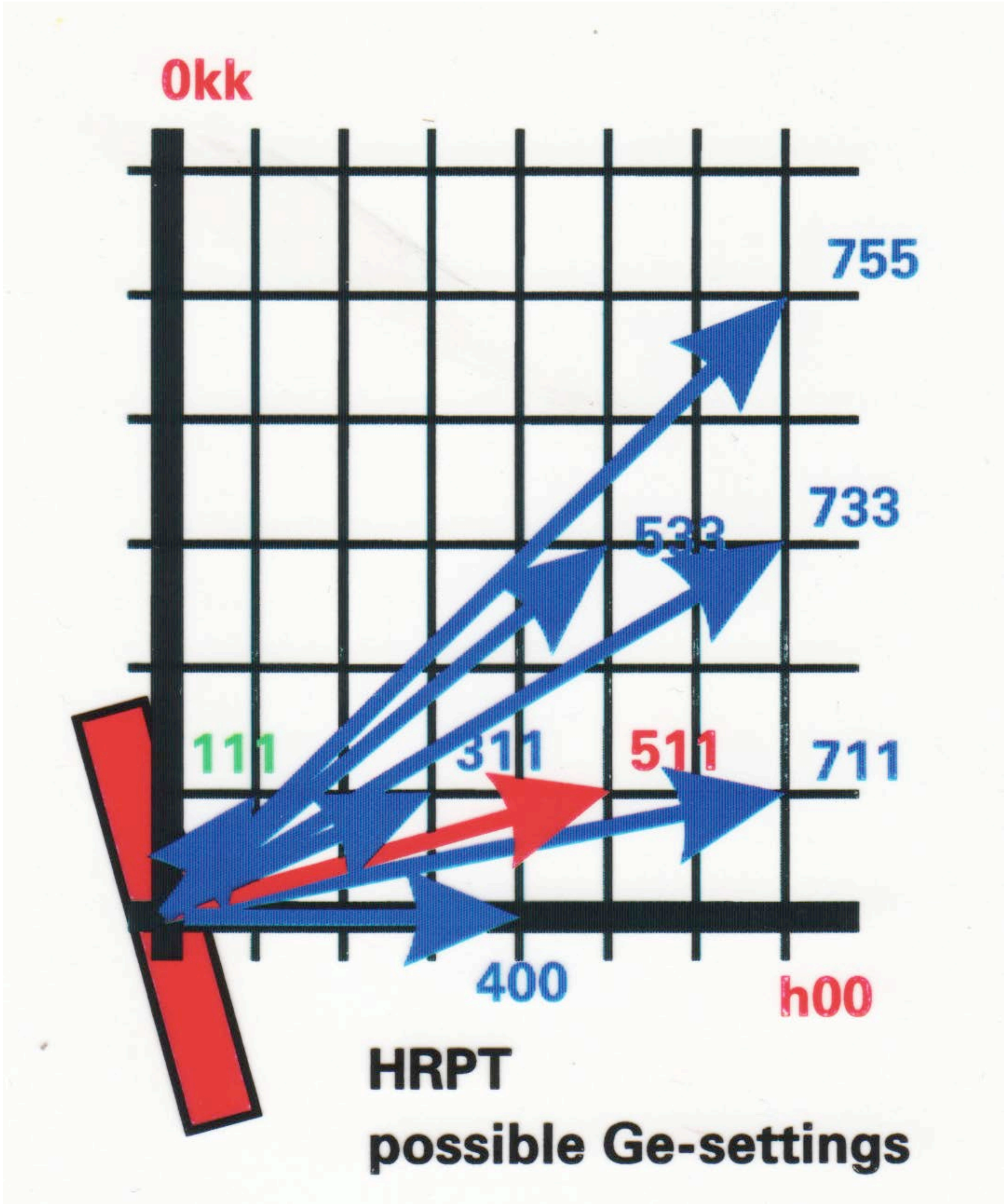

Ge hkk focusing monochromator

<u>Monochromator hight</u>: 11slabs*25=255mm
<u>Beam spot hight</u> at sample position
is smaller due to vertical focusing: 60mm
<u>Wavelength</u> is chosen by rotation along (hkk)
<u>Mosaic</u> 15’

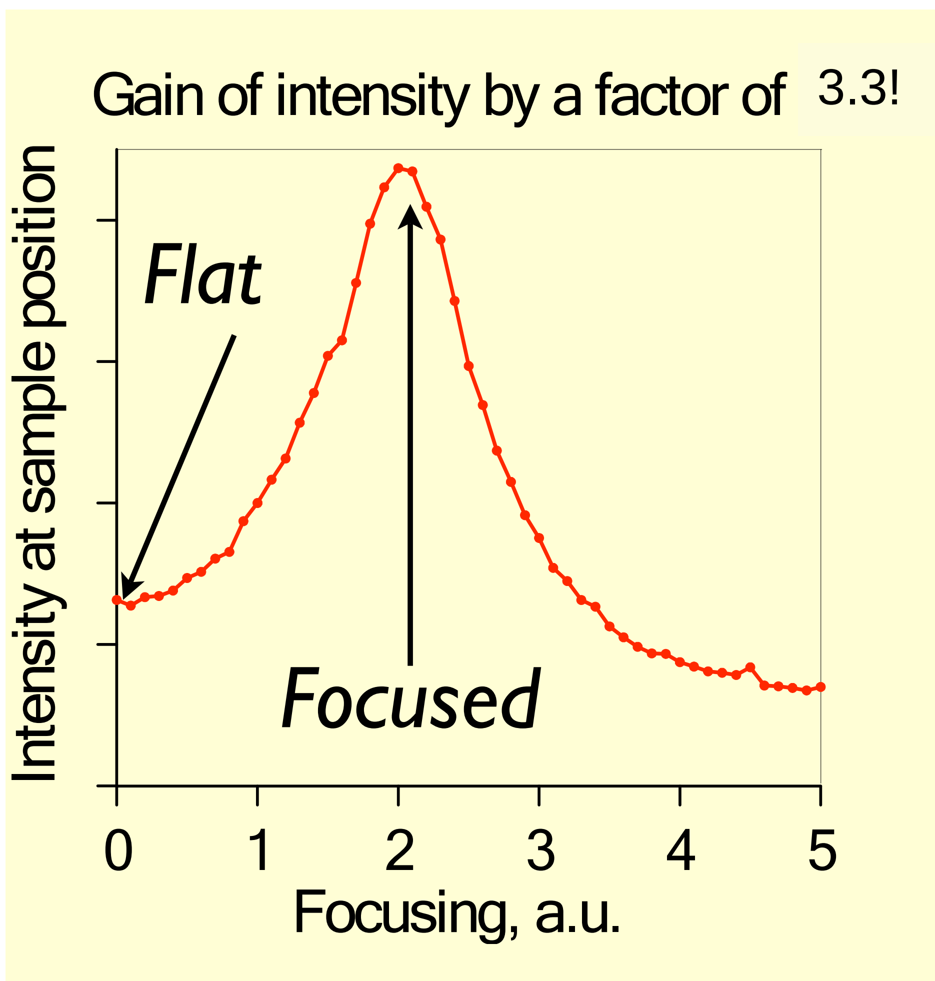

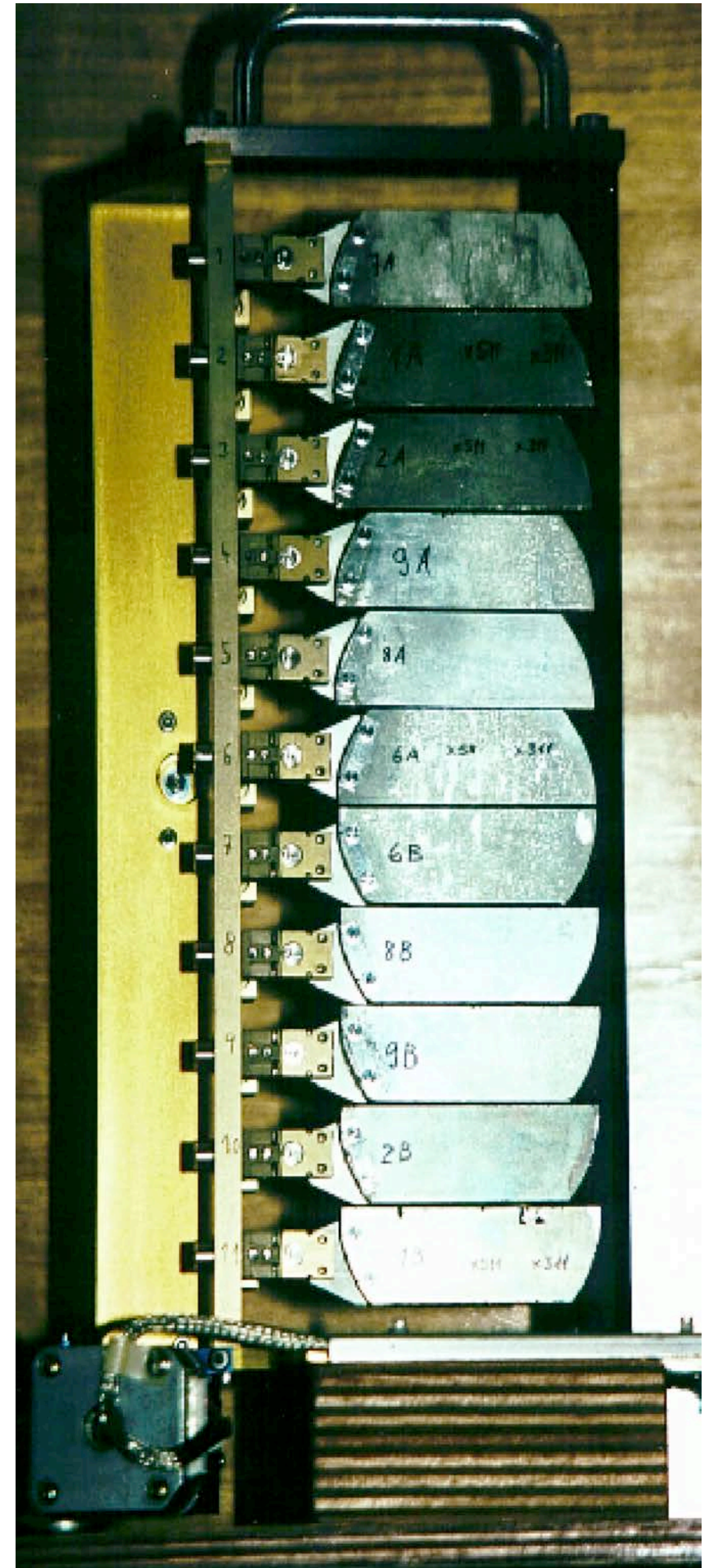

Flexible choice of wavelength, resolution/intensity

- Wavelength is selected by (hkk) plane of Ge-monochromator
- Resolution and intensity are controlled by appropriate primary/secondary collimations and take-off-angle of the monochromator (120° or 90°)

	$2\theta_M$=90°		$2\theta_M$ = 120°	
(hkk) Ge	λ, Å	Effective intensity	λ, Å	Effective intensity
311	2.40971	0.64	2.9536	~0.16
400	1.9984[4,5]		2.449[1,3]	0.19
133	1.8324	1.00	2.246[1,2]	
511	1.5384	1.55	1.886	1.0
533	1.2183	0.83	1.494	0.90
711	1.1194	0.60	1.372	0.71
733	0.9763	0.34	1.197	0.63
822	0.9419	0.48	1.154	0.79
466			1.044	0.27

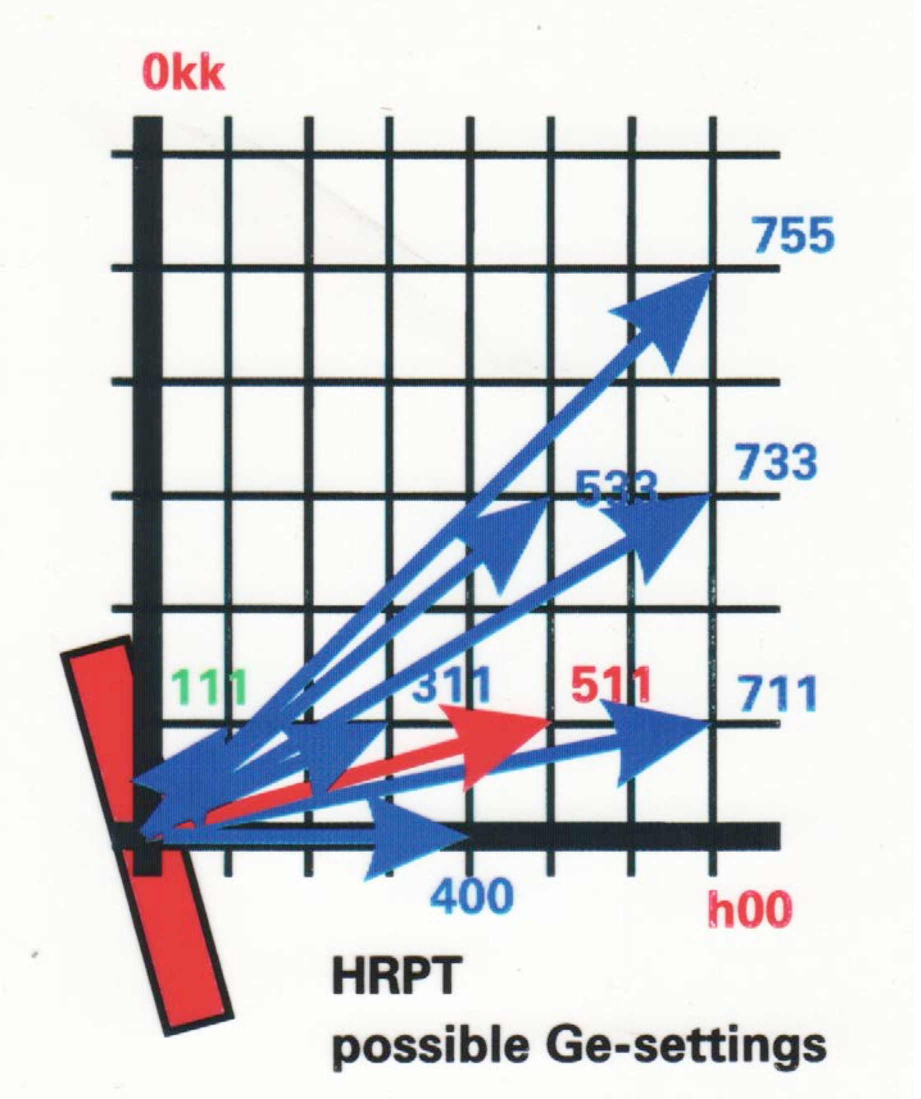

HRPT resolution
horizontal angular divergence control

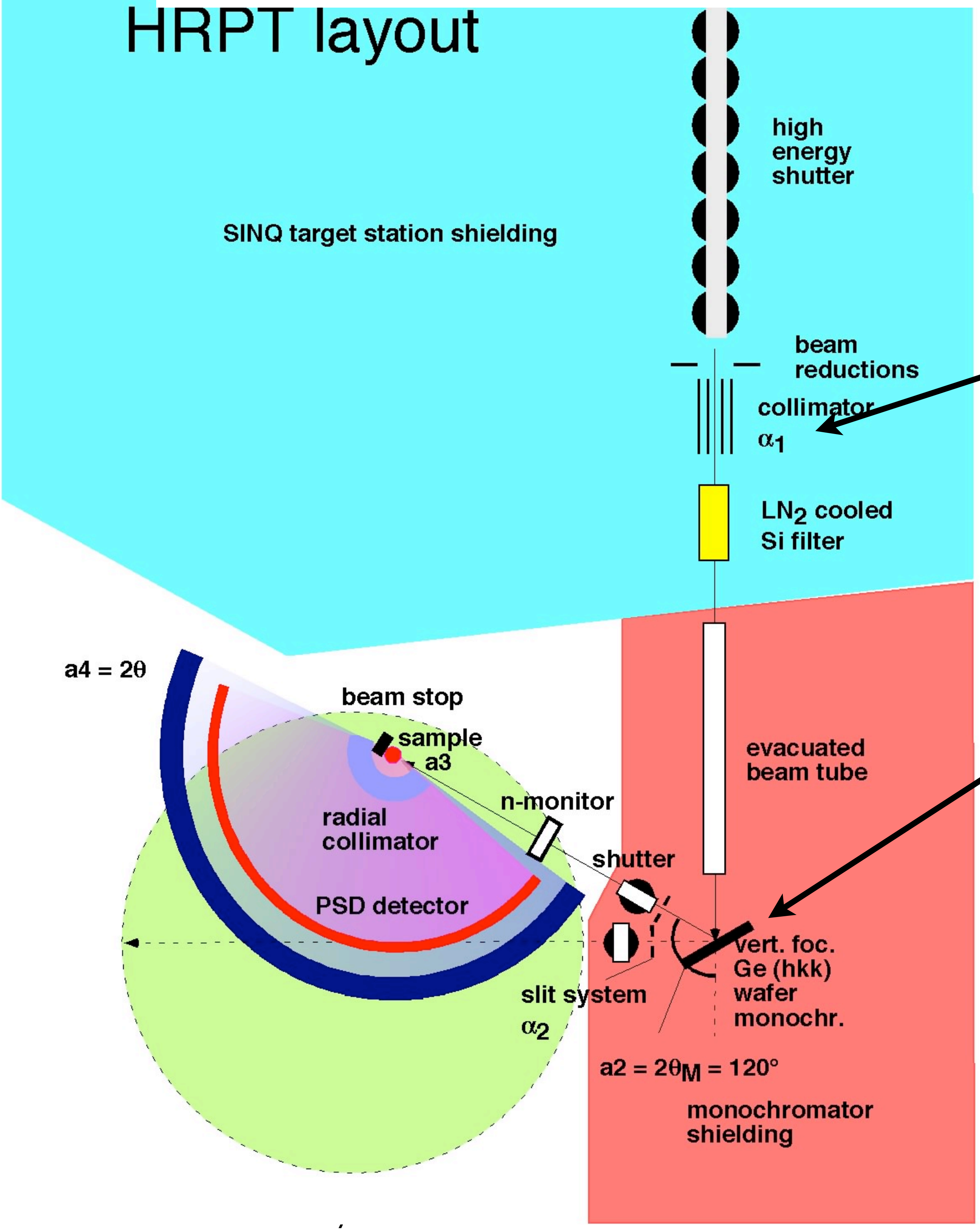

α_1

primary beam collimator(s):
6', 12', 24', 30'

α_2

mosaic spread of the monochromator 15'

α_3

slit system for
monochromatic beam
and
sample diameter

Resolution calibration

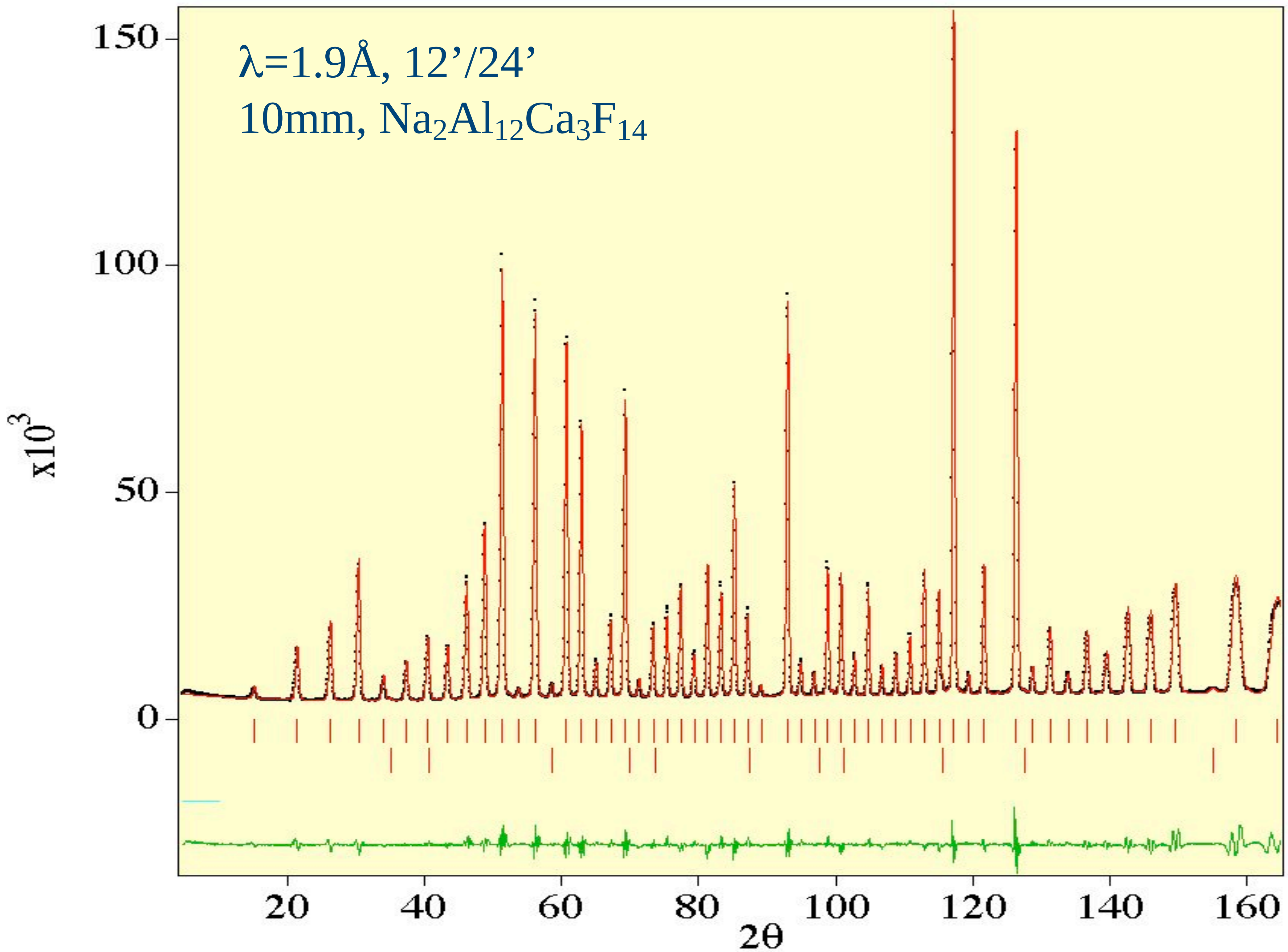

Resolution and intensity (2)

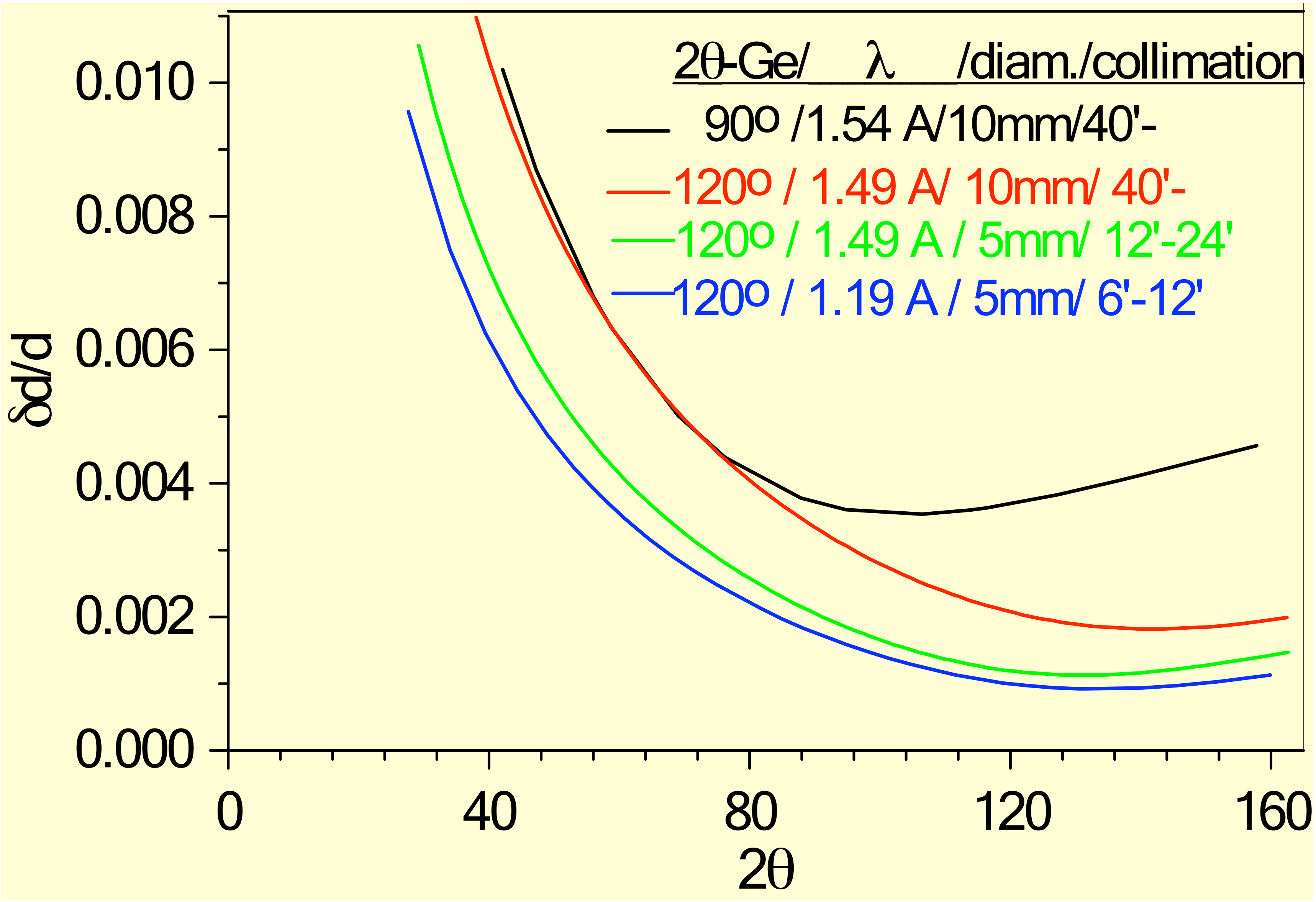

Comparison of resolution functions for different primary-secondary collimations. Typical modes are HI:40'-, MR:12'-24', HR:6'-12'. Counting rates are decreased by a factor of ~3 and ~(8-10) for MR and HR, respectively.

Detector

- ^{3}He (3.6 bar) + CF_4 (1.1 bar), effective detection length 3.5 cm, 15 cm hight
- Volume 100L, Voltage -6.7kV
- Efficiency 80% @ 1.5 Å
- 1600 wires with angular separation 0.1° (2.6 mm), 1500 mm to sample

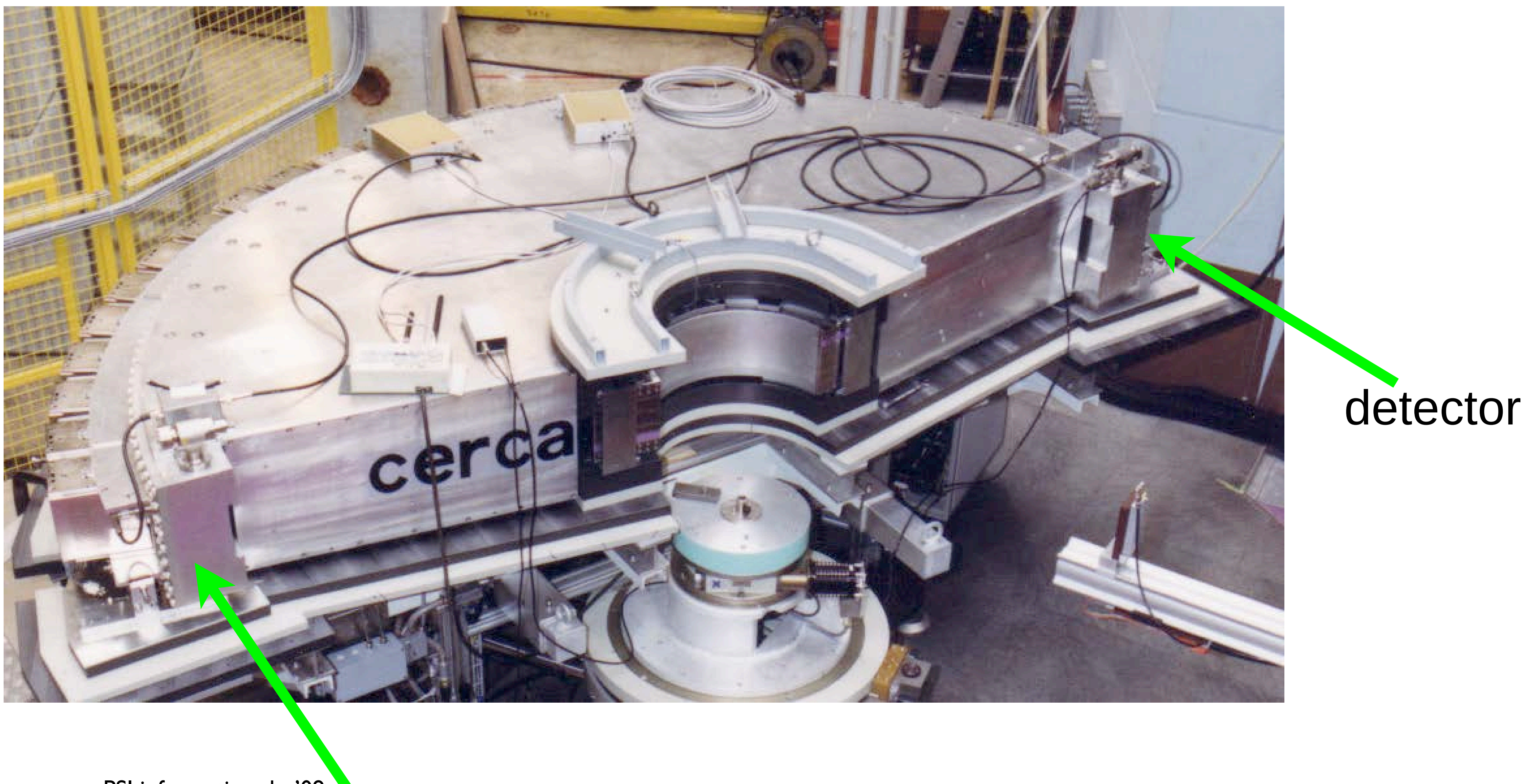

Detector chamber. 1600 wires

1600 wires with angular separation 0.1^o (2.6mm)

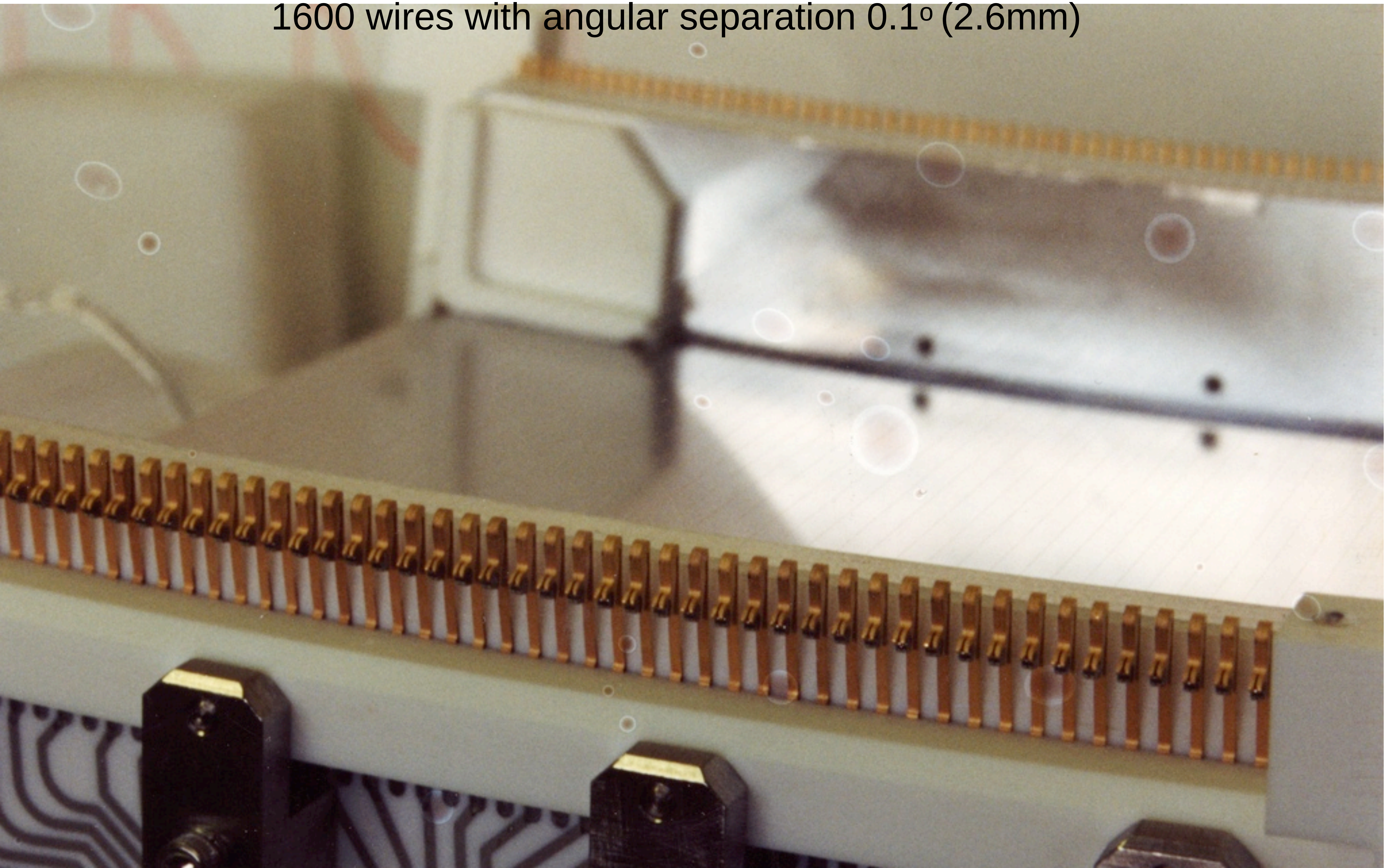

Oscillating radial collimator to avoid scattering from sample environment.

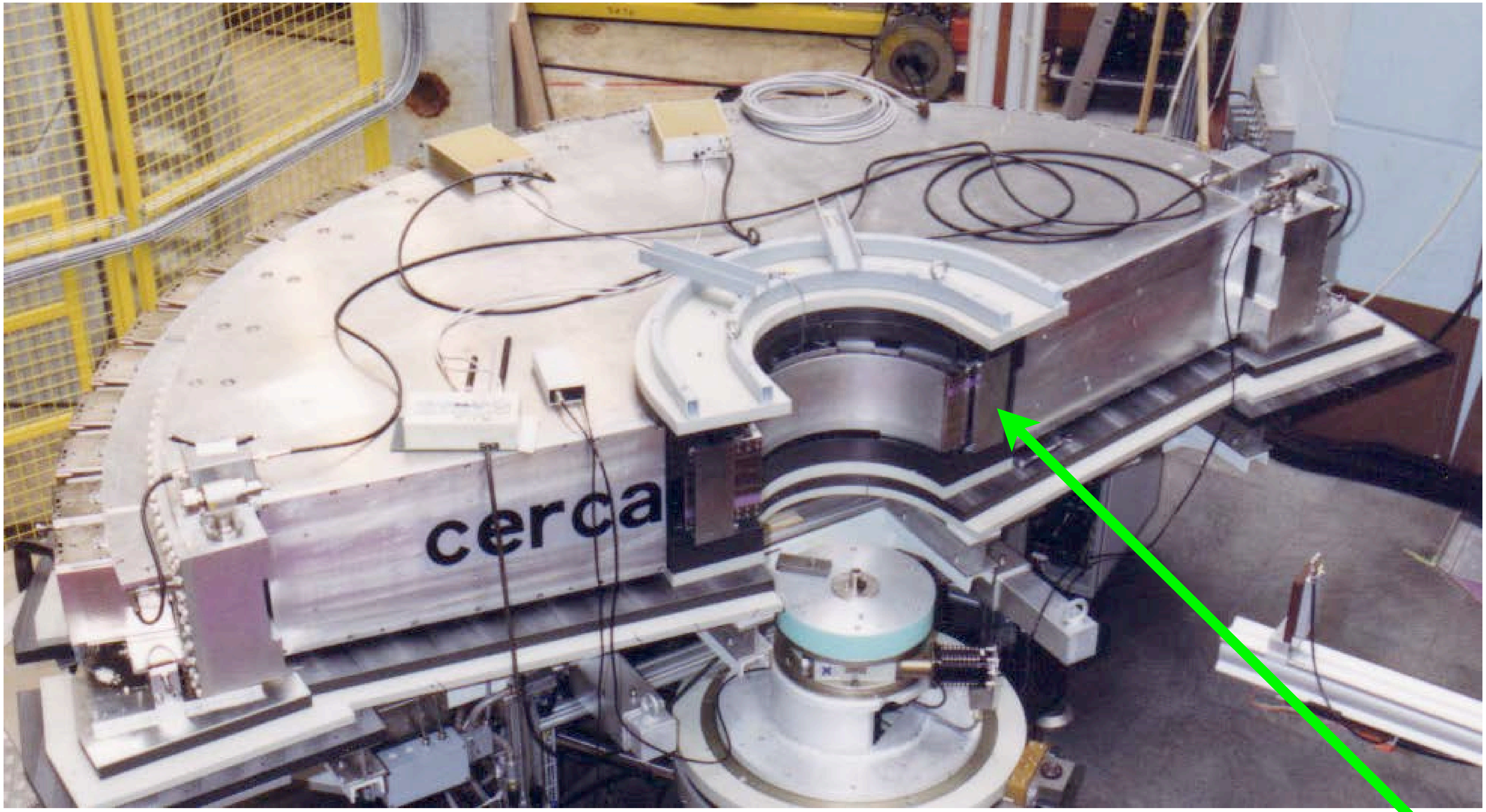

radial
collimator

HRPT radial collimators

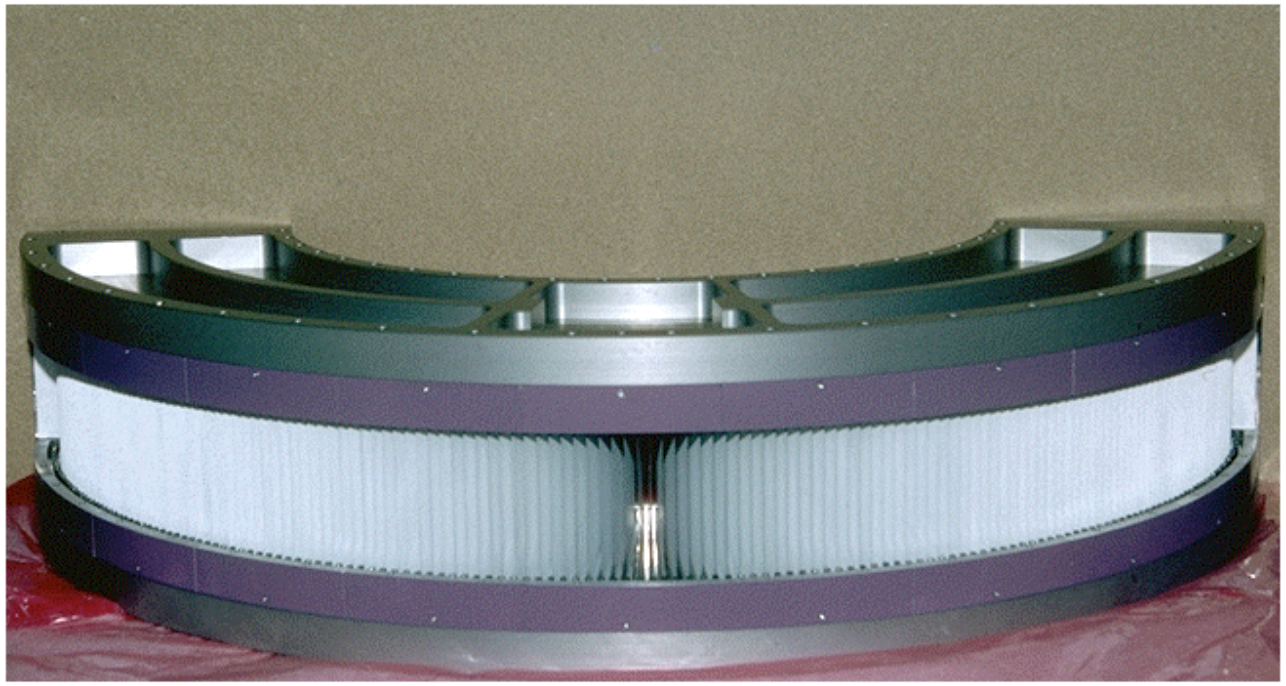

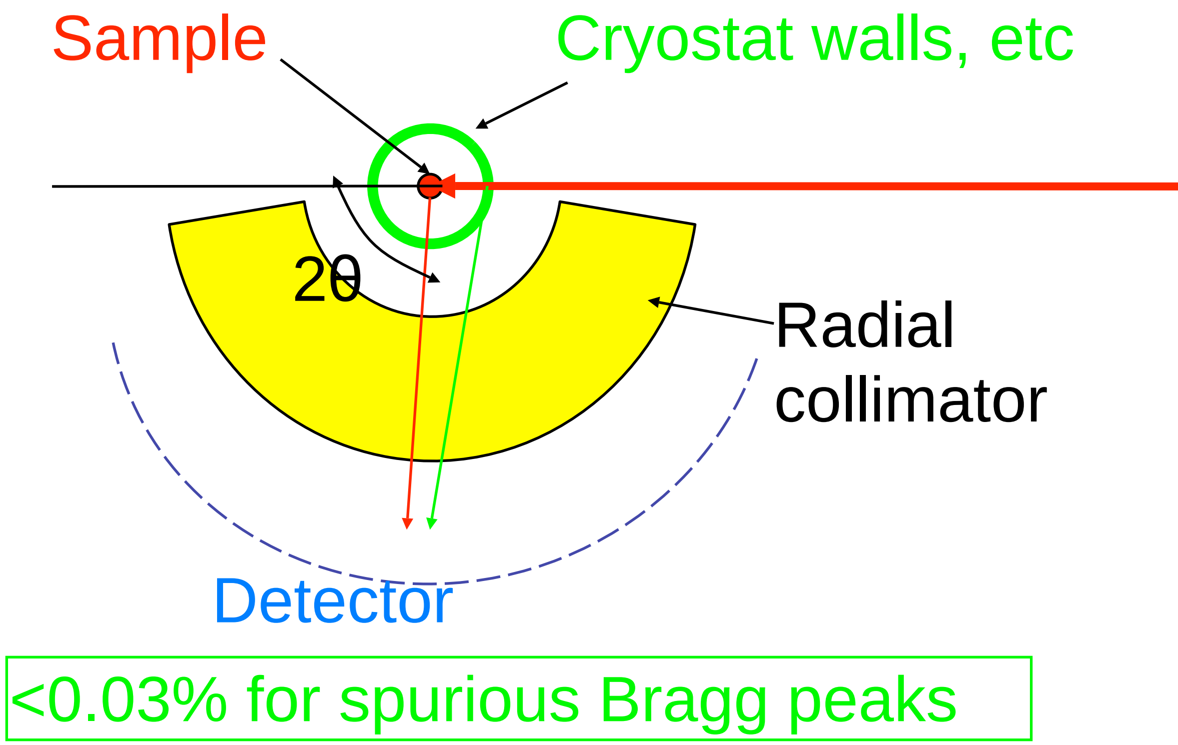

Radial collimator with the shielding.

There are two radial collimators with 14mm and 28mm full width full maximum triangular transmission function.

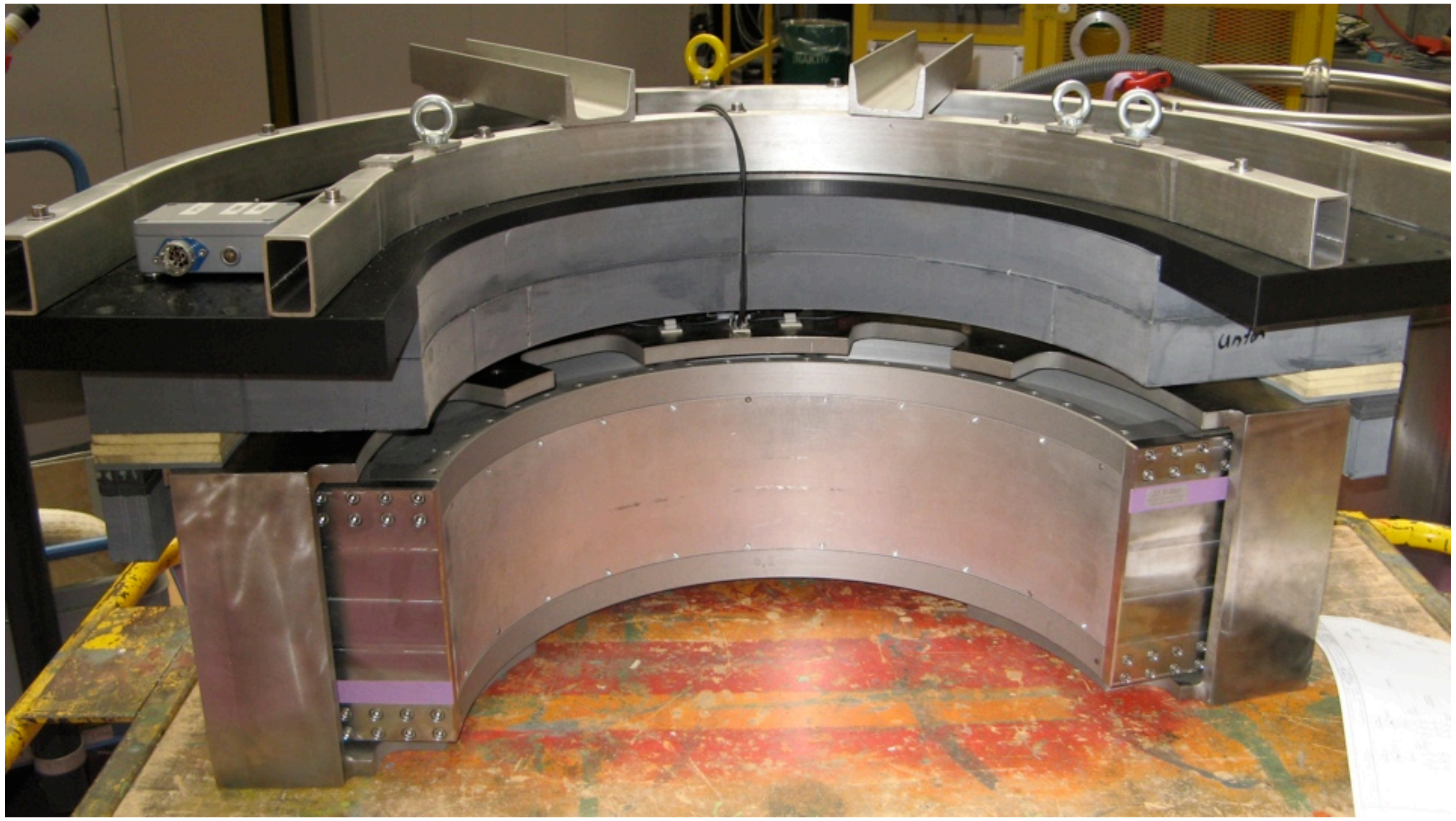

Samples, T, P, H and other equipment

- **standard sample container: 6-10 mm dia x 50 mm (<4cm^3)**
- due to low background small samples can be measured (30 mm^3)
- zero matrix high pressure cells:
  - clamp cells for 9 and 15 kbar
  - Paris Edinburgh cell 100 kbar
- standard LNS sample environment:
  - Temperature = 50 mK—1800K,
  - Magnetic field H = 4 T (vertical)
- Sample changers 4-8 samples, T=1.5-300 K

standard sample containers: 6-10 mm dia x 50 mm (<4cm^3)

Samples, T, P, H and other equipment

- standard sample container: 6-10 mm dia x 50 mm (<4cm^3)
- **due to low background small samples can be measured (30 mm^3)**
- zero matrix high pressure cells:
  - clamp cells for 9 and 15 kbar
  - Paris Edinburgh cell 100 kbar
- standard LNS sample environment:
  - Temperature = 50 mK—1800K,
  - Magnetic field H = 4 T (vertical)
- Sample changers 4-8 samples, T=1.5-300 K

Samples, T, P, H and other equipment

- standard sample container: 6-10 mm dia x 50 mm (<4cm^3)
- due to low background small samples can be measured (30 mm^3)
- **zero matrix high pressure cells:**
  - **clamp cells for 9 and 15 kbar**
  - **Paris Edinburgh cell 100 kbar**
- standard LNS sample environment:
  - Temperature = 50 mK—1800K,
  - Magnetic field H = 4 T (vertical)
- Sample changers 4-8 samples, T=1.5-300 K

clamp cells for 9 and 15 kbar

Paris Edinburgh cell 100 kbar

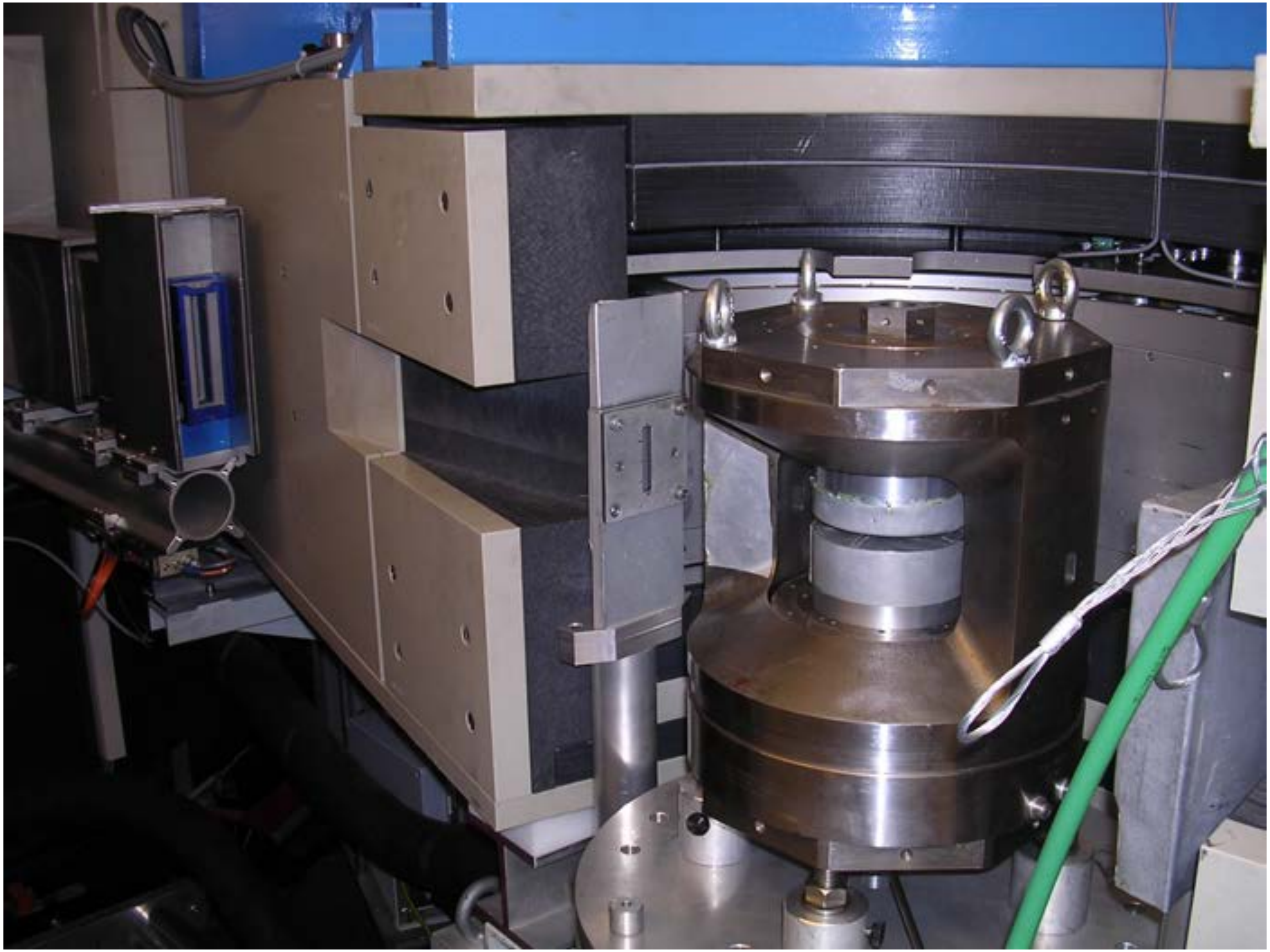

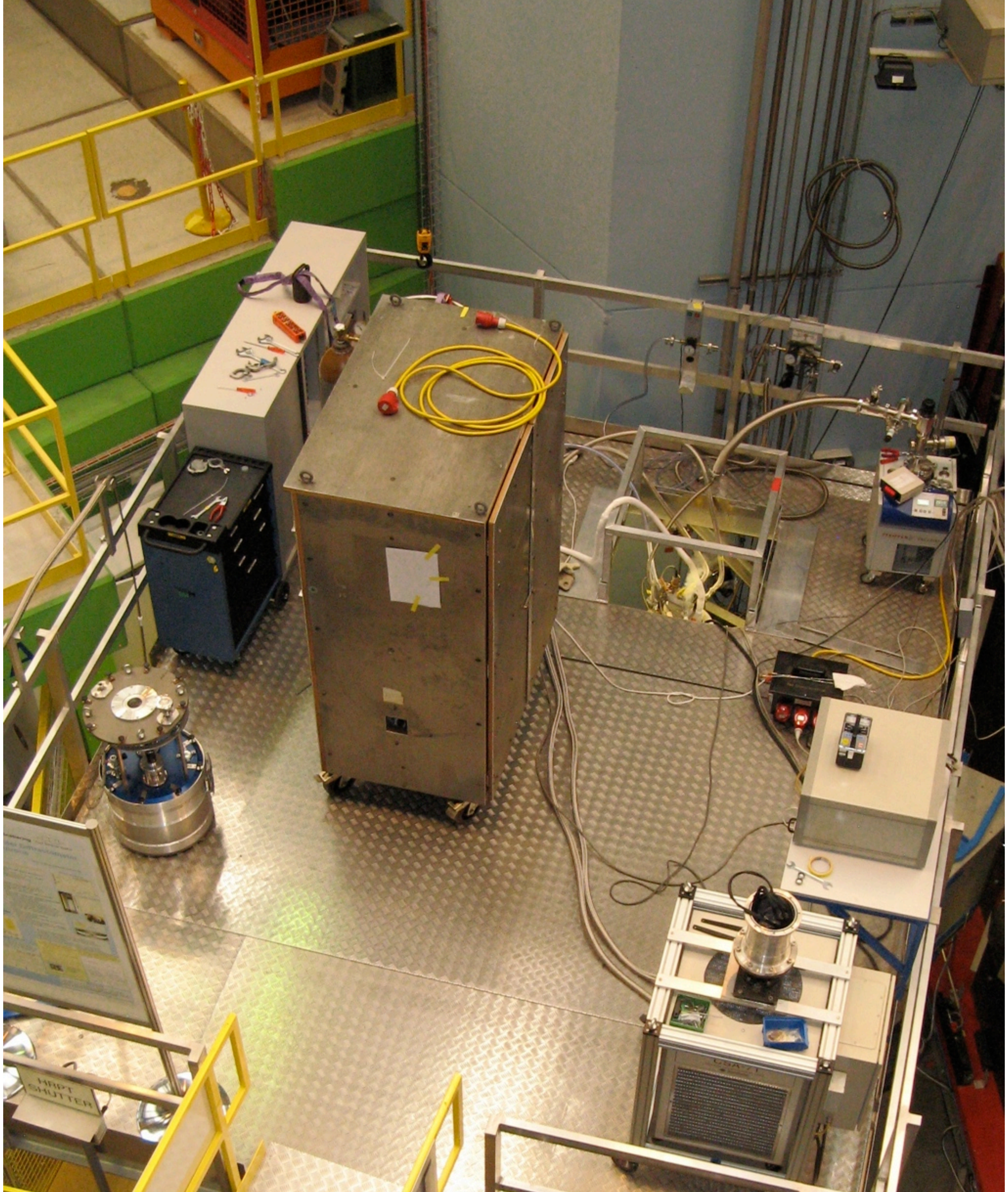

PSI information

Samples, T, P, H and other equipment

- standard sample container: 6-10 mm dia x 50 mm (<4cm^3)
- due to low background small samples can be measured (30 mm^3)
- zero matrix high pressure cells:
  - clamp cells for 9 and 15 kbar
  - Paris Edinburgh cell 100 kbar
- **standard LNS sample environment:**
  - **Temperature = 50 mK—1800K,**
  - **Magnetic field H = 4 T (vertical)**
  - **Automatic He, N_2 refilling systems**
- Sample changers 4-8 samples, T=1.5-300 K

Samples, T, P, H and other equipment

- standard sample container: 6-10 mm dia x 50 mm (<4cm^3)
- due to low background small samples can be measured (30 mm^3)
- zero matrix high pressure cells:
  - clamp cells for 9 and 15 kbar
  - Paris Edinburgh cell 100 kbar
- standard LNS sample environment:
  - Temperature = 50 mK—1800K,
  - Magnetic field H = 4 T (vertical)
  - Automatic He, N_2 refilling systems
- **Sample changers 4-8 samples, T=1.5-300 K**

HRPT room temperature 8-sample changer

- Eight samples mounted on a caroussel-type changer, few seconds to bring the next one into the measurement position;

- Independent sample rotation mechanism – for reducing the preferred orientation aberrations.

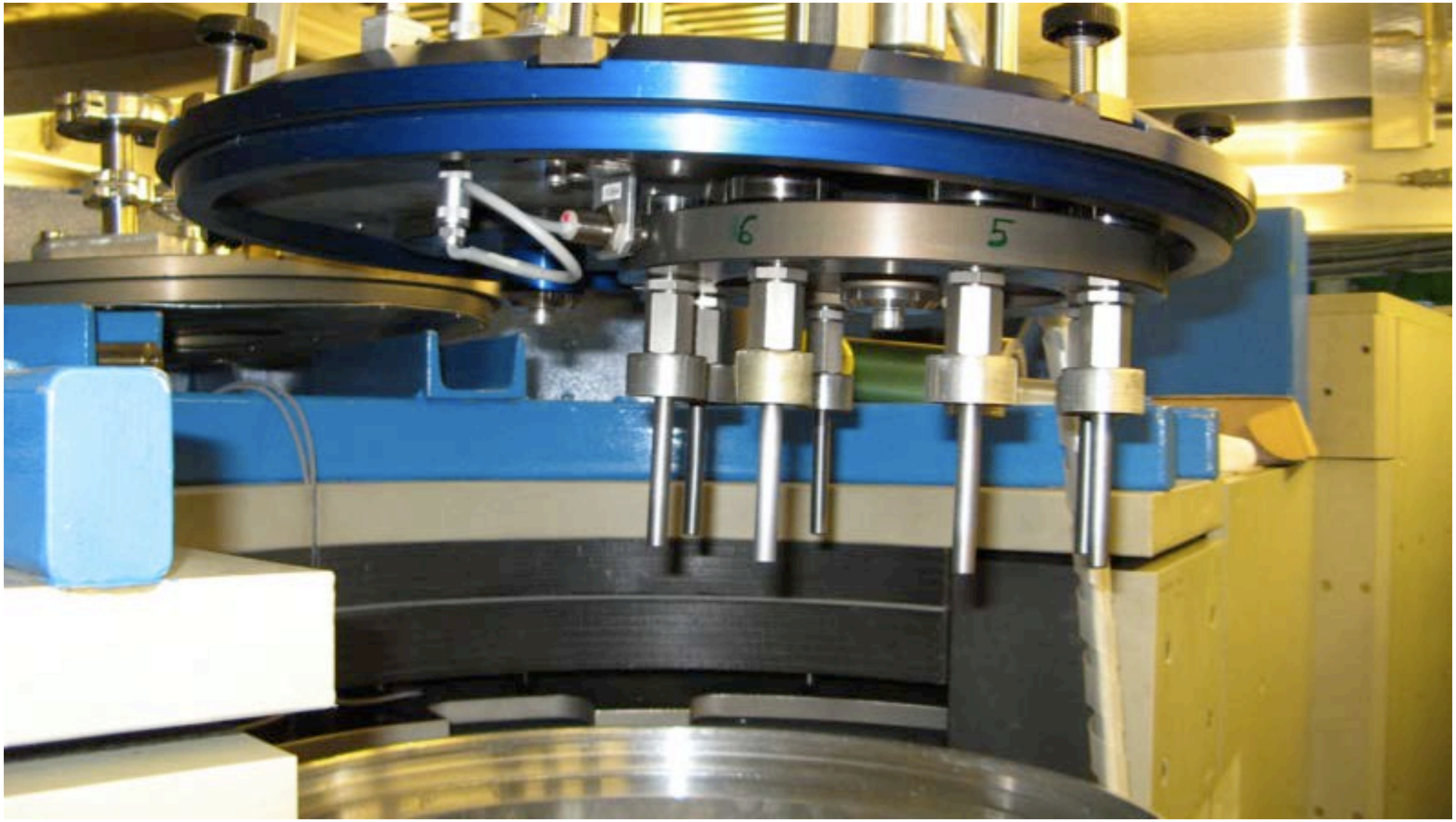

Fully loaded with 8 samples, the sample changer is ready to be installed in-place on the HRPT sample table.

HRPT room temperature 8-sample changer

- Eight samples mounted on a caroussel-type changer, few seconds to bring the next one into the measurement position;

- Independent sample rotation mechanism – for reducing the preferred orientation aberrations.

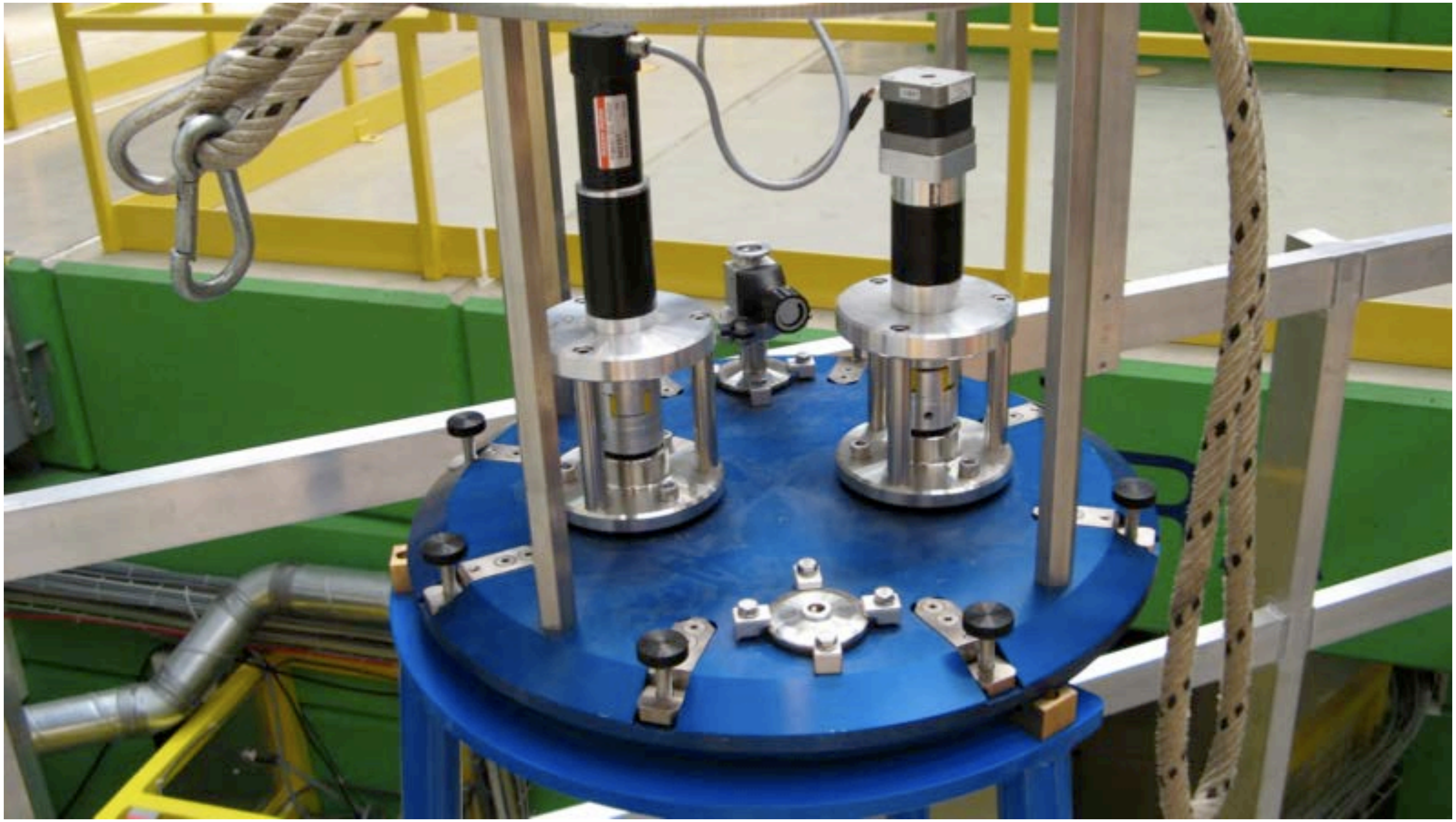

Fully loaded with 8 samples, the sample changer is ready to be installed in-place on the HRPT sample table.

HRPT low temperature 4-sample changer

A device for routine powder diffraction measurements at temperatures between 1.5K -300K.

- All samples have the same temperature, i.e. time for temperature change is saved;
- Four samples mounted on a caroussel-type changer, that is a special inset for an orange cryostat

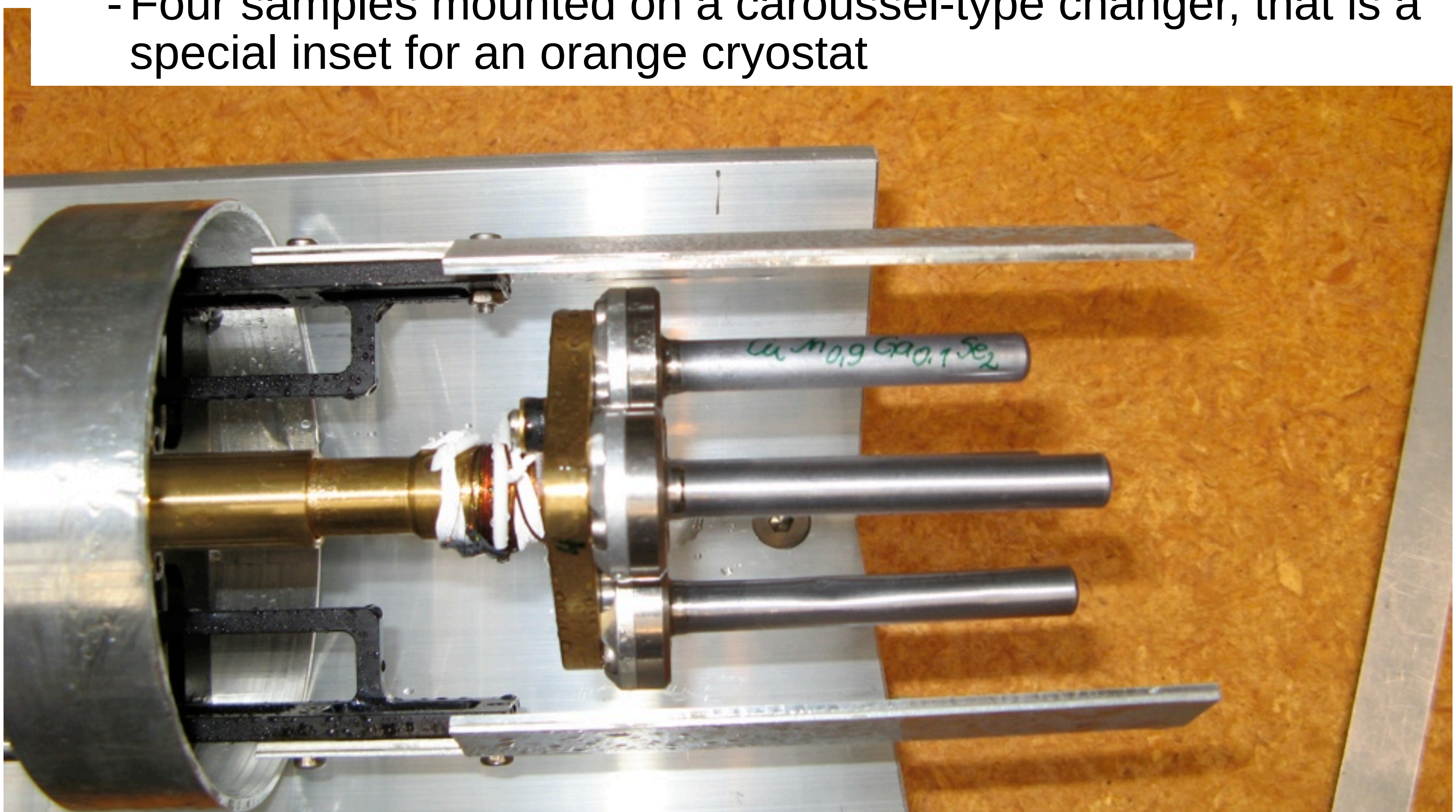

HRPT low temperature 4-sample changer

HRPT low temperature 4-sample changer

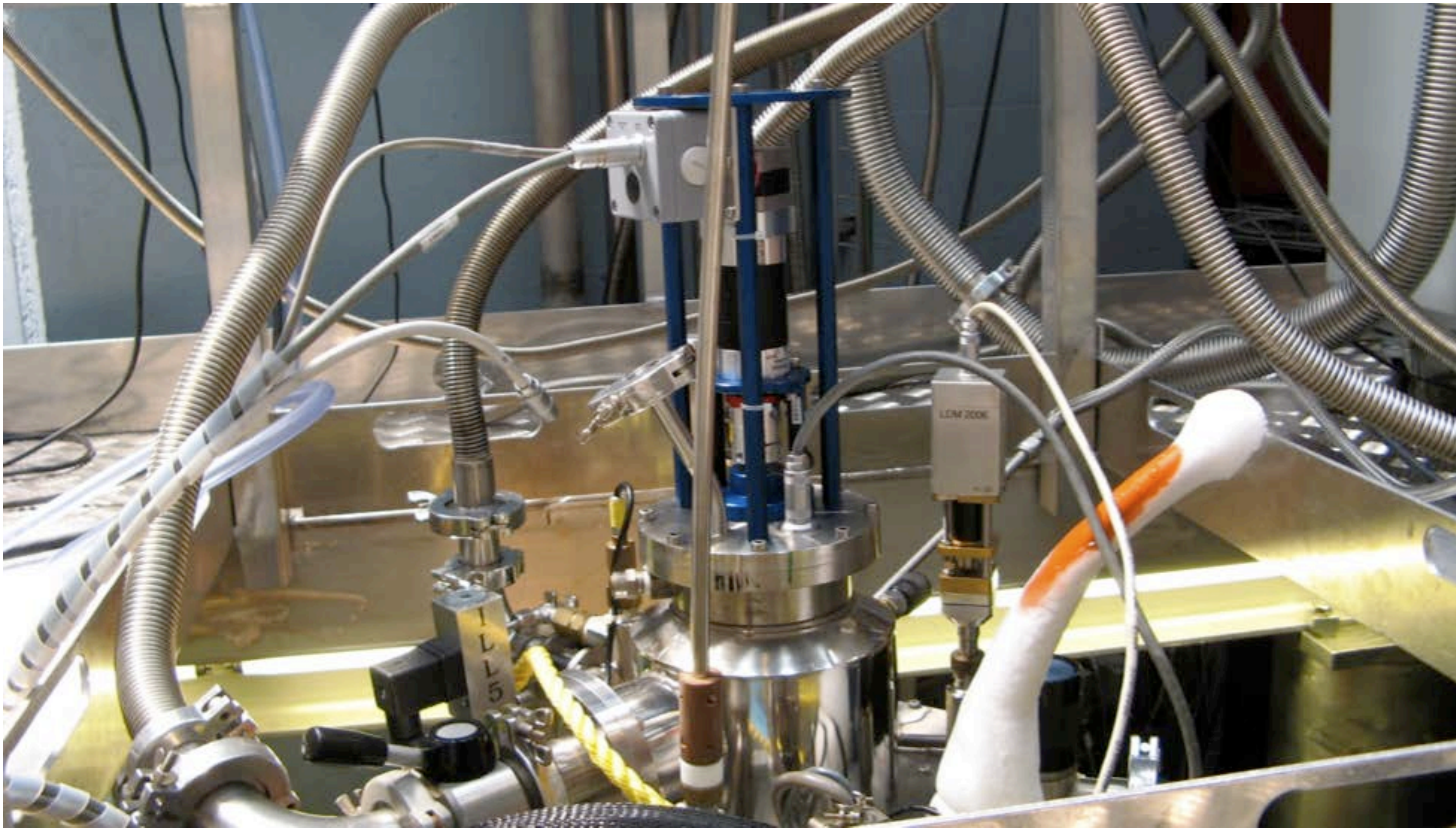

Examples of HRPT applications

Mn-O bond lengths

$(La_{1-y}Pr_y)_{0.7}Ca_{0.3}(Mn^{3+})_{0.7}\,(Mn^{4+})_{0.3}O_3$

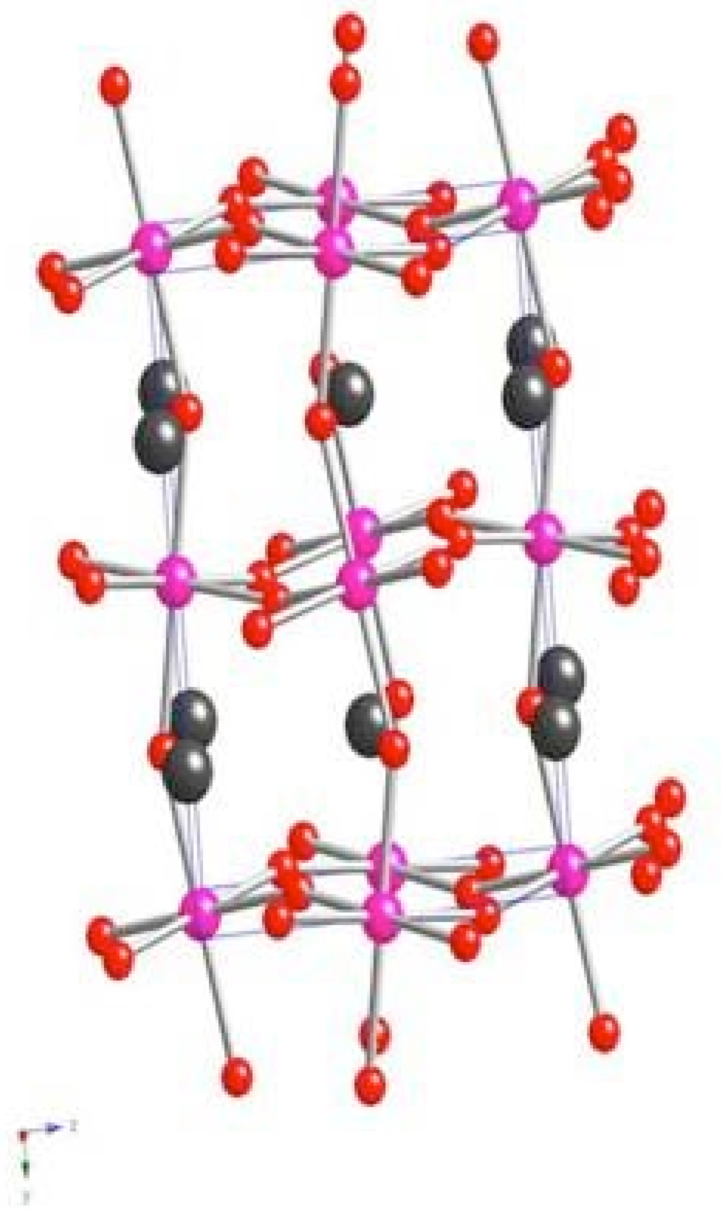

$$|\theta\rangle = \cos\frac{\theta}{2}|3z^2 - r^2\rangle + \sin\frac{\theta}{2}|x^2 - y^2\rangle$$

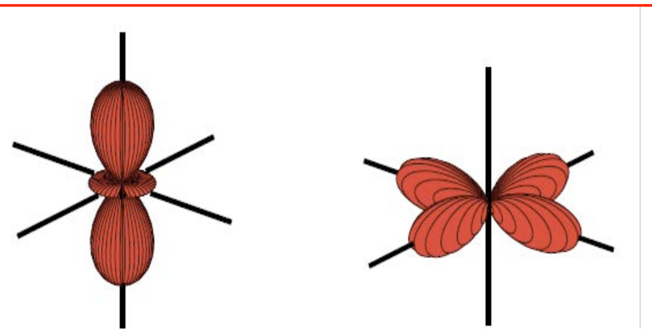

Orbital and charge ordering OO/CO

$(La_{1-y}Pr_y)_{0.7}Ca_{0.3}(Mn^{3+})_{0.7}(Mn^{4+})_{0.3}O_3$

$$|\theta\rangle = \cos\frac{\theta}{2}|3z^2 - r^2\rangle + \sin\frac{\theta}{2}|x^2 - y^2\rangle$$

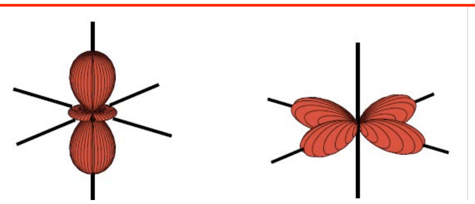

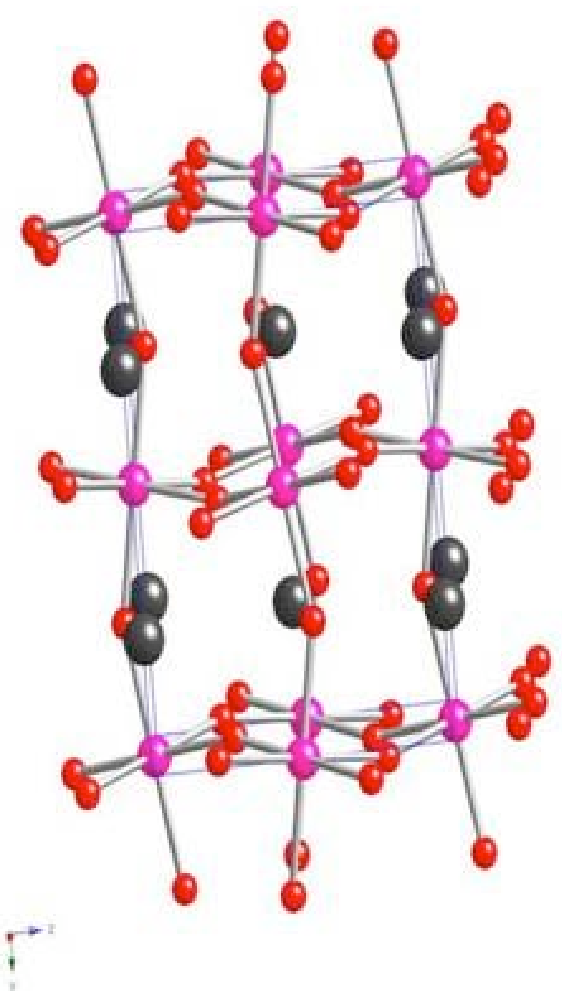

Mn-O bond lengths in LPCM (y=0.7)

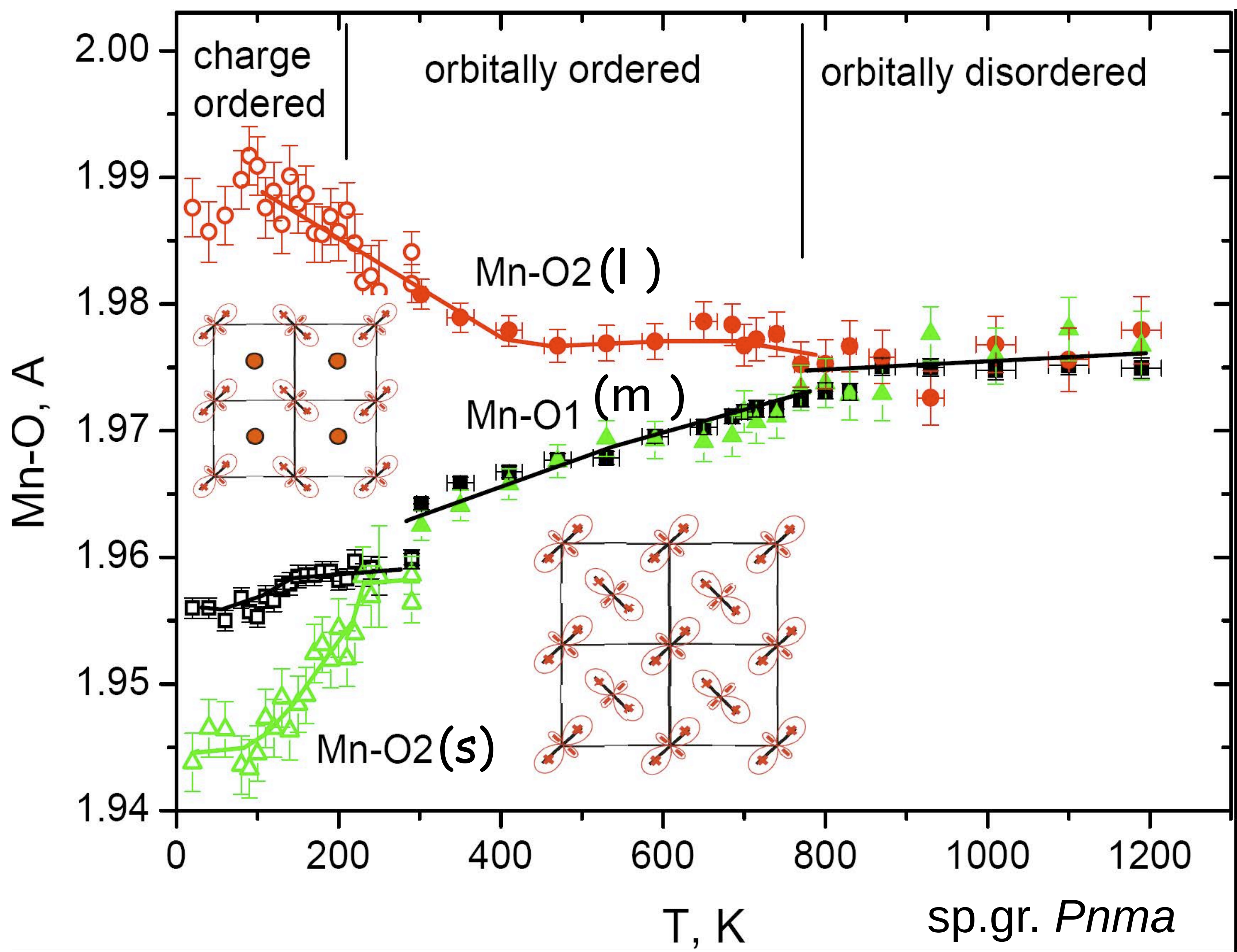

Where are Ni ions in the trimer?

$Ca_3Cu_{3-x}Ni_x(PO_4)_4$ (x=0,1,2)

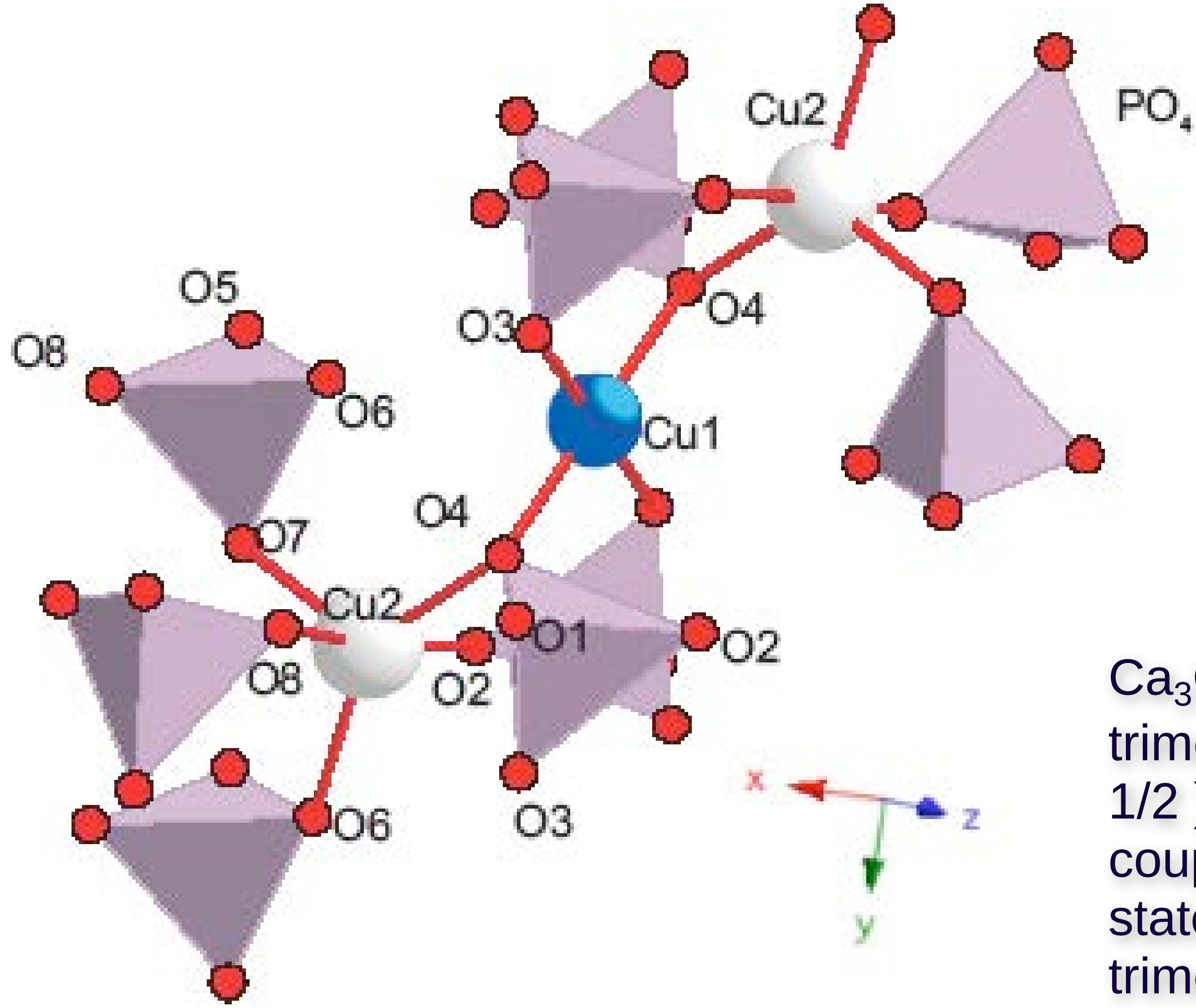

$Ca_3Cu_3(PO_4)_4$ is a novel quantum spin trimer system in which the three Cu^{2+}(S = 1/2) spins are antiferromagnetically coupled giving rise to a doublet ground state. By substituting a Cu^{2+} spin in the trimer by Ni^{2+} (S = 1) a singlet ground state could be in principle realized offering the observation of the Bose-Einstein condensation in a quantum spin trimer system.

Crystal and magnetic structures and magnetic excitations spin-trimer system $Ca_3Cu_{3-x}Ni_x(PO_4)_4$ (x=0,1,2)

Where are Ni ions in the trimer?

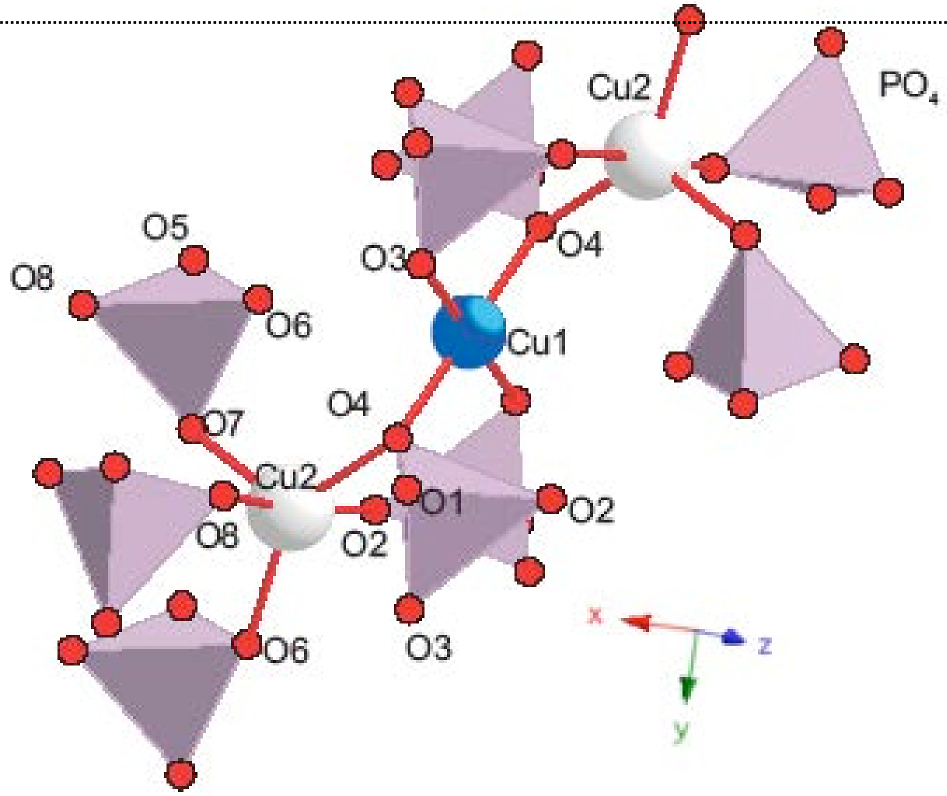

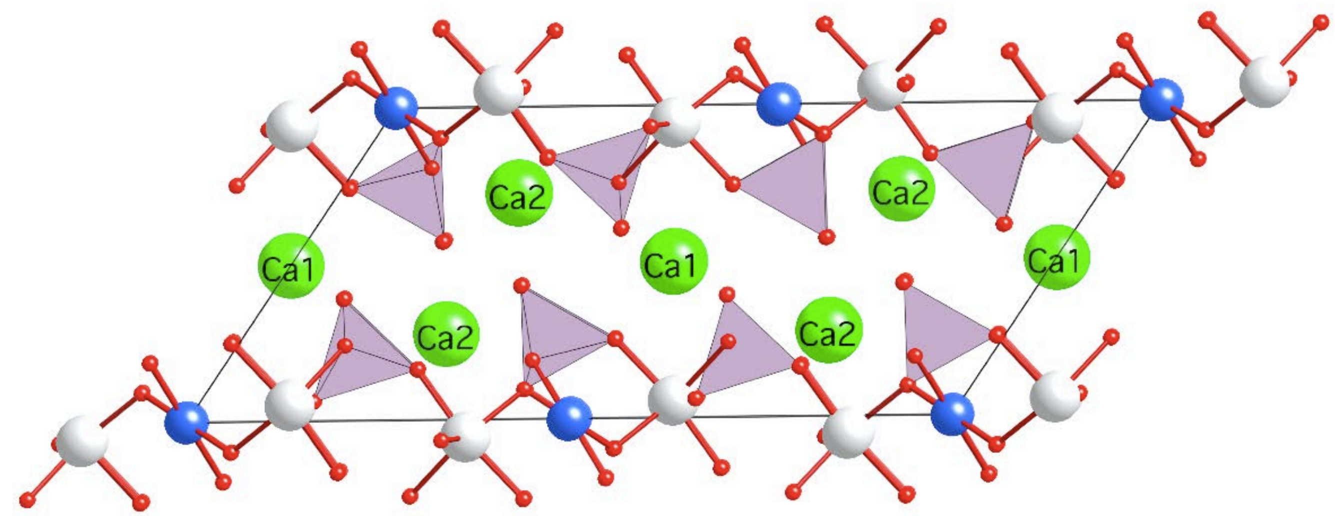

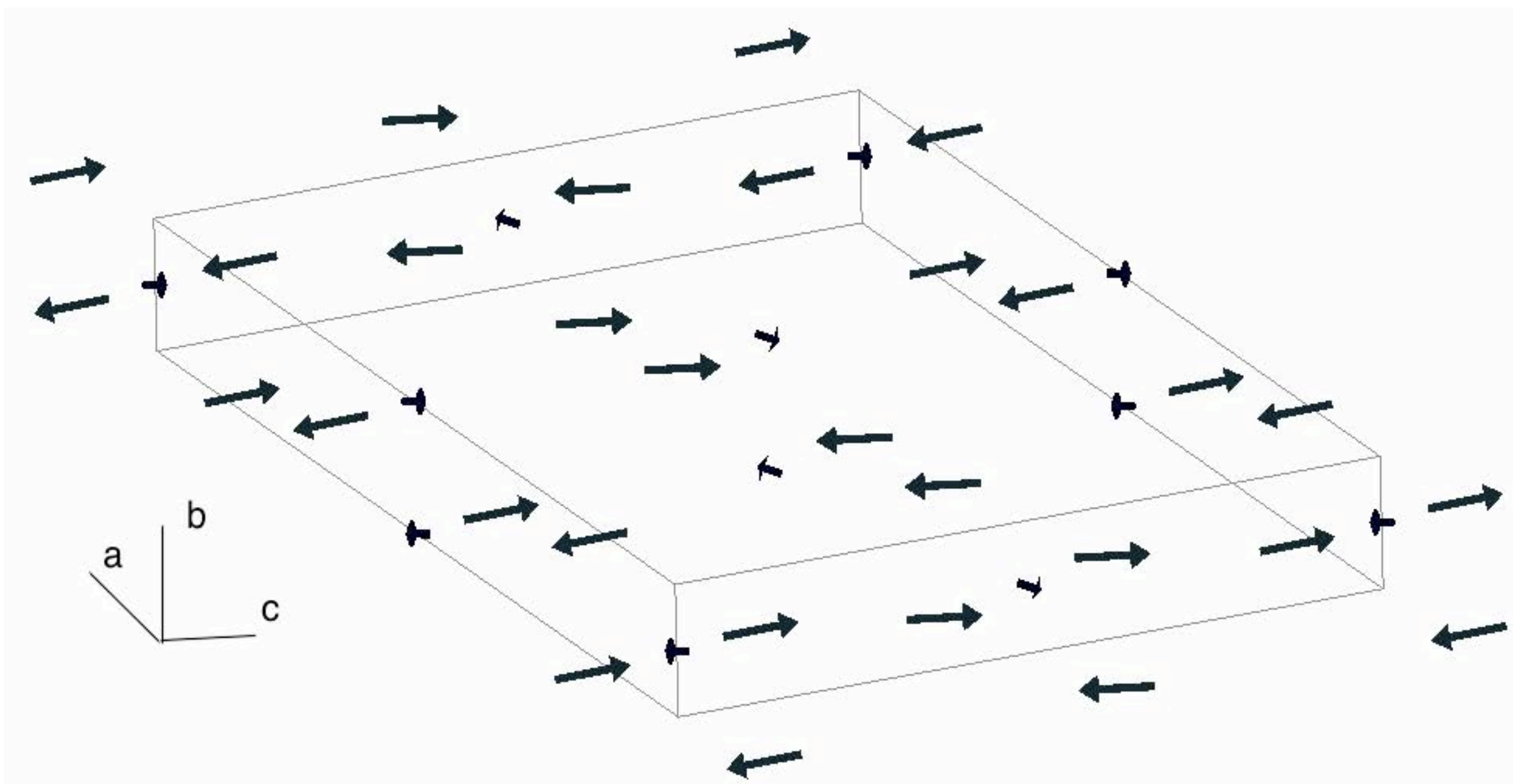

$Ca_3Cu_3(PO_4)_4$ is a novel quantum spin trimer system in which the three Cu^{2+}(S = 1/2) spins are antiferromagnetically coupled giving rise to a doublet ground state. By substituting a Cu^{2+} spin in the trimer by Ni^{2+} (S = 1) a singlet ground state could be in principle realized offering the observation of the Bose-Einstein condensation in a quantum spin trimer system.

$C(CrBr)_4$-liquid in gas pressure cell. T-P phase diagram

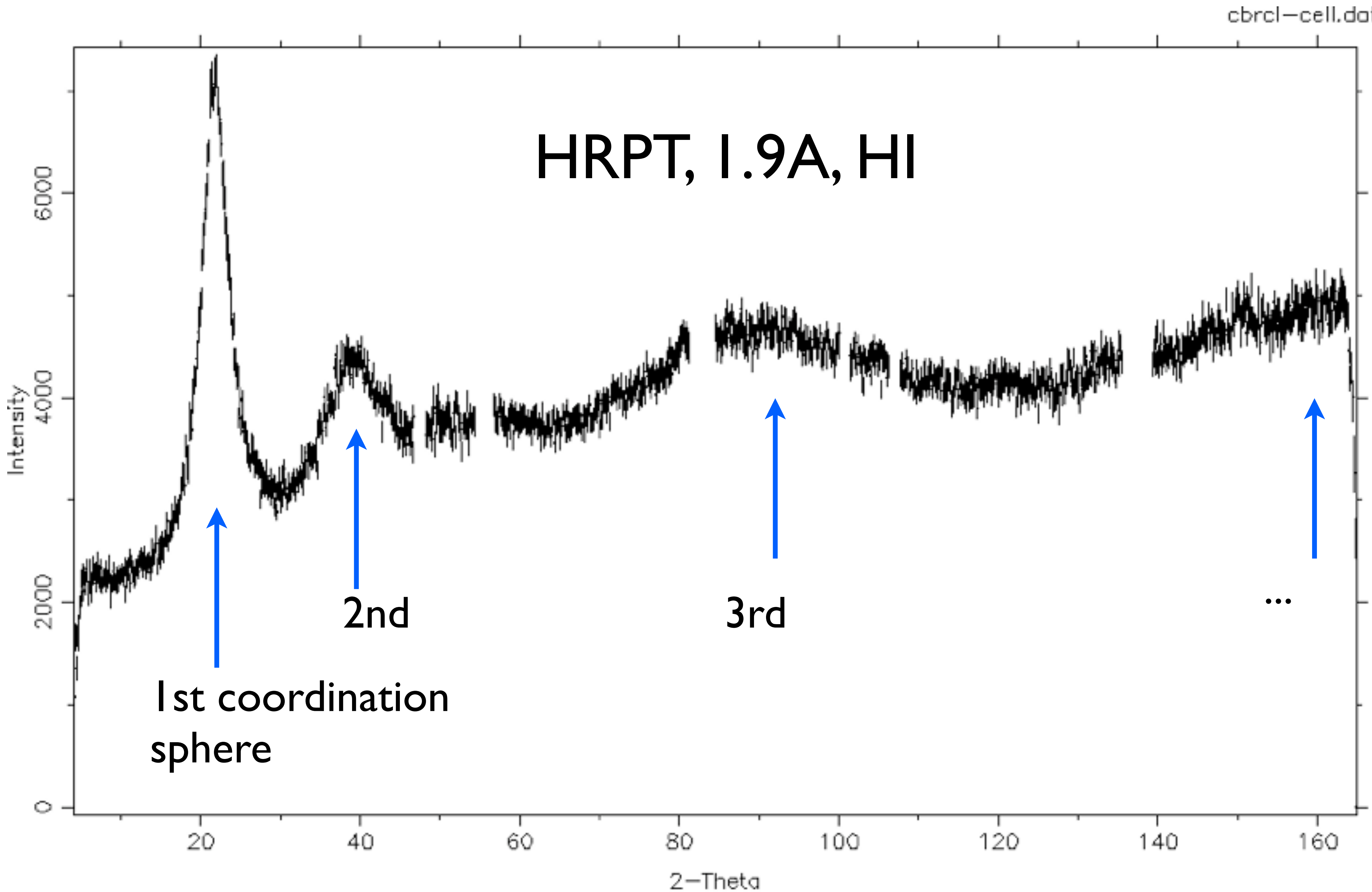

M.Barrio, et al (2009)

High pressure structure transition in quantum dimer system $SrCu_2(BO_3)_2$

Anvil pressure cell installed at HRPT diffractometer

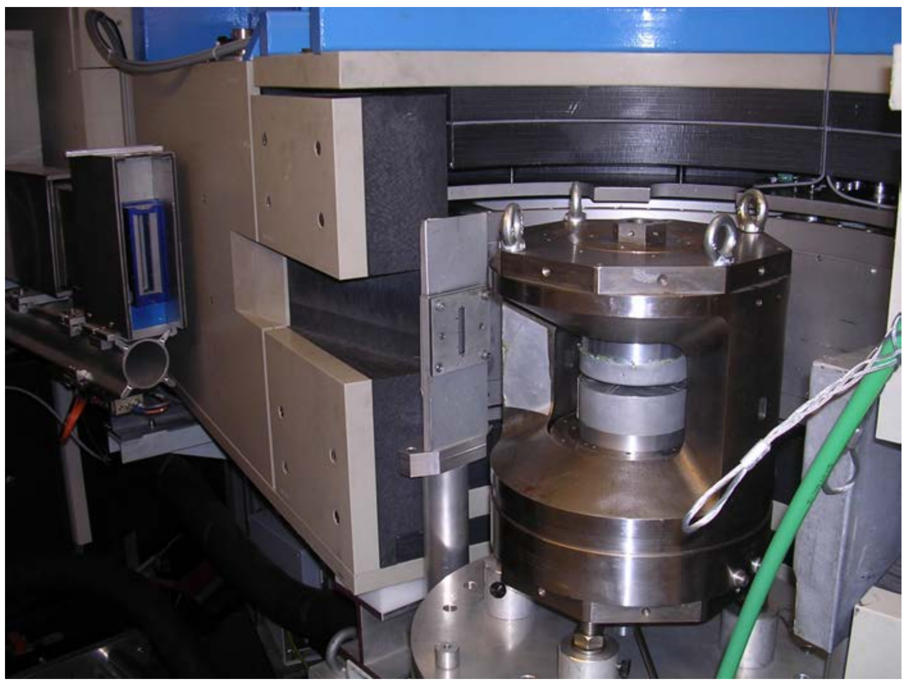

detector shielding + radial collimator + BN anvils + low noise ellectronics = excellent peak to background ratio

LNS, PSI: V. Pomjakushin, Th. Strassle, K. Conder, E. Pomjakushina
EPFL: M. Zayed, H. Ronnow

p=8GPa: monoclinic *C2*: the new structure solved from the HRPT data!

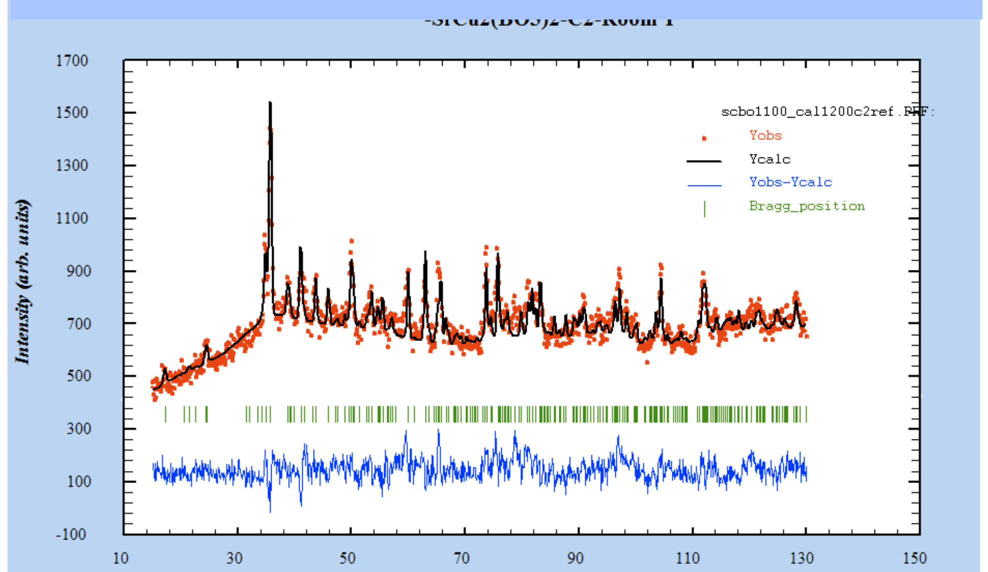

p=3.7GPa, known tetragonal *I-42m* structure

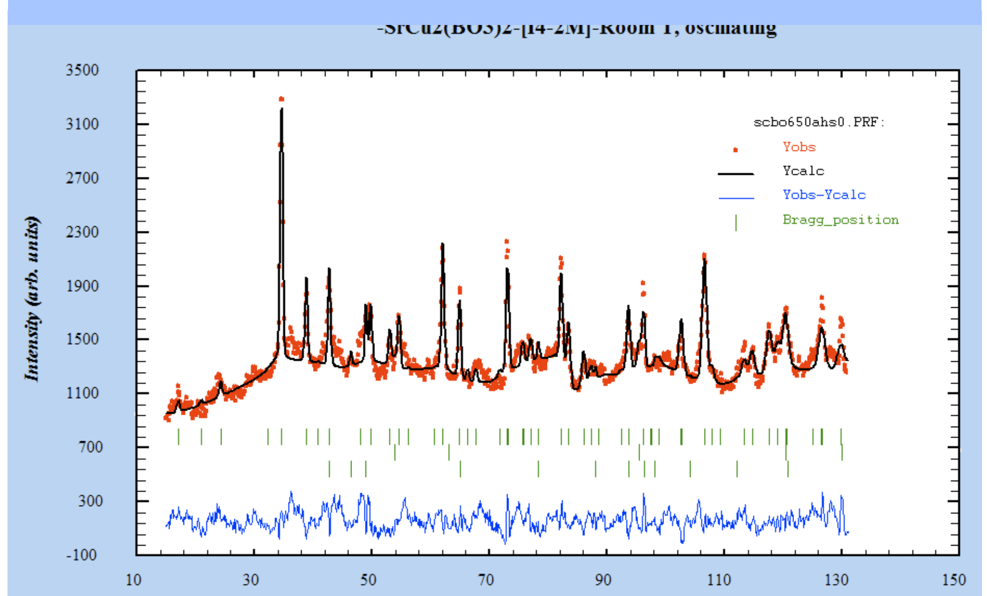

The S=1/2 moments of the Cu^{2+} ions are arranged in a 2D lattice of strongly coupled dimers (J=85 K).

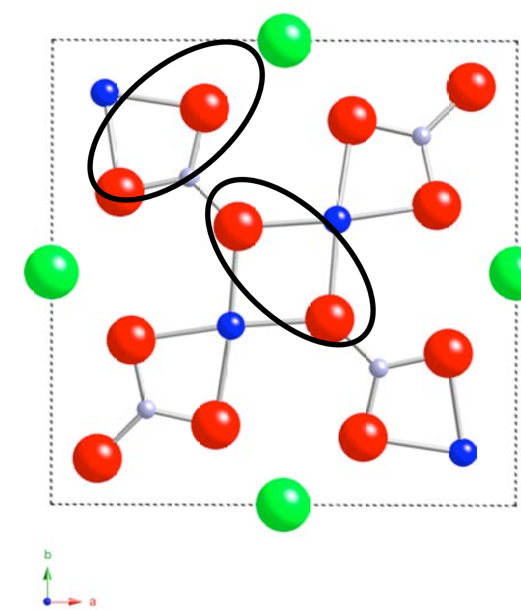

- The material is predicted to undergo a quantum phase transition by application of hydrostatic pressure.
- To fully understand the magnetic properties of the material the knowledge of the exchange paths as a function of pressure is mandatory.

High pressure structure transition in quantum dimer system $SrCu_2(BO_3)_2$

Anvil pressure cell installed
HRPT diffractometer

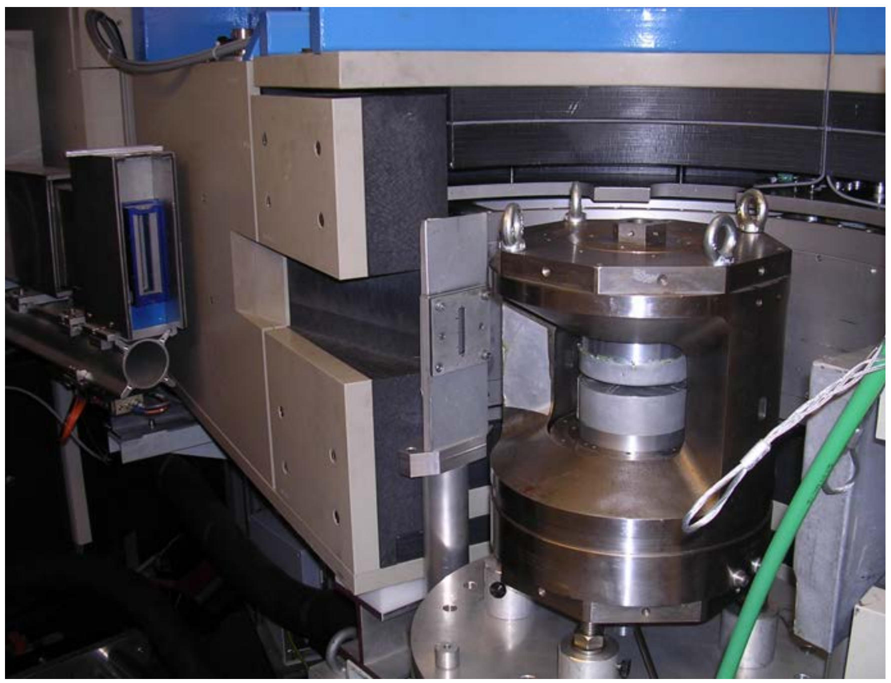

detector shielding + radial collimator + BN anvils + low noise ellectronics = excellent peak to background ratio

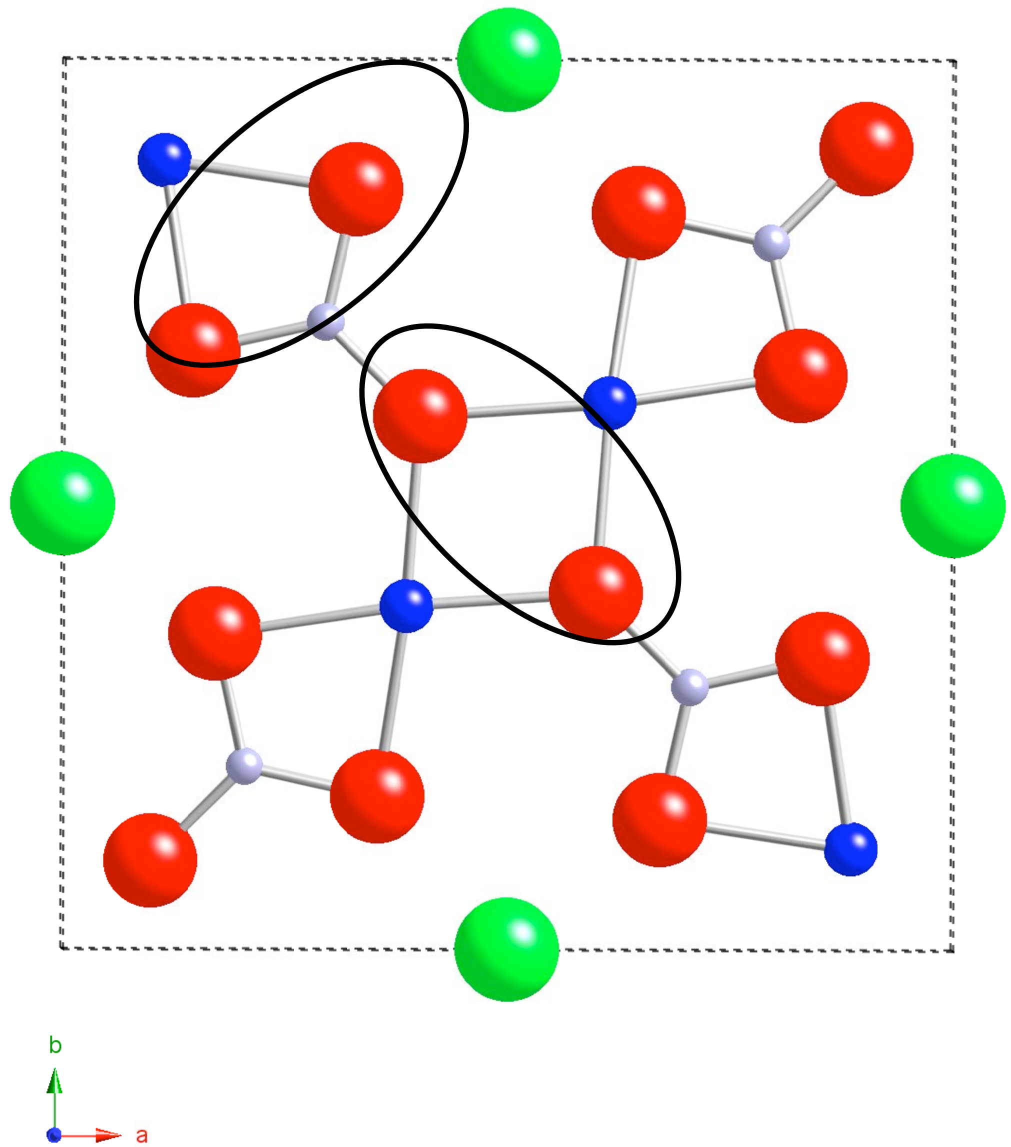

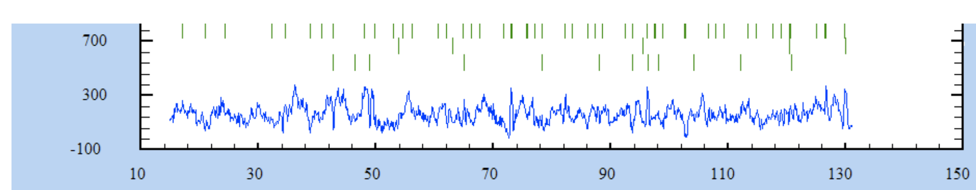

The S=1/2 moments of the Cu^{2+} ions are arranged in a 2D lattice of strongly coupled dimers (J=85 K).

- The material is predicted to undergo a quantum phase transition by application of hydrostatic pressure.
- To fully understand the magnetic properties of the material the knowledge of the exchange paths as a function of pressure is mandatory.

LNS, PSI: V. Pomjakushin, Th. Strassle, K. Conder, E. Pomjakushina
EPFL: M. Zayed, H. Ronnow

High pressure structure transition in quantum dimer system $SrCu_2(BO_3)_2$

p=8GPa: monoclinic *C2:* the new structure solved from the HRPT data!

p=3.7GPa, known tetragonal *I-42m structure*

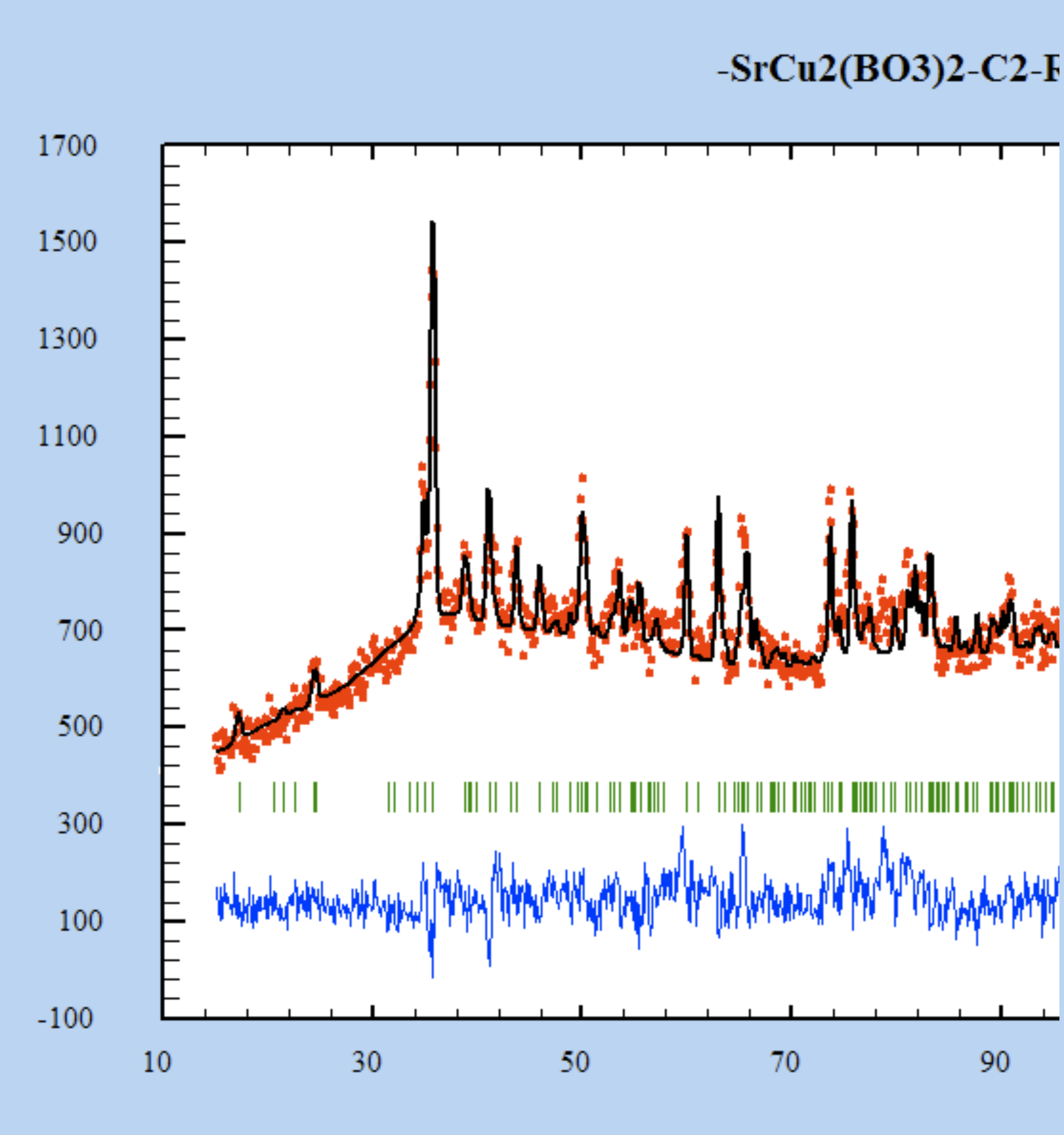

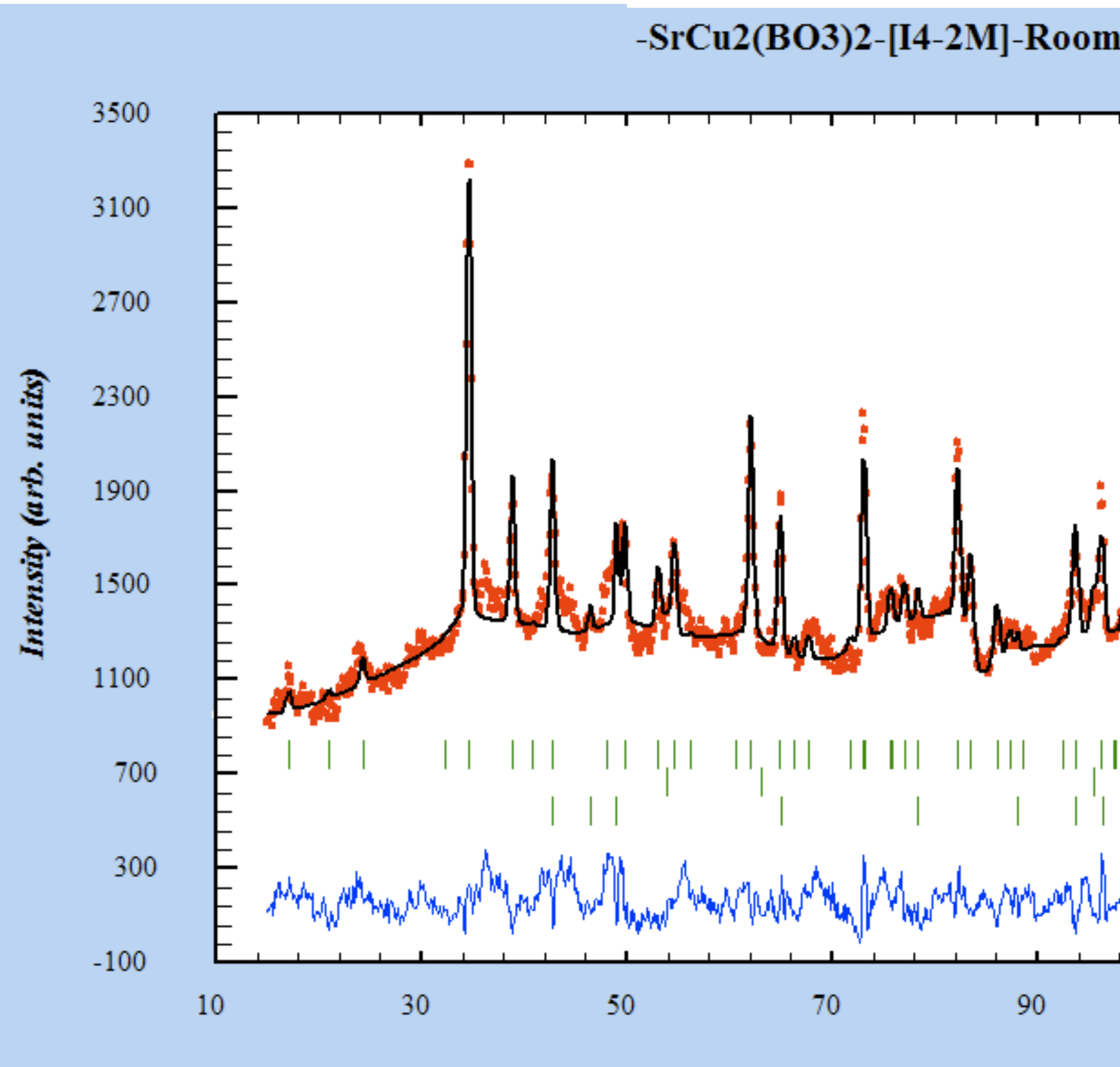

Magnetic structure of $Cu_2CdB_2O_6$ exhibiting a quantum-mechanical magnetization plateau and classical antiferromagnetic long-range order

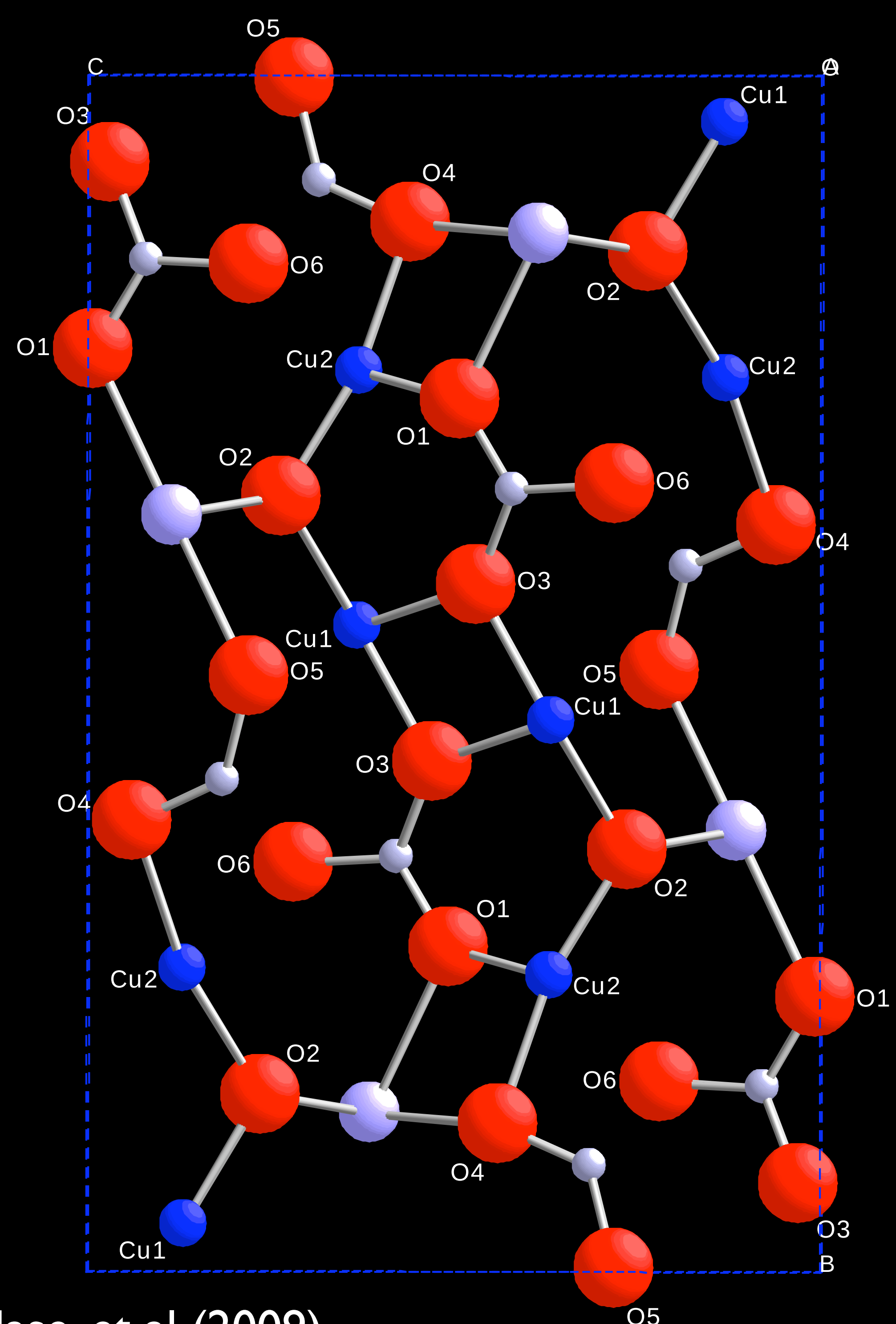

M.Hase, et al (2009)

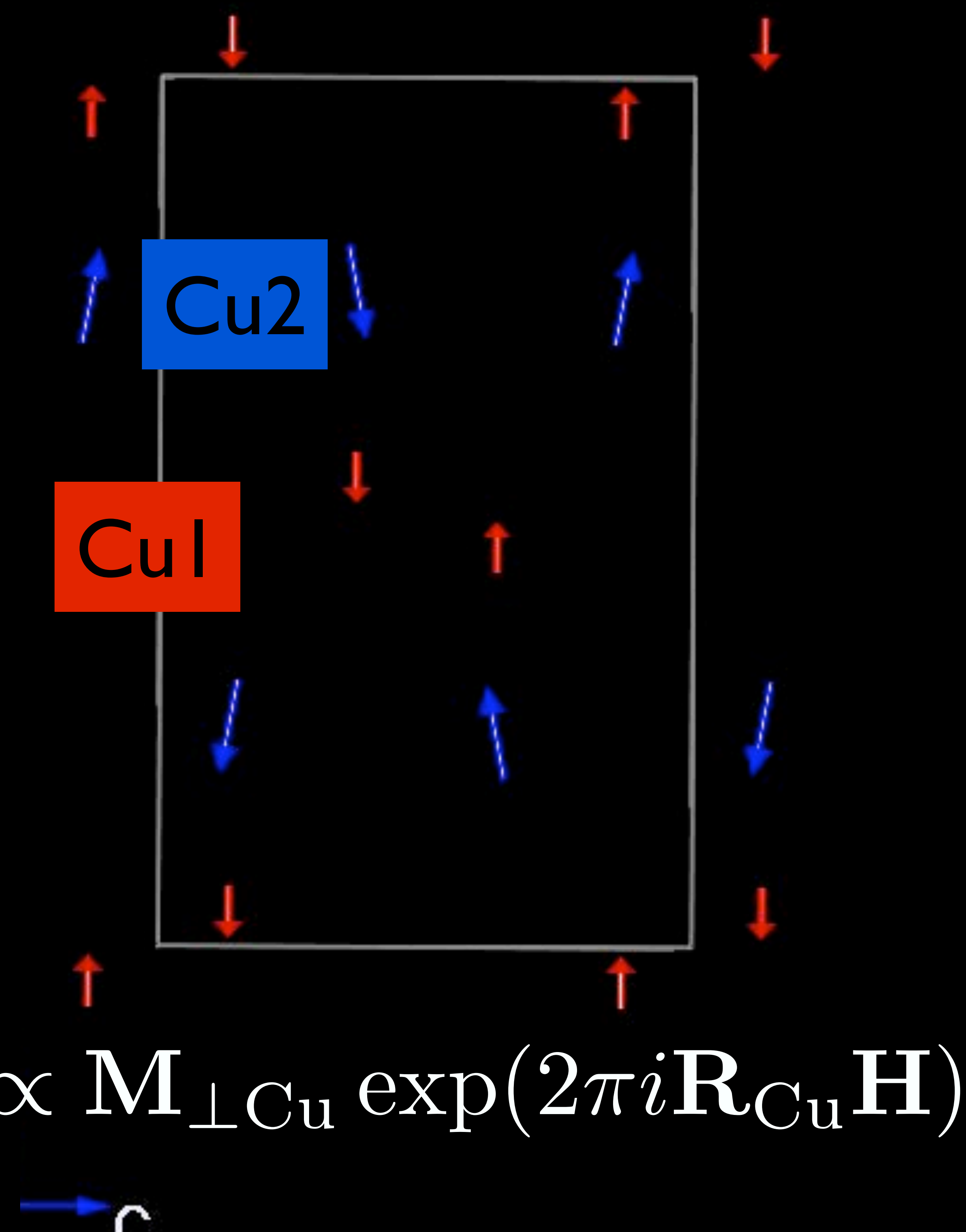

$$\mathbf{F(H)} \propto \mathbf{M}_{\perp \mathrm{Cu}} \exp(2\pi i \mathbf{R}_{\mathrm{Cu}} \mathbf{H})$$

Lattice distortion (0.1%) and magnetic structure in NiO under high pressures (up to 130kbar) at HRPT

@ p=1bar: μ_{Ni}=1.73(9) μ_B, k =[½ ½ ½] in *Fm3m*
R3-m: a=2.9534(2)Å, α=60.061(2)º

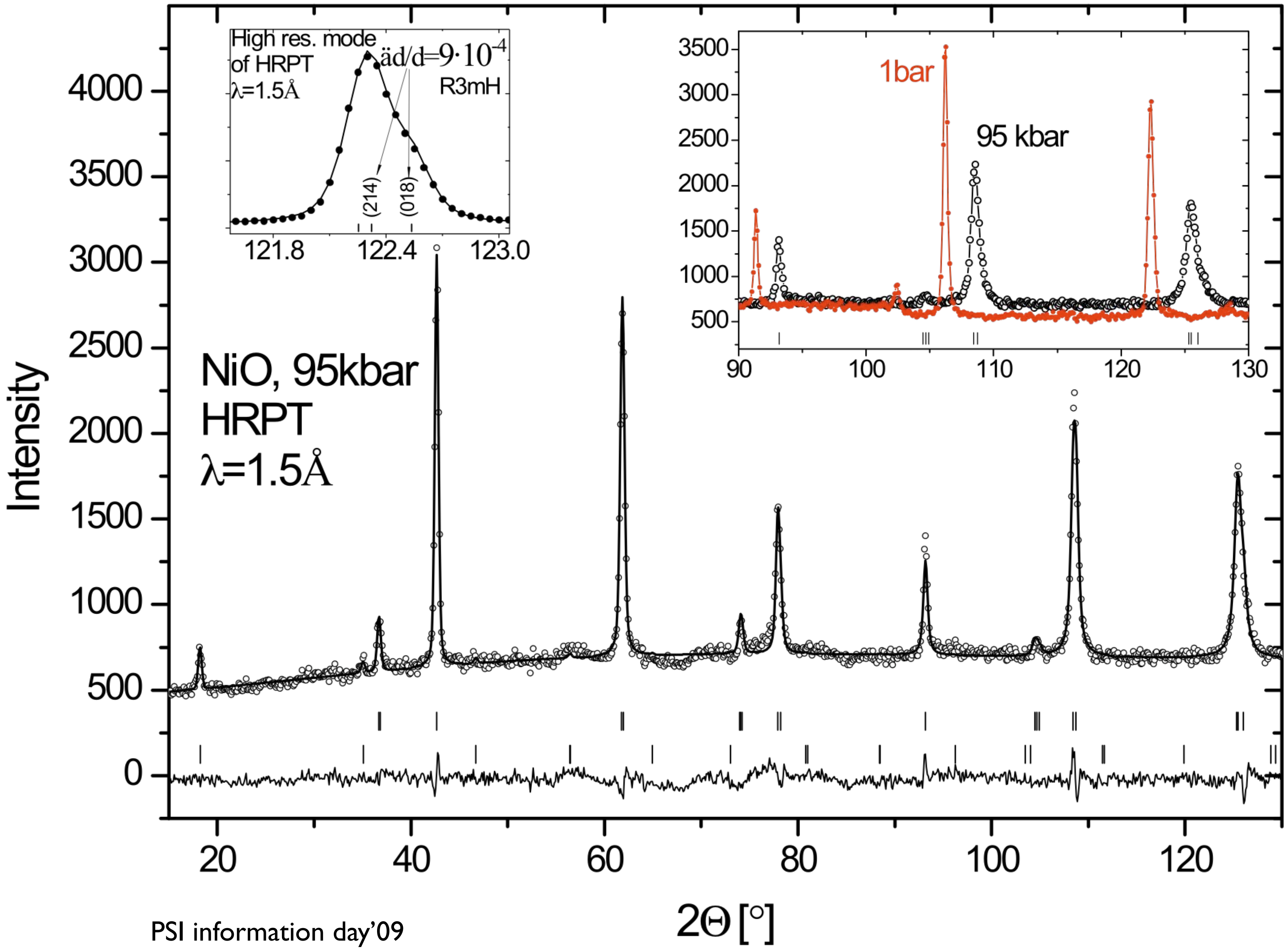

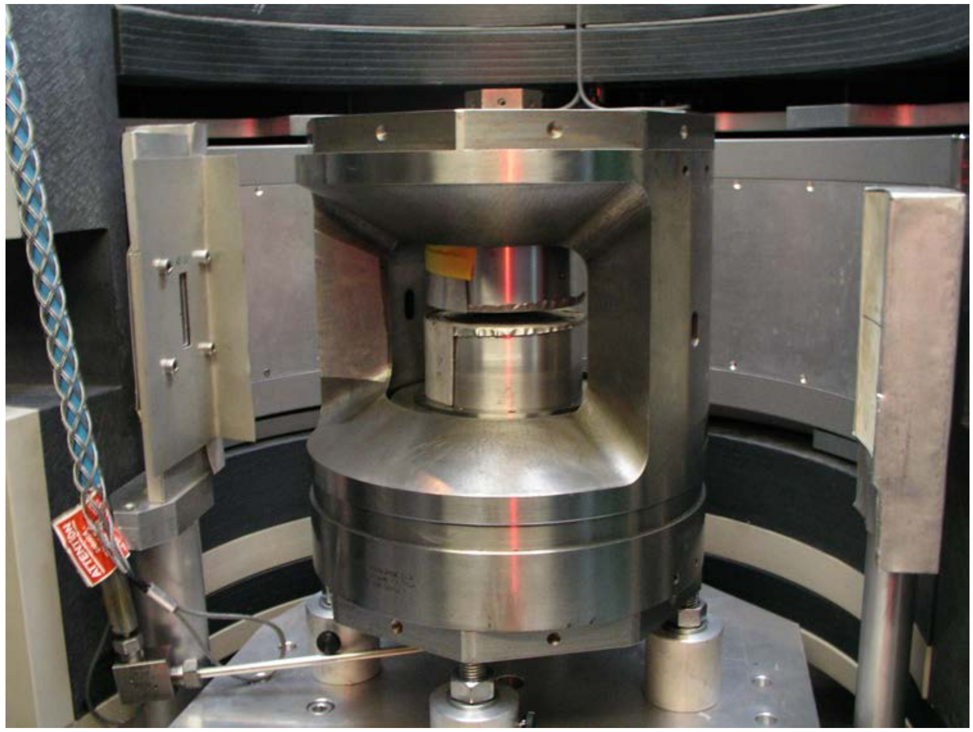

S. Klotz, Th. Strässle, G. Rousse, G. Hamel, V. Pomjakushin, *APL 2005.*

High-pressure studies of $PbMg_{1/3}Ta_{2/3}O_3$ relaxor ferroelectric

S. Gvasaliya, V. Pomjakushin, B. Roessli, Th. Strässle, S. Klotz, S. Lushnikov

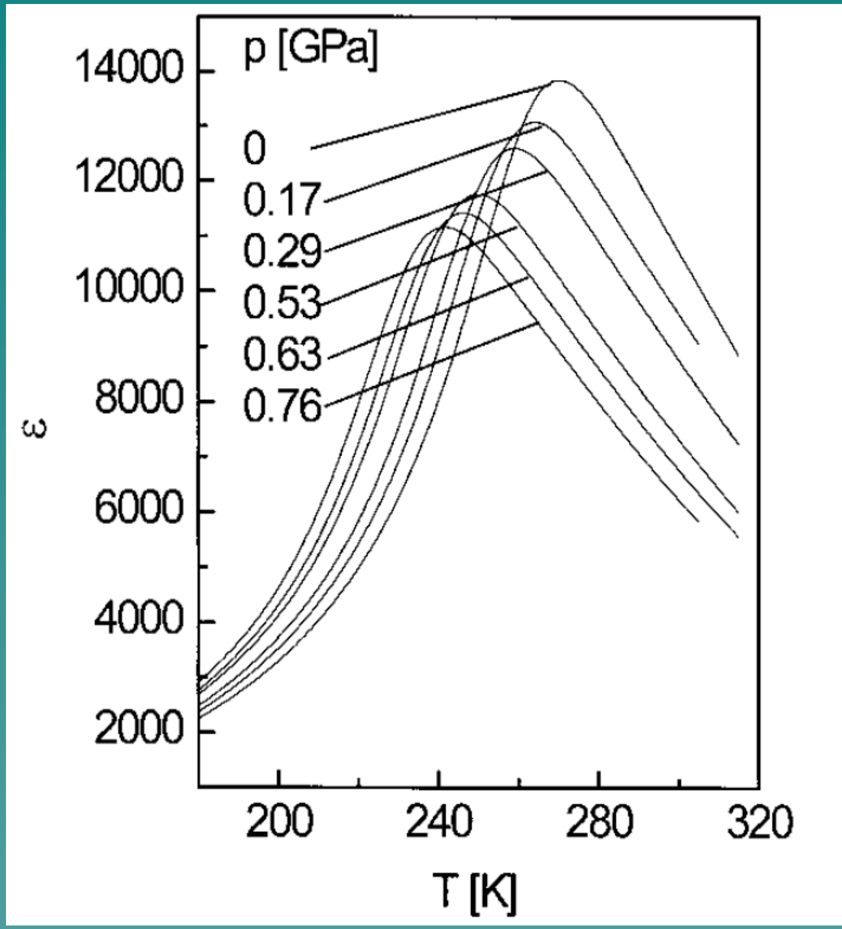

Relaxor ferroelectrics are peculiar crystals where the giant dielectric permittivity appears without structural phase transition. There is no theory which describe their properties. Among other anomalies, there is a suppression of the peak in the dielectric permittivity and of the intensity of diffuse scattering under hydrostatic pressure. In order to understand underlying physics the structure of a model relaxor was studies up to hydrostatic pressure P~7 GPa

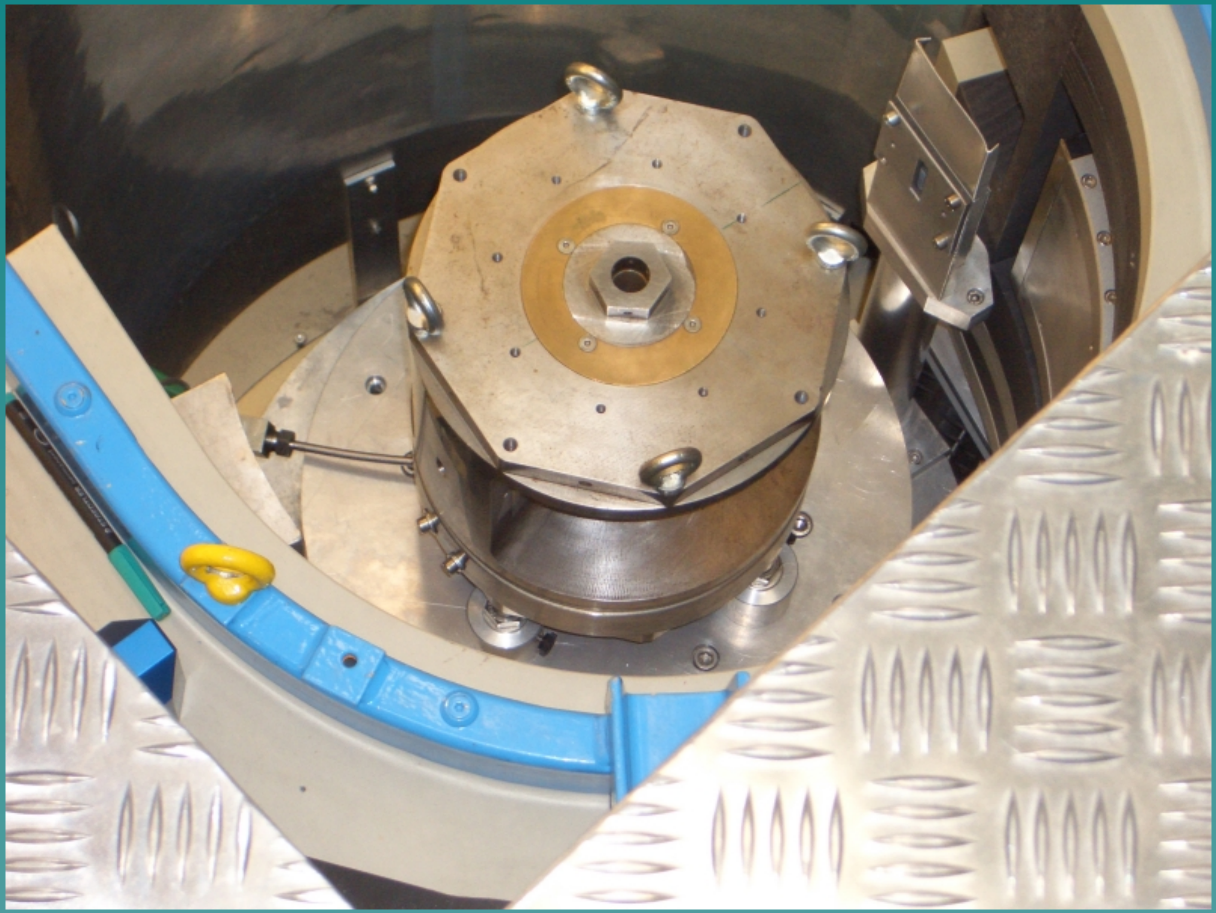

Photo of a high pressure setup using Paris-Edinburgh pressure cell at HRPT diffractometer. The sample volume is less than 100 mm^3, approximately two orders of magnitude smaller than in a standard setup.

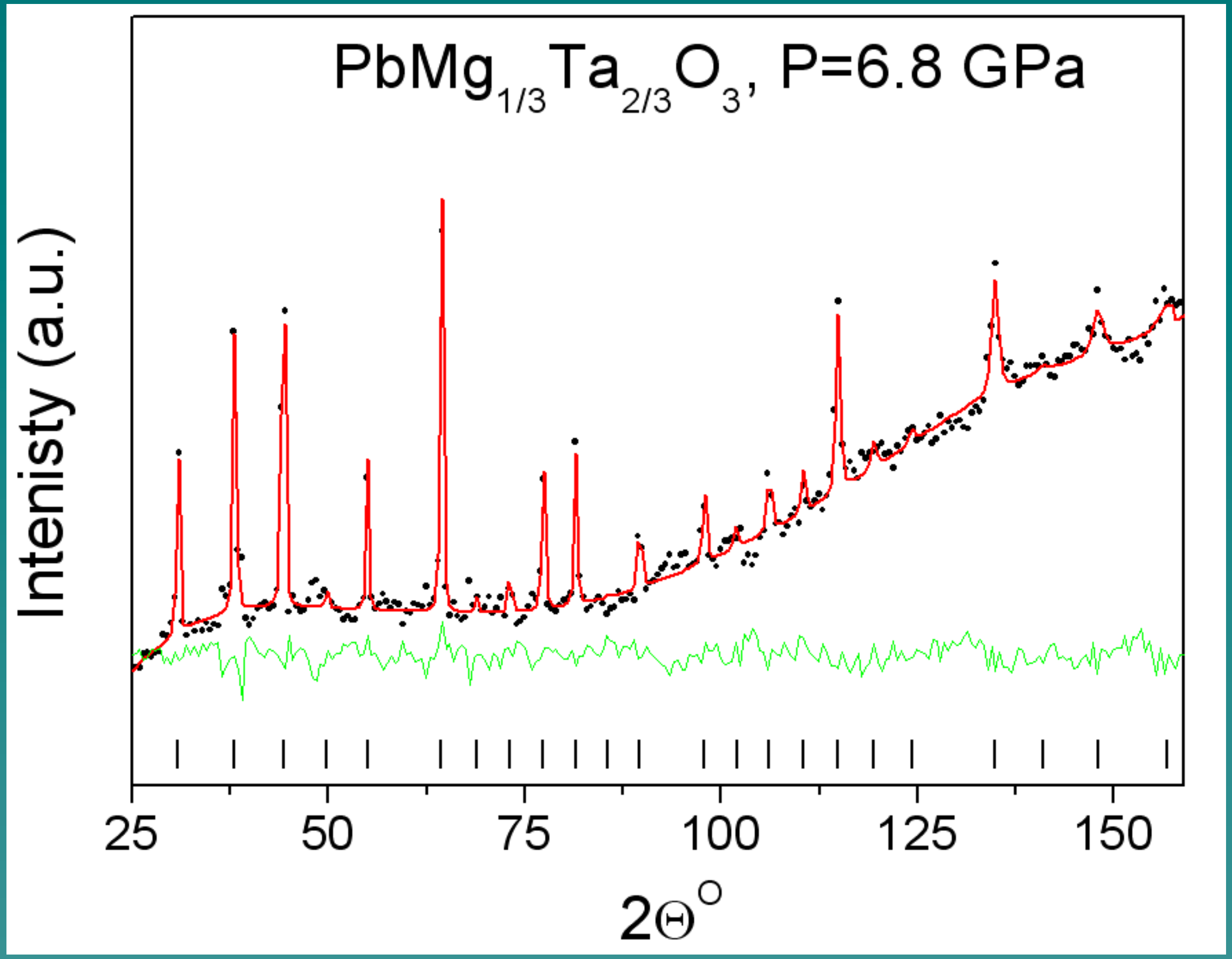

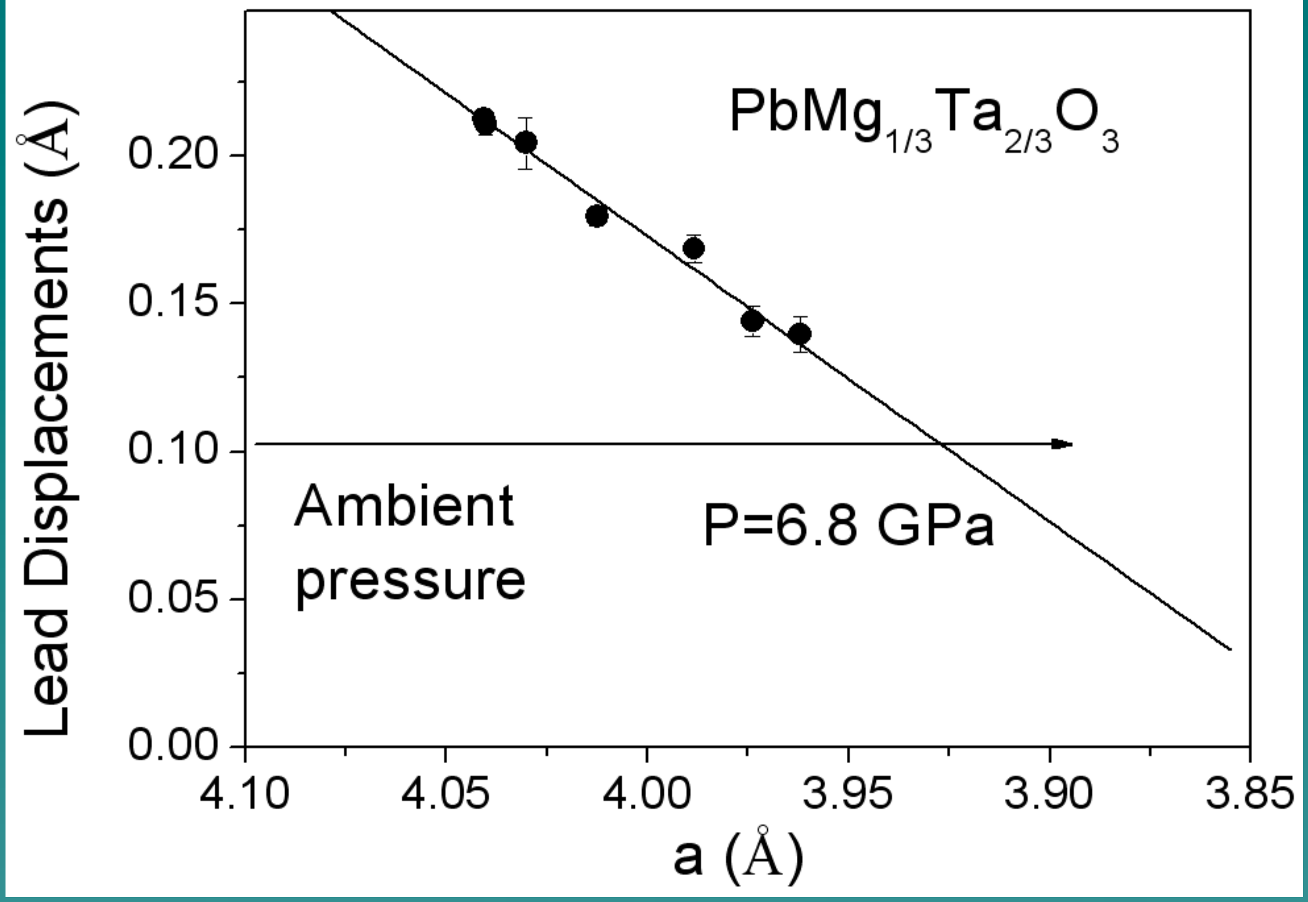

Observed and calculated diffraction spectrum from $PbMg_{1/3}Ta_{2/3}O_3$. Increased background is probably due to the unmasked part of the steel leg of the pressure cell. The crystal structure remains cubic at all pressures. The important changes are: (i) Reduction of the Lead displacements at increased pressures (ii) Appearance of the anisotropy in the Oxygen thermal motion – its ellipsoid becomes significantly elongated toward the Lead ions. Thus these change are responsible for the suppression of the peak in dielectric permittivity and of the diffuse scattering. Similar behaviors were never reported earlier.

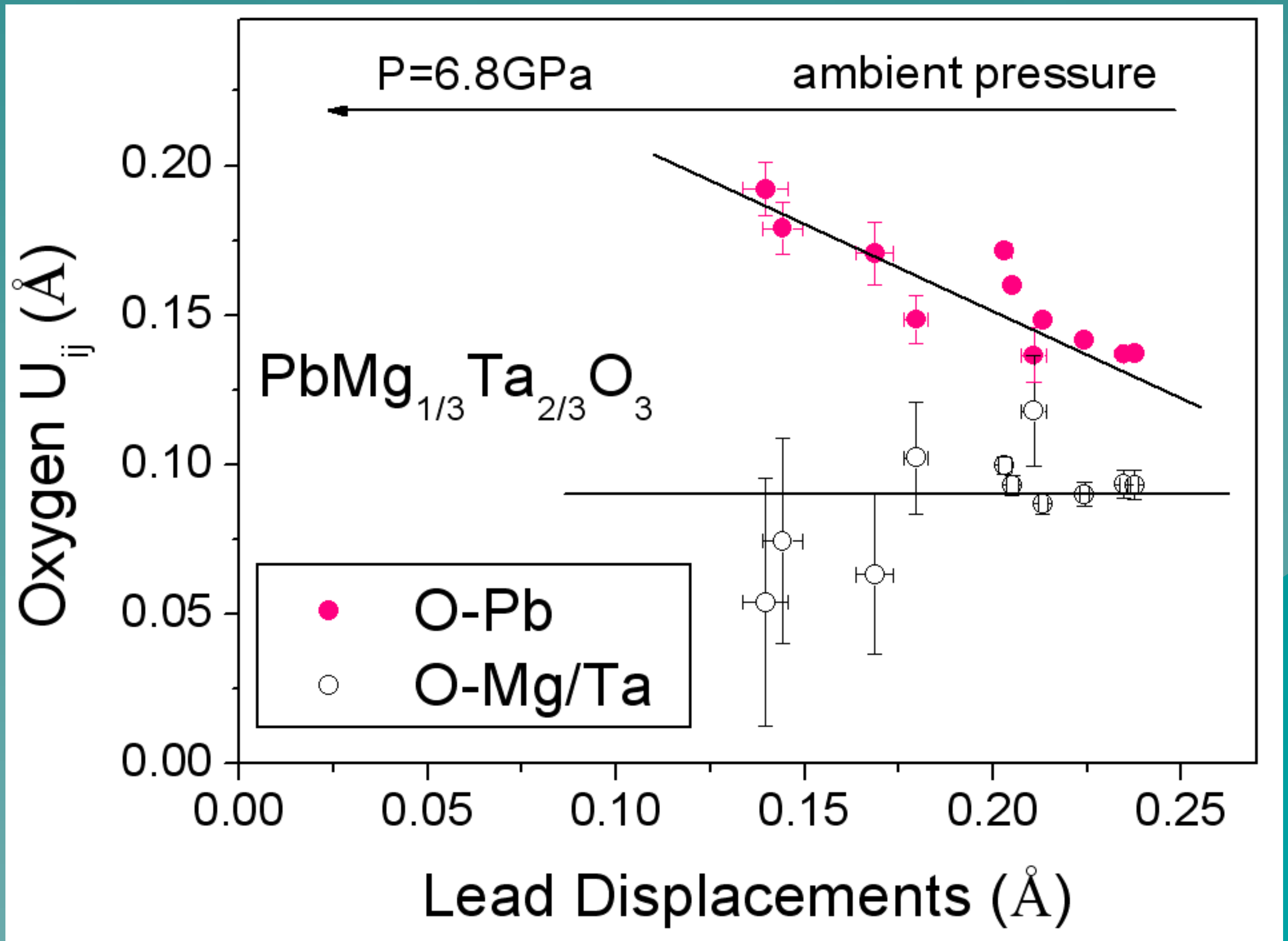

More information about HRPT

http://sinq.web.psi.ch/hrpt

OR

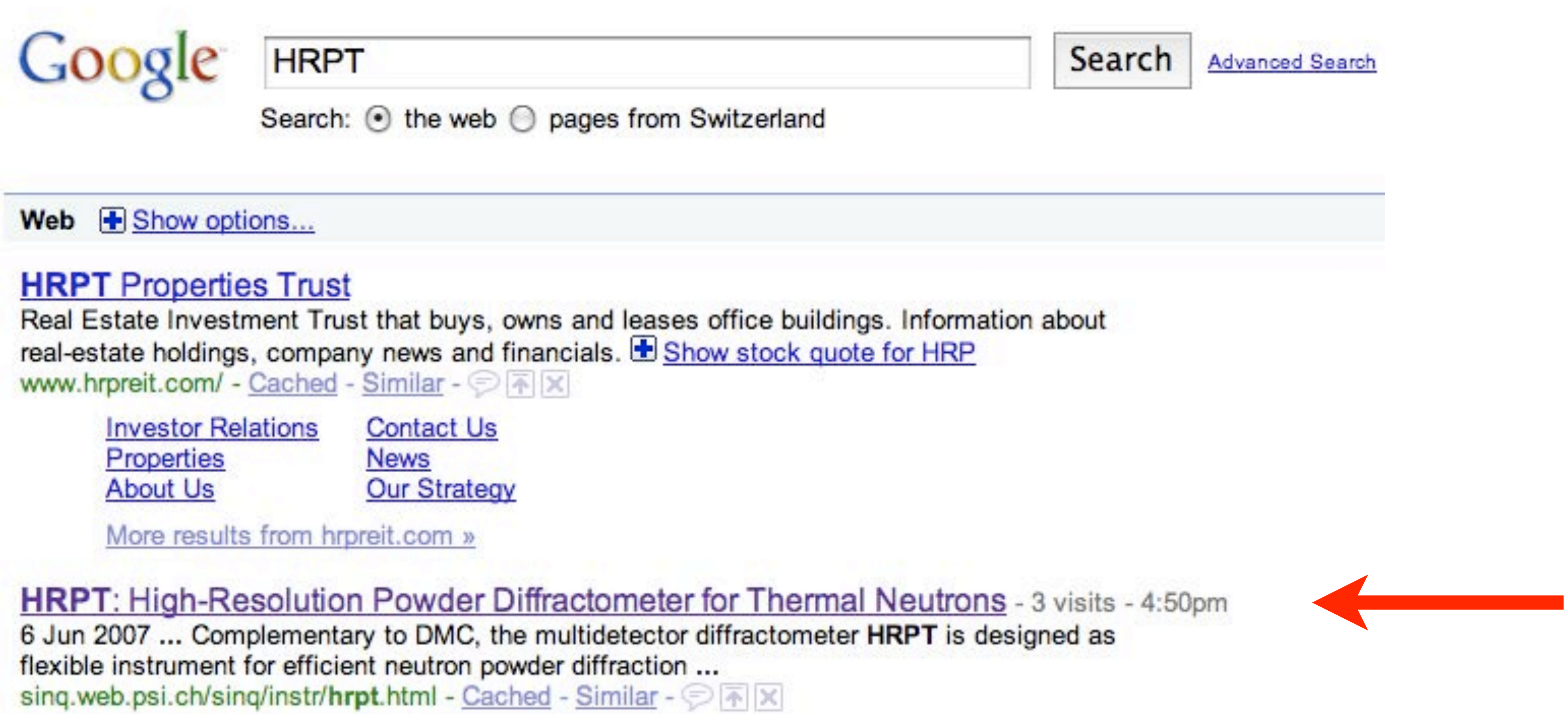

The End